The development of a posterior dynamic stabilisation implant indicated for thoraco-lumbar disc degeneration

Chris Parker

20721579

Thesis submitted in fulfillment of the requirements for the degree *Magister Ingeneriae* in Mechanical Engineering at the Potchefstroom Campus of the North-West University

Supervisor: Prof. Leon Liebenberg

November 2013

Abstract

Posterior lumbar spinal dynamic stabilisation devices are intended to relieve the pain of spinal segments while prolonging the lifespan of adjacent intervertebral discs. This study focuses on the design of such a device, one that has the correct stiffness to stabilise the spinal segment by the correct amount.

An initial literature survey covers contemporary topics related to the lumbar spine. Included topics are lumbar anatomy and kinematics, pathology of degenerative disc disease and treatment thereof, other spinal disorders such as spondylolisthesis and spinal stenosis, as well as the complications associated with lumbar dynamic stabilisation. The influence of factors such as fatigue and wear, as well as the properties of appropriate biomaterials are considered when determining the basis of the device design and development.

Stabilising the spinal segment begins with correct material selection and design. Various designs and biomaterials are evaluated for their stiffness values and other user requirements. The simplest design, a U-shaped spring composed of carbon fibre-reinforced poly-ether-ether-ketone (CFR-PEEK) and anchored by polyaxial titanium pedicle screws, satisfies the most critical user requirements. Acceptable stiffness is achieved, fatigue life of the material is excellent and the device is very imaging-friendly. Due to financial constraints, however, a simpler concept that is cheaper and easier to rapid prototype was chosen. This concept involves a construct primarily manufactured from the titanium alloy Ti6Al4V extra-low interstitial (ELI) and cobalt-chrome-molybdenum (CCM) alloys. The first rapid prototype was manufactured using an additive manufacturing process (3D-printing).

The development of the device was performed in three main stages: design, verification and validation. The main goal of the design was to achieve an acceptable stiffness to limit the spinal segmental range of motion (ROM) by a determined amount. The device stiffness was verified through simple calculations. The first prototype's stiffness was validated in force-displacement tests. Further validation, beyond the scope of this study, will include fatigue tests to validate the fatigue life of the production-ready device.

Acknowledgements

The work presented in this study is an outcome of having the privilege of working in a creative and positive environment. In addition to this the engineering product development process in this environment is applied by enthusiastic and innovative people with incredible minds. I would like to thank the following people for their immeasurable contributions to my work in this study. Firstly, to my study leader **Leon Liebenberg** for his constant motivation and eagerness about my studies and for inspiring me to persevere. **Malan de Villiers** has always provided a work environment where there is a great freedom to design and develop products. To **Karl Grimsehl** who provided some helpful insight and experience in developing designs. To the two anonymous reviewers whose comments resulted in a much improved manuscript. To my friends and in particular my family, **Mike**, **Karen**, **Olga**, **Jonjon**, **Nick** and **Gizela** for your support, love and encouragement throughout my studies.

-Thank you-

Table of Contents

List of Figures

List of Tables

List of Symbols

Symbol	Definition	Unit
c	The maximum distance from the neutral line during bending	m
F	Force	N
I	Moment of inertia	m^4
M	A moment at a point caused by a force acting at a certain distance from that point	Nm
σ_{max}	The maximum average stress in a component	MPa
σ	The average normal stress in a component	MPa

Nomenclature

ASD	Adjacent segment degeneration
ASTM F136	Standard Specification for Wrought Titanium-6 Aluminium-4 Vanadium ELI (Extra-Low Interstitial) Alloy for Surgical Implant Applications
ASTM F799	Standard Specification for Cobalt-28Chromium-6Molybdenum Alloy Forgings for Surgical Implants
ASTM F1058	Standard Specification for Wrought 40Cobalt-20Chromium-16Iron-15Nickel-7Molybdenum Alloy Wire and Strip for Surgical Implant Applications
ASTM F2026	Standard Specification for Poly-ether-ether-ketone Polymers for Surgical Implant applications
ASTM F2624	Standard Test Method for Static, Dynamic, and Wear Assessment of Extra-Discal Spinal Motion Preserving Implants
BMD	Bone mineral density
CCM	Cobalt-chromium-molybdenum
CFM	Composite flow moulding
CFR	Carbon fibre-reinforced
CP	Commercially pure
CT	Computed tomography
DDD	Degenerative disc disease
DSS	Dynamic Stabilisation System by Paradigm Spine
EDM	Electrical discharge machining
FDA	Food and Drug Administration, USA
FEA	Finite element analysis
FSU	Functional spinal unit
HA	Hydroxyapatite
ICR	Instantaneous centre of rotation
ISO	International Organisation for Standardisation
ISO 13485	A quality management system where an organisation needs to demonstrate its ability to provide medical devices and related services that consistently meet customer requirements and regulatory requirements applicable to medical devices and related services.
IVD	Intervertebral disc
L1...L5	Lumbar vertebra 1 to lumbar vertebra 5

L4-L5	Reference to a specific intervertebral disc, for example: between the fourth and fifth lumbar vertebrae
LSS	Lumbar spinal stenosis
MRI	Magnetic resonance imaging
ODI	Owestry Disability Index
PDB	Posterior disc bulge
PDS	Posterior dynamic stabilisation
PEEK	Poly-ether-ether-ketone
PMMA	Poly-methyl-methacrylate
ROM	Range of motion
SP	Spinous process
VAS	Visual analogue scale

Glossary

Anterior	Positioned toward the front
Arthrodesis	Removal of a joint
Arthroplasty	Replacement of a joint
Cadaveric spine	A harvested human spine
Cage	An intervertebral arthrodesis intended to fuse the vertebrae
Cancellous bone	Soft, porous bone
Caudal	Pertaining to the hind part or inferior to another structure
Cephalad	Toward the head or anterior end of the body
Characteristics	A feature or quality belonging to the specific object
Claudication	Pain, cramping in the leg due to inadequate blood flow to the muscles
Cortical bone	Hard, dense bone
Degeneration	A natural process of aging of the intervertebral disc
Degeneration grades (I, II, III, IV, V)	Grade I: Homogenous; Grade II: Horizontal dark bands; Grade III: Grey tone; Grade IV: Bright and dark regions; Grade V: Gross loss of disc height
Discectomy	Surgical removal of a herniated disc material cause compression of a nerve root
Disc herniation	A portion of the disc's nucleus pulposus pushes through the outer annulus fibrosus
Facetectomy	Surgical removal of portions of the facet joints that cause nerve compression
Functional spinal unit	The smallest physiological motion unit of the spine to exhibit biomechanical characteristics similar to those of the entire spine
Fusion	The process of osseointegration, or bone growth, between two bones
Kinematics	Motion of an object without consideration of the forces on the object causing the motion
Kyphosis	The anatomical curvature of the cervical spine
Ligamentoplasty	A device that replaces a ligament; generally between spinous processes
Lordosis	The anatomical curvature of the lumbar spine
Neutral zone	The area on the load-displacement curve of an FSU where the passive osteoligamentous stability mechanisms exert little or no influence
Pseudarthrosis	Failed previous fusion of a spinal segment
Retrolisthesis	Backward slippage of one vertebra onto the vertebra immediately below
Spinal stenosis	Compression of the spinal nerve roots due to a narrowing of the spinal canal
Spondylolisthesis	Forward slippage of the cephalad vertebra onto the caudal vertebra
Subluxation	Partial dislocation of the lumbar vertebra

Chapter 1: Overview of the Study

1.1. Background

Lower back pain affects 60%-80% of the adult population at various stages in their lifetime and results in significant impacts on the medical and economic sectors of a country (Gulbrandsen *et al.* 2010). The ailments of the lower back account for about a fifth of all visits to physicians and time lost from work (Hart *et al.* 1995).

Intervertebral fusion has been considered the standard treatment of lower back pain over the last three decades. This technique, however, has not significantly increased the success of clinical outcomes. While being considered the standard treatment for lumbar spinal disorders, fusion is generally also associated with an accelerated degeneration of the adjacent intervertebral discs (Serhan *et al.* 2011). The known disadvantages of fusion techniques have prompted a higher interest in the development of motion-preserving devices (Courville *et al*. 2008).

The main goals of posterior dynamic stabilisation devices have been postulated by current developers as the restoration of the normal behaviour of the spinal column and the potential prevention of adjacent segment disease (Khoueir *et al*. 2007). Dynamic, or non-fusion, devices are relatively new and only recently has literature reporting the clinical outcomes of these devices been published. One such example is that of the Isobar, where Li *et al.* (2013) have reported its clinical and radiological outcomes.

The first dynamic stabilisation device to be reported on is the Graf ligamentoplasty in 1992. The device that has been reported on the most is the Dynesys, developed by Dubois (Stoll *et al.* 2002). Since the Dynesys was developed, many new devices have emerged resulting in a vast range of dynamic coupler mechanisms.

There are two categories for posterior dynamic stabilisation (PDS) systems; semi-rigid systems intended for intervertebral fusion and soft PDS systems intended to control segmental motion (Barrey *et al.* 2008). Figure 1 illustrates this and highlights the two types of devices pertaining to this research.

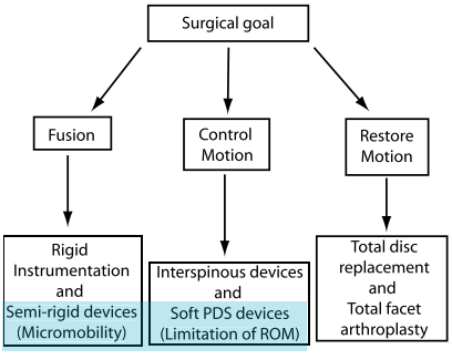

Figure 1: Surgical goals of various devices (Barrey *et al.* 2008)

1.2.Motivations for Development

It has been suggested in a study by Boos and Webb (1997) that spinal fusion devices have been developed to provide fusion success rates close to 98%, but have failed to improve the overall clinical success of decreasing lower back pain.

The failure to improve clinical outcomes of fusion can be attributed to developers not accounting for patients having been diagnosed with pseudarthrosis, resulting in a false-positive finding when studying radiographs (McAfee 1999). Another large factor overlooked with fusion, specifically cages, is abnormal load transmission through the bone-metal interface, where a small cage-footprint size might result in a load distribution that is 500% higher than anywhere else on the endplate, even after fusion (Polikeit & Nolte 2000).

It is therefore fair to deduce that the improvement of clinical outcomes with regards to lower back pain requires a device that produces a more uniform distribution of load through the spinal joint. A solution is the use of a dynamic, or soft, intervertebral device that stabilises without fusion.

Figure 2: Currently FDA approved DSS devices; A: Dynesys®, B: AccuFlex®, C: Graf System (Serhan et al. 2011)

Current dynamic stabilisation devices are prone to fatigue failure and/or screw-loosening, especially if the device does not match the kinematics of the spinal motion segment. These devices should also help in transferring load that was previously transferred through the intervertebral disc and facet joints

(Courville *et al.* 2008). Figure 2 shows three of the currently FDA-approved devices; the Dynesys® (Zimmer Spine, Inc., Warsaw, IN) system is arguably the most widely used device (Gédet *et al.* 2009).

The main goal of a posterior dynamic stabilisation device is to stabilise the affected spinal segment without the use of bone graft and rigid fixation. Allowing motion at the instrumented level will theoretically decrease the incidence of adjacent segment disease and restore the segmental neutral zone (Park *et al.* 2012).

1.3. Objective of the Study

The objective of this study is to develop a dynamic stabilisation device, which meets the determined user requirements, to the first prototype phase.

A posterior lumbar dynamic stabilisation device, which meets the specific user requirements, is defined as a device that stabilises the lumbar spine enough to prevent excessive spinal segment motion. The load-distribution characteristics of the device construct should be designed such that the incidence of adjacent segment disease (ASD) is reduced as far as possible.

The development of the stabilisation device will be done in three main phases: detail design, design verification and prototype validation.

1.4. Scope of the Study

The scope of this study includes a study of contemporary literature relating to the user requirements of posterior lumbar dynamic stabilisation implants, conceptualisation, detail design, and manufacture and stiffness testing of a prototype device.

Verification of the design is performed on the chosen concept through simple calculations. A rapid prototype device is manufactured and is load tested to validate the design; this prototype is representative of the final product, although it is not composed of the same materials.

Due to financial constraints the study concludes at the first rapid prototype phase.

Chapter 2: Literature Review

This chapter summarises the literature reviewed relating to lumbar spine functioning, anatomy, kinematics and degenerative disc disease (DDD). The latest literature that the author could obtain has been cited, whilst ensuring that it is as relevant as possible to the current project.

2.1. Introduction

The functions of the human spine include providing a strong, mobile structure onto which the skeletal frame is applied and providing protection to the spinal cord and peripheral nerves that stem from it (Bao *et al.* 1996).

The spinal column is composed of hard tissue and soft tissue. The hard tissue is in the form of vertebrae that make up the strong spinal column. The soft tissue forms the intervertebral discs (IVDs), muscles and connective tissues that give the spine stiffness and stability by holding the spine together (Gambrandt *et al.* 2005).

2.2. Anatomical Planes

When describing the anatomy of the human body, three anatomical planes are used. The sagittal plane intersects the body in an anterior-posterior direction, the coronal plane in a lateral direction, and the axial plane sections the anatomy into superior and inferior portions. The anatomical planes are illustrated in Figure 3.

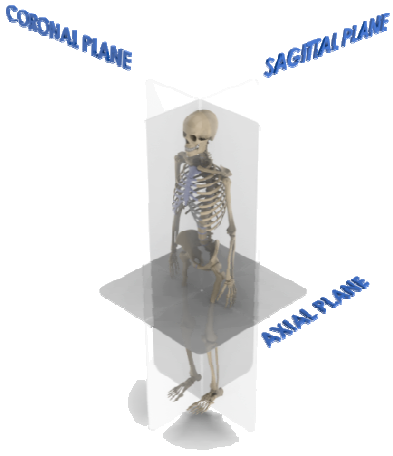

Figure 3: Anatomical planes (Jansen 2010)

The movements of the spine are described using three mutually orthogonal planes, according to Spenciner *et al.* (2006). These movements are illustrated in Figure 4; the principal anatomical directions include flexion/extension, described as bending forwards or backwards; lateral bending in the coronal plane; and axial rotation, a twisting of the spine observed from the axial plane.

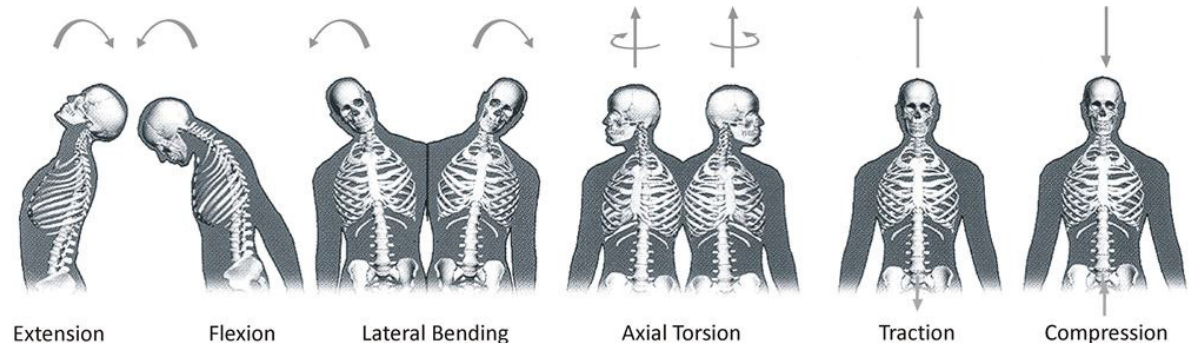

Figure 4: Movements of the spine (Adapted from Austin 2008)

2.3.Functional Spinal Unit (FSU)

The spinal column consists of 33 vertebrae with 23 intervertebral discs. The spine is grouped into 5segments; the cervical spine (C1 to C7), the thoracic spine (T1 to T12), the lumbar spine (L1 to L5), the sacral spine (S1-S5) and the coccygeal spine (Drake *et al.* 2010). Figure 5 illustrates the spinal column showing the anterior, lateral and posterior views along with the different spinal segments.

When the spine is viewed laterally, in the sagittal plane, there are three clear curvatures; sacral kyphosis of the sacrum, lumbar lordosis from L1 to L5, thoracic kyphosis from T1 to T12, and cervical lordosis from C1 to C7 (Roussouly 2011).

When viewed in the coronal plane, the spine should be positioned in a straight upright position; this indicates that it is balanced laterally. A lateral imbalance can result in a condition known as scoliosis.

Figure 5: Artistic illustration of the spinal column anteriorly, left laterally and posteriorly (Netter 2011)[1]

The functional spinal unit (FSU) is defined as at least two vertebrae with an intervertebral disc between them with all the ligaments, muscles and other soft tissue intact. A healthy FSU has spring-like properties; when the FSU is loaded axially it responds with a certain deflection and results in increasing lordotic and kyphotic curvatures. When the FSU is no longer healthy it experiences excessive movements under these loads and can result in conditions known as hyperlordosis and hyperkyphosis.

2.3.1. Lumbar Spine

The lumbar spine is a system of vertebrae, articulation joints, muscles and connective tissue that provides motion for the trunk, mechanical support and protection to neural elements. The lumbar spine consists of five vertebrae (Ebraheim *et al.* 2004).

[1] "Celebrated as the foremost medical illustrator of the human body and how it works, Dr. Frank H. Netter's career as a medical illustrator began in the 1930's when the CIBA Pharmaceutical Company commissioned him to prepare illustrations of the major organs and their pathology. Dr. Netter's incredibly detailed, lifelike renderings were so well received by the medical community that CIBA published them in a book. This first successful publication in 1948 was followed by the series of volumes that now carry the Netter name - The Netter Collection of Medical Illustrations. Even 12 years after his death, Dr. Netter is still acknowledged as the foremost master of medical illustration. His anatomical drawings are the benchmark by which all other medical art is measured and judged." (www.netterimages.com)

Figure 6 shows an illustration of the lumbar spine from a left lateral view. Note the lumbar lordotic curvature and how the lumbar vertebrae dimensions increase from cephalad to caudal. Note also how the intervertebral lordotic angle becomes more oblique down where the L5-S1 joint would be. This level is crucial for balance and is one of the most commonly degenerated levels; shear forces are also high in this disc due to its oblique angle (Rousseau *et al.* 2006).

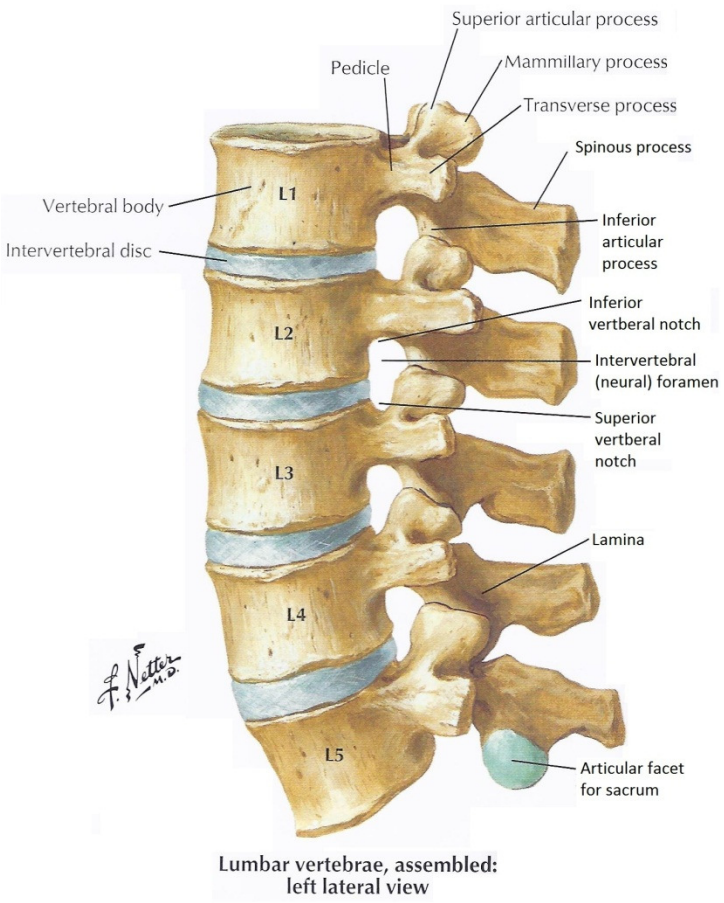

Figure 6: Artistic illustration of the lumbar spine from a left lateral view (Netter2011)

2.3.2. Anatomy of the Lumbar Vertebrae

The lumbar vertebrae and its geometry, bone mineral density and structure are important factors to consider when designing a posterior lumbar dynamic stabilisation device as these devices are generally anchored in the vertebrae using pedicle screws. Therefore, the screw design is dependent on these factors.

There are five lumbar vertebrae in the spinal column, followed by the sacrum at the bottom. The depth of the vertebral body varies, depending on gender, age and level, between 25 and 35mm (Ouelette and Arlet 2004). The vertebral body can be defined as consisting of two parts: the vertebral body and the neural arch. The neural arch is located posterior to the vertebral body, and is formed by two laminae that join at the spinous process, a protrusion on the posterior end of the vertebral body to which

muscle and ligaments attach. The laminae are attached to the upper portion of the vertebral body by two pedicles (Ebraheim *et al.* 2004).Figure 7 illustrates the L2 lumbar vertebra from a superior view.

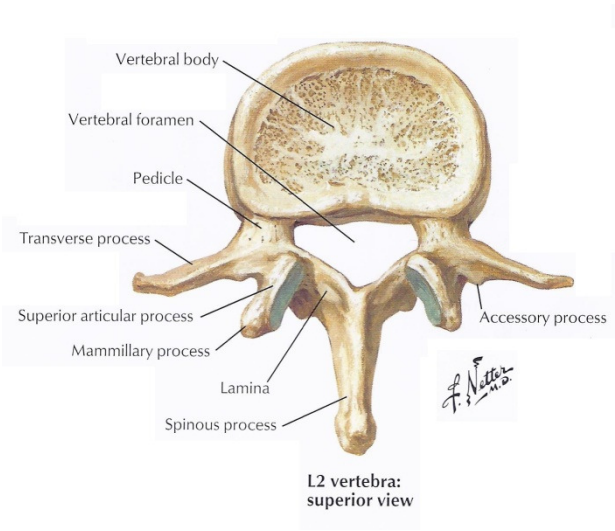

Figure 7: Artistic impression of the L2 lumbar vertebra, superior view (Netter 2011)

In a study to determine the bone mineral density (BMD) of the cervical and lumbar vertebrae, Yoganandan *et al.* (2006) measured the BMD of 57 young adult males, the results of which are provided in Table 1. The results show the statistical BMD for various vertebrae. Bone mineral density in each vertebra is distributed between the hard, dense outer shell of cortical bone and the inner, more porous cancellous bone. Bone mineral density is important for implant screws as osteoporotic, or abnormally low-density, bone will not anchor them correctly.

Table 1: BMD measurements (mg/cm^3) for cervical, thoracic and lumbar vertebrae (Yoganandan *et al.* 2006)

BMD (mg/cm^3) for cervical, thoracic, and lumbar vertebrae

Level	Sample size	Mean	Minimum	Maximum	Standard deviation
C2	57	274.0	190.9	427.5	53.1
C3	57	256.2	162.9	429.9	49.1
C4	57	270.1	193.1	412.6	44.7
C5	57	268.3	189.5	392.9	44.6
C6	57	242.6	162.6	361.4	40.6
C7	57	224.9	154.5	327.8	36.9
T1	55	194.3	106.2	322.1	44.2
L2	57	173.9	110.5	263.8	27.4
L3	57	169.7	123.0	262.0	28.5
L4	57	173.1	123.7	260.5	29.4
All	568	224.8	106.2	429.9	57.7

The cross sectional view in Figure 8 illustrates the higher density cortical bone around the perimeter of the vertebra and the lower density cancellous bone in the centre.

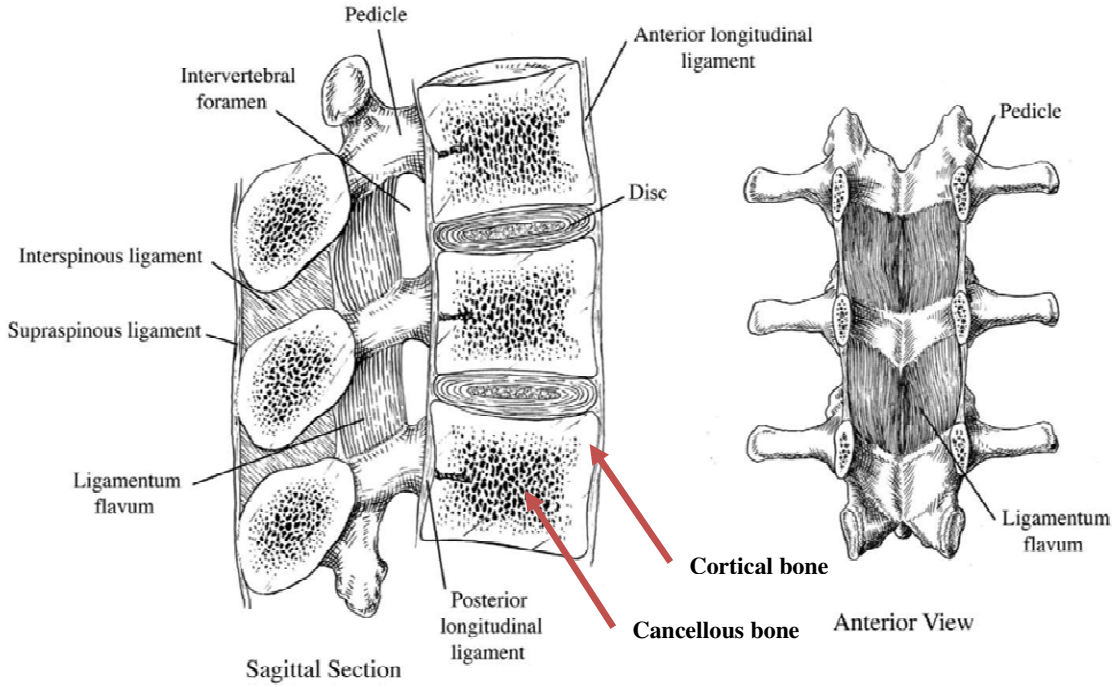

Figure 8: Sagittal section and anterior view of part of the lumbar spine illustrating the ligaments (adapted from Ebraheim *et al.* 2004)

Bone mineral density is an important factor to consider when developing an orthopaedic implant; Wittenberg *et al.* (1991) described how the BMD can affect screw stability by demonstrating that pedicle screw pull-out occurs in cadaveric vertebrae with BMD below 74±17mg/cc when subjected to physiological loads.

2.3.3. Ligaments

A cadaveric spine without its ligaments or musculature is inherently unstable. According to Bogduk and Twomey (1991) the passive combination effect of the musculoligamentous system provides the stabilisation of the spine in flexion.

Figure 8 illustrates the ligaments of the lumbar spine with sagittal section and anterior views. The anterior longitudinal ligament extends all the way from the superior base of the skull to the anterior surface of the sacrum. The posterior longitudinal ligament is attached along its length to each of the vertebral bodies on the anterior surface of the vertebral canal. The ligament flavum attach to the posterior surface of the vertebral canal and pass the laminae of the adjacent vertebrae. Interspinous ligaments pass between the adjacent spinous processes and are attached to the apex of each spinous process. These ligaments merge with the ligamentum flava anteriorly and supraspinous ligament

posteriorly on each side (Drake *et al.* 2010). These ligaments all play a vital role in the stabilisation of the lumbar spine (Ebraheim *et al.* 2004).

2.3.4. The Intervertebral Disc

In order to understand the reason for lower back pain as a result of degenerative disc disease, discussed later, the structure of the intervertebral disc needs to be reviewed. There are a number of reasons for the degeneration of the disc and its structure is critical to its function.

The intervertebral disc has a structure consisting of the nucleus pulposus core which is surrounded by the annulus fibrosis, or multi-layered fibres (Markolf *et al.* 1974).Figure 9illustrates the composition of the disc.

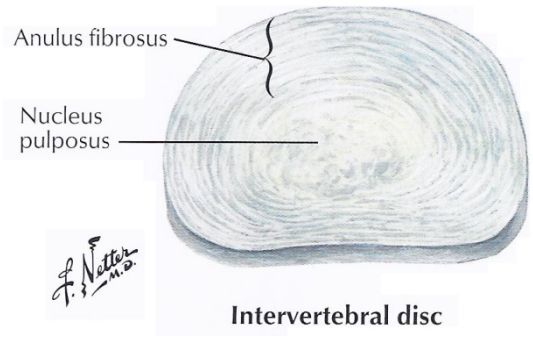

Figure 9: Artistic illustration of the intervertebral disc (Netter 2011)

The nucleus pulposusis composed of a mucoid that contains 70%-90% water. This water percentage decreases with age and this decrease is considered a major factor in disc degeneration (Ebraheim *et al.* 2004).

2.4.Spinal Nerves

Spinal nerves transmit sensory and motor function signals between the central nervous system (CNS) and target organs (Kayalioglu 2009). A large part of the CNS is formed by the spinal cord which extends from the foramen magnum to approximately the level of the L1-L2 disc in adults (Drake 2010).

According to Drake (2010) there are 31 pairs of spinal nerves along the spinal cord; eight cervical (C1-C8), twelve thoracic (T-T12), five lumbar (L1-L5), five sacral (S1-S5) and one coccygeal nerve (Co). All these nerves leave the cord through the intervertebral foramina and after the ganglion (5 in Figure 10) split into anterior and posterior rami; two or four smaller meningeal nerves from each re-enter the intervertebral foramen to supply blood vessels, dura, ligaments and IVDs.

Figure 10 illustrates the nerve roots in the spinal canal; the vertebrae are sectioned through the pedicles (1). The ventral (2) and dorsal (3) nerves roots are shown leaving the spinal cord as small rootlets (4). As the nerve roots leave the spinal canal there is a bulge called the ganglion (5). The spinal dura wraps the nerve roots as a central cylindrical sac (7). This is split into separate root sleeves (8) (Olmarker 1990).

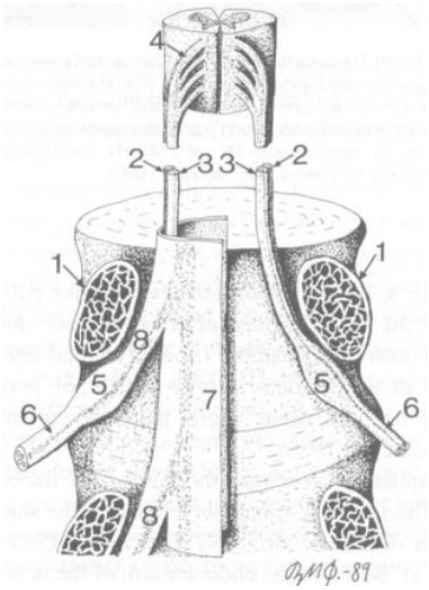

Figure 10: Illustration of the nerve roots with the vertebrae section through the pedicles (Olmarker 1990)

2.5.The Pedicle

The pedicle and its anatomical properties such as dimensions and angles, bone density and other morphometric values are important when considering the design of pedicle screws for anchoring a posterior lumbar device.

The pedicle is the portion of the vertebrae that connects the spinous process to the vertebral body. A vertebra consists of two pedicles; the space between them is known as the vertebral foramen. The length of the pedicle averages between 40mm and 50mm between the dorsal and ventral cortex (Ebraheim *et al*. 2004). Figure 11 shows a cross-section of the vertebra through the pedicle.

According to Weinstein *et al.* (1992) the transverse pedicle diameters range from 4.5mm at the vertebrae T5 to 18mm at L5, with the sagittal diameter being slightly larger than the transverse in general. The angle at which the pedicle protrudes from the vertebra in the transverse plane also changes between levels; starting around 10 degrees in the thoracic spine and increasing to a maximum of 30 degrees, from posterolaterally to anteromedially, in the lumbar spine.

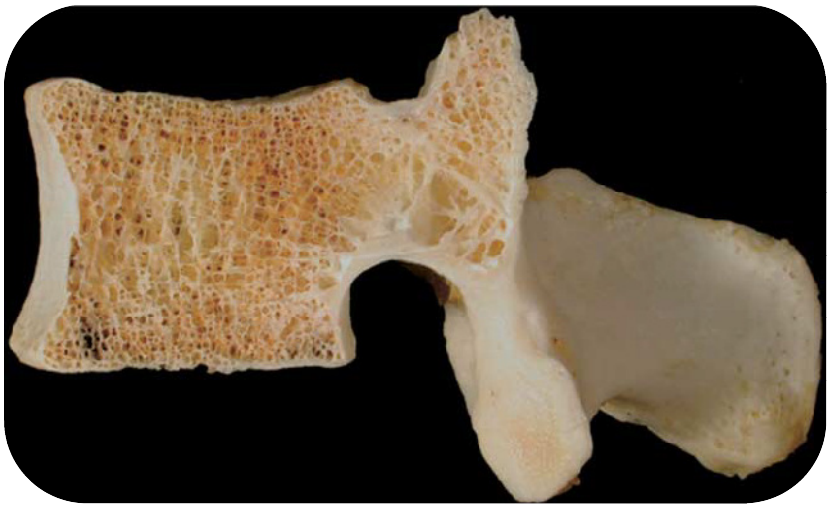

Figure 11: Sagittal section of the L3 vertebra at the pedicle level (Ouelette and Arlet 2004)

2.6. Vertebral Loading

The loading experienced by the lumbar vertebrae have been described by various authors; Dolan *et al.* (2001) have suggested that the typical loading is around 1kN and that below the L3 vertebra this force acts axially. The typical intact spinal segment is inherently unstable, according to Crisco *et al.* (1992), as it buckles under a compressive load of 88N and this value decreases with injury.

A preload on the spine affects the movement and displacement curve of the spine; the spine becomes more flexible when a preload with lateral or anterior forces or lateral bending or flexion and extension moments. The spine becomes less flexible with a preload when the spine is in traction or axial rotation (Panjabi *et al.* 1977). Fatigue testing of a posterior dynamic stabilisation device is crucial, and using loads that mimic those of an actual spine is important. The preload specified by the testing standard ASTM F2624-07 uses an estimate from the studies of Nachemson (1965, 1981) of a 1kN axial load with approximately a third of the load carried by posterior elements, i.e. a 300N preload.

2.7. Kinematics of the Lumbar Spine

A lumbar spinal segment consists of 6 degrees of freedom; 3 translational and 3 rotational (Kulkarni and Diwan2005). Motion in the lumbar spine varies such that lateral bending is predominant in the upper segments.

2.7.1. Instantaneous Centre of Rotation (ICR)

The centre of rotation for a spinal segment changes with movement of that segment; flexion and extension, lateral bending and axial rotation all cause a change in the ICR (Gambrandt *et al.* 2005). Figure 12 shows the model used by Schmidt *et al* (2008). to determine the ICR of the L4-5 with the use of finite element modelling (FEM).

According to Schmidt *et al.* (2008), the instantaneous centre of rotation (ICR) is important in the development of dynamic stabilisation devices. The device's ICR must mimic that of a healthy motion segment in order to avoid facet joint arthritis. In their study it was found that the facet, otherwise known as zygapophyseal, joints were only slightly loaded when small moments were applied. They determined that the facet joints were always unloaded in flexion, as expected. It was also shown that the hypothesis that the highest facet joint forces occurred when the ICR was located outside the IVD was indeed correct.

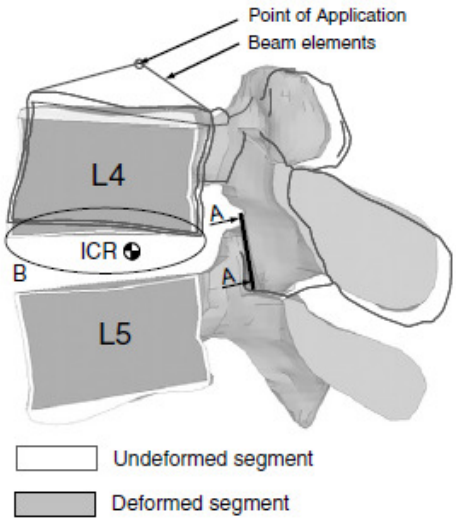

Figure 12: Model used for FEM in determining the ICR of the L4-5 motion segment (adapted from Schmidt *et al.* 2008)

The ICR is initially located in the centre of the IVD and moves posteriorly upwards, under an increasing moment, and under a maximum of 7.5 Nm the ICR is located completely outside the IVD. The path of the ICR was studied by Rousseau *et al.* (2006) and is illustrated in Figure 13.

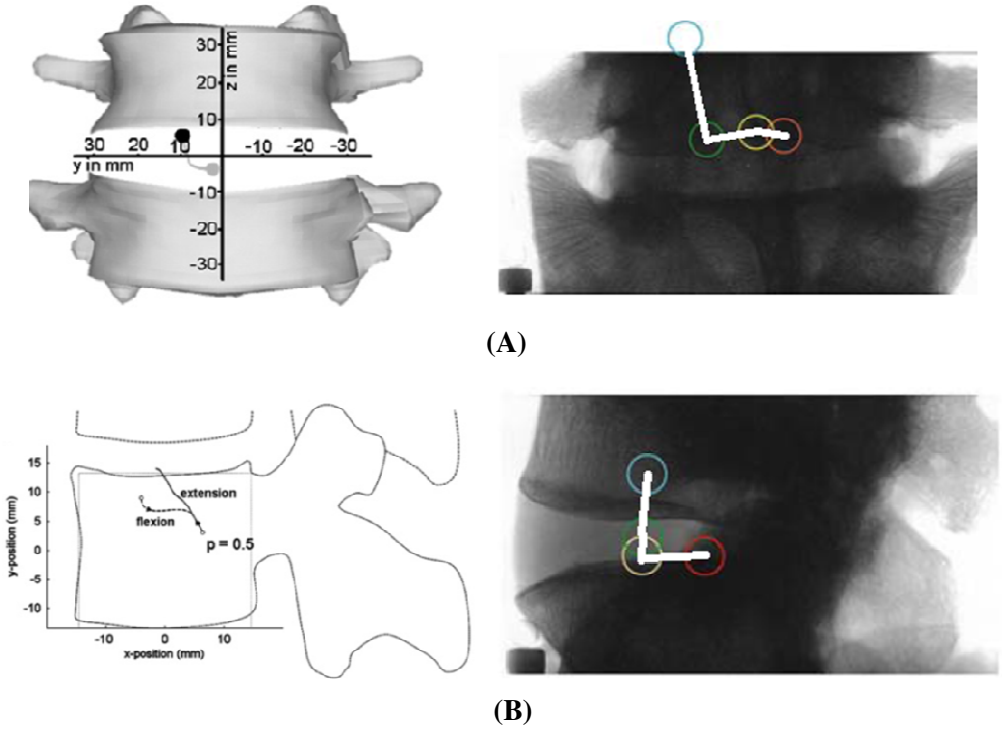

Figure 13: Comparisons between ICR paths during (A) Lateral bending: Schmidt *et al.* (2008) vs. Rousseau *et al.* (2006), and (B) Flexion/extension: Bifulco *et al.* (2012) vs. Rousseau *et al.* (2006)

2.7.2. Range of Motion (ROM)

Eijkelkampand Groningen (2002) summarised the data collected on range of motion (ROM) of lumbar IVDs from three sources; White and Panjabi (1990), and Pearcy (1984a, 1984b). The data from Pearcy distinguishes the differences between flexion and extension ROM. The authors also note that the more flexible a spinal segment is the more likely that it will become unstable.

Table 2: ROM and its range in degrees summarised for lumbar IVDs. The numbers in brackets indicate the ROM range for each case (adapted from White & Panjabi (1990), Pearcy (1984a, 1984b)

Source	Motion	L1-L2	L2-L3	L3-L4	L4-L5	L5-S1
White (1990)	Axial rotation	2 (1-3)	2 (1-3)	2 (1-3)	2 (1-3)	1 (1-3)
White (1990)	Lat. bending	6 (3-8)	6 (3-10)	8 (4-12)	6 (3-9)	2 (2-6)
White (1990)	Flex. and ext.	12 (5-16)	14 (8-18)	15 (6-17)	16 (9-21)	17 (10-24)
Pearcy (1984)	Flexion	8 (5)	10 (2)	12 (1)	13 (4)	9 (6)
Pearcy (1984)	Extension	5 (2)	3 (2)	1 (1)	2 (1)	5 (4)

2.8.Degenerative Disc Disease (DDD)

Degenerative disc disease is a common disorder in the lumbar spine. This condition remains a controversial one as biochemical and mechanical factors may influence its progress in various ways. The biochemical alterations in the intervertebral disc may be brought on by an initial mechanical failure, whereas the mechanical failure of the disc may be as a result of the biochemical changes (Adams *et al.* 200).

It has been suggested that the changes in the intervertebral disc due to degeneration are related to the biomechanical function of the lumbar spine (Kirkaldy-Willis *et al.* 1982). A study performed by Tanaka *et al.* (2001) was aimed at showing the relationship between disc degeneration and spinal flexibility. Their study found that in the upper lumbar spine, the motion under axial rotation was increased during grade IV degeneration and decreased during grade V, while the motion in lateral bending was increased in grade III. In the lower lumbar spine, the motion in axial rotation and lateral bending was increased in grade III degeneration. Figure 14 illustrates these degeneration grades.

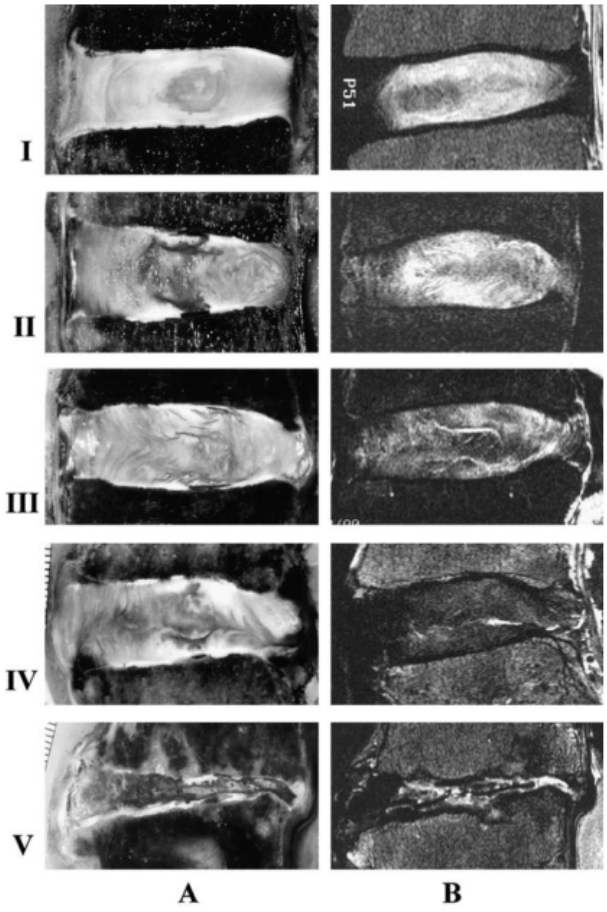

Figure 14: Mid-saggital sections of the intervertebral disc with grades I to V of degeneration; photographs (left), magnetic resonance imaging (right) (adapted from Tanaka *et al.* (2001))

The intervertebral disc undergoes biological changes including an altered cell type, cell density, cell proliferation and cell death among many others. These changes result in the disc's inability to bear normal loading (Zhao *et al.* 2007). In a healthy spine about 70% of spinal load is transferred through the intervertebral disc, while the rest is transferred though the facet joints, this loading changes as the disc degenerates (Shiraz-Adl *et al.* 1987).

According to Errico (2004), disc degeneration in the hypermobility phase results in either frank subluxation or axial setting of the disc. With the former either spondylolisthesis or retrolisthesis, depending on which level is affected, occurs. With the latter, the disc simply collapses, or decreases in height significantly, and as a result the lumbar lordosis, which is provided by a well-hydrated disc, is lost. In either case, when the disc collapses, the motion segment stiffens and osteophyte and facet arthrosis form. After the segment stiffens the adjacent level becomes hypermobile and begins degenerating itself. This adjacent segment degeneration can happen in a cascading manner in either direction from the initially affected segment.

2.8.1. Mechanical Loading

The mechanical properties of the intervertebral disc (IVD) contribute largely to the shock-absorbing characteristics of the lumbar spine. Because of the complex motion of the spine and the visco-elastic behaviour that the IVD exhibits, the stiffness of the IVD is time-dependent. The IVD's visco-elastic properties result in its ability to absorb energy, releasing it during a typical loading-unloading of the disc, demonstrated by the hysteresis curves in Figure 15 (Kulkarni & Diwan 2005).

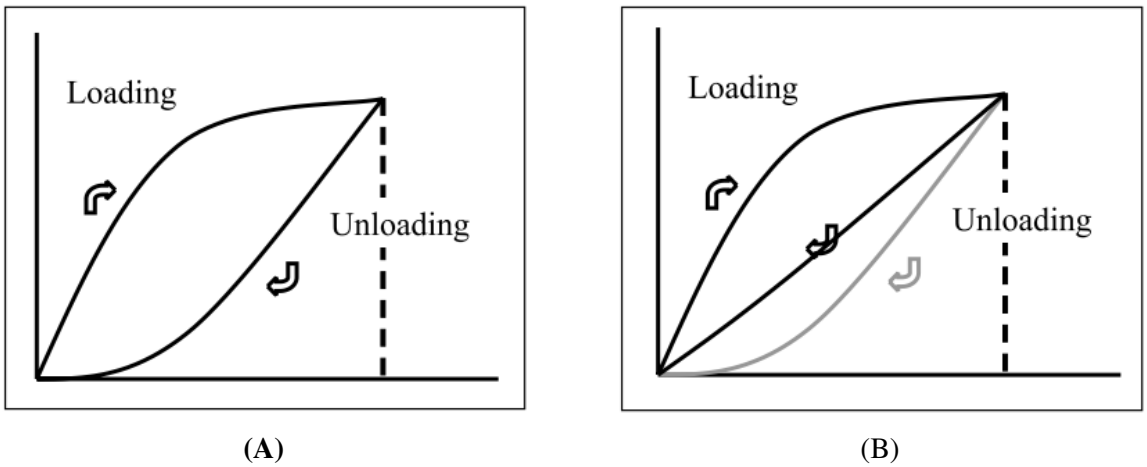

(A) (B)

Figure 15: Hysteresis curves demonstrating the visco-elastic properties, or absorption and equal-dissipation of energy, of (A) a normal IVD and (B) a degenerated IVD (Kulkarni & Diwan 2005)

The ability of the intervertebral disc to absorb shock is decreased; the hysteresis curve is smaller, indicating that less energy is absorbed when the disc is loaded. This means that the disc deformation in creep and relaxation is reached faster than usual (Kulkarni & Diwan 2005).Eijkelkamp and

Groningen (2002) have also summarised simple representations of the various stiffness values of the FSU, of which the IVD forms a part, (cf. Table 3).

Table 3: Simple representations of various stiffness values of the FSU (Eijkelkamp & Groningen 2002)

Force/Moment	Stiffness
Tension	770 N/mm
Compression	2000 (700-2500) N/mm
Anterior shear	121 N/mm
Posterior shear	170 N/mm
Lateral shear	145 N/mm
Flexion	1.36 (0.8–2.5) Nm/deg
Extension	2.08 Nm/deg
Lateral bending	1.75 Nm/deg
Axial rotation	5.00 (2-9.6) Nm/deg

A combination of bending and compression can cause a healthy IVD to prolapse and herniate (Adams & Dolan 2005). Figure 16 shows a midsagittal section through a healthy disc that prolapsed; note how the nucleus pulposus has herniated and created a fissure posteriorly.

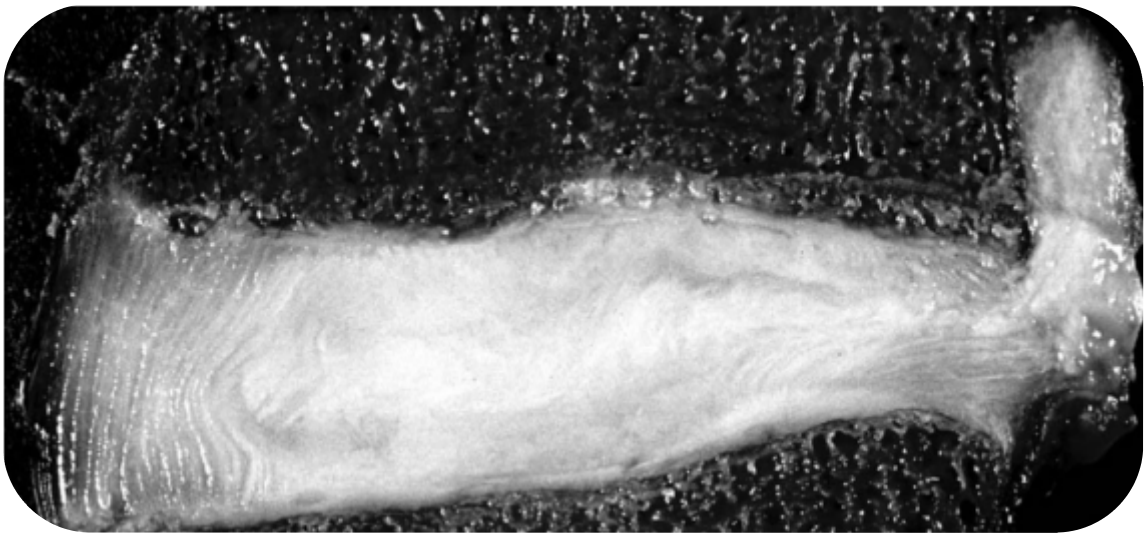

Figure 16: Midsagittal section through a cadaveric, prolapsed lumbar intervertebral disc (Adams & Dolan 2005)

A herniated intervertebral disc is usually treated with discectomies; this method of treatment is not always successful and a disc may continue to herniate recurrently. This condition is an indication of posterior dynamic stabilisation. In a study by Kaner *et al.* (2010) the authors evaluated two-year follow-up clinical outcomes of posterior dynamic stabilisation in 40 patients suffering from recurrent

spinal segment disc hernias. Figure 17 shows imaging after microdiscectomies to address the herniated disc and postoperative imaging of the Cosmic (Ulrich GmbH & Co. KG, Ulm, Germany) device implanted at the affected level in a 34-year-old man. Visual Analogue Scales (VAS) and Owestry Disability Index (ODI) scores were significantly improved as a result of the implanted devices at 3, 12 and 24 months follow-up.

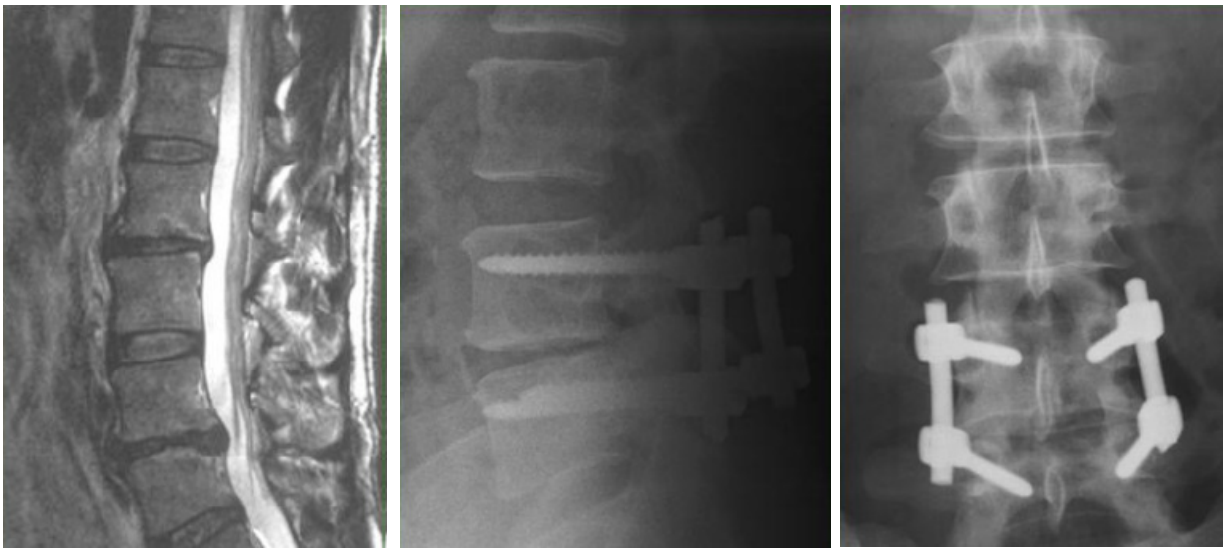

(A) **(B)** **(C)**

Figure 17: L4-L5 recurrent herniated intervertebral disc, indicated by the arrow, after microdiscectomy (A), radiographs of the Cosmic dynamic stabilisation device from a lateral (B) point of view and a posterior (C) point of view (adapted from Kaner *et al.* 2010)

2.8.2. Genetic Predisposition

Disc degeneration may, according to Urban *et al.* (2003), have a strong familial predisposition. Two studies have been done on the genetic factors in twins (by determining heritability) of disc degeneration both support this statement. In the study by Sambrook *et al.* (1998), for instance, the authors found that heritability of the disease was 64%. Urban *et al.* (2003) go on to note that there is evidence for gene-environment interaction that affects the heritability of degenerative disc disease.

2.8.3. Nutritional Effects

The intervertebral disc is large and avascular. Its cells depend on blood vessels to provide nutrients and to remove metabolic waste (Holm *et al.* 1981). The blood vessels travel through the intervertebral body and end just above the cartilaginous end-plate and then must diffuse through the endplate and through the cells to the nucleus which, according to Urban *et al.* (2003), may be as far as 8mm away from the capillaries.

One of the main causes of degenerative disc disease is believed to be a discontinued supply of nutrients to the intervertebral disc (Nachemson *et al.* 1970). As with any cell in the human body it is critical that it receives nutrients (e.g. glucose) and oxygen to remain healthy. According to Horner *et al.* (2001) the cells do not survive when exposed to low levels of glucose concentrations or acidic pH for extended periods of time.

Urban *et al.* (2003) also note that even if the nutrients are not disturbed, the supply of them to the disc may be inhibited by the calcification of the cartilaginous endplate.

2.9. Conclusion

The functional spinal unit serves in transmitting physiological loads through the three-joint complex, while also transmitting sensory information to and from target organs and the brain. Abnormalities in the spinal column, such as degenerative disc disease, may lead to conditions that impinge spinal nerves and cause pain.

The intervertebral disc serves as a shock absorber and is critical for support of the upper parts of the spinal column. The disc determines how the spinal segment moves and rotates and therefore where the instantaneous centre of rotation (ICR) is located. The ICR changes position as the functional spinal unit (FSU) moves; it begins in the centre of the disc and moves posteriorly upwards during extension.

Disc degeneration is a natural process, however if degenerative disc disease (DDD) occurs it accelerates the degeneration. The degeneration is thought to be a result of various factors such as; mechanical loading, genetic predisposition and nutritional effects.

A posterior dynamic stabilisation device should unload the degenerated disc enough, although not completely, and should limit the range of motion. It is ideal that the ICR as a result of the device is as close to the natural ICR path during any motion of the segment.

Chapter 3: Lower Back Pain (LBP)

3.1. Overview of Lower Back Pain

Lower back pain is highly prevalent, according to Adogwa *et al.* (2011), and affects almost 85% of the US population with 1- and 10-year occurrence rates of 45% and 80% respectively.

Lower back pain, or mechanical back pain, is traditionally a chronic condition caused by degenerative diseases of the lumbar spine (Sengupta 2005). It is also generally accepted that disc degeneration reduces the movement of the spine, except in early stages (Fujiwara *et al.* 2000).

A normal intervertebral disc consists of a homogeneous gel of collagen and proteoglycan and transmits a uniformly distributed load, whereas disc degeneration changes the isotropic characteristics of the structure of the disc (Krag *et al.*1987). A degenerated disc consists of a non-homogenous mixture of fragmented collagen, fluids and, in some cases, gases.

The non-homogeneity of the structure of the degenerated disc causes high-load spots that are considered a precursor to lower back pain. Two methods are used in the assessment of the intensity of pain: the visual analogue scale (VAS) and the four-point category scale. The VAS method is considered to be more sensitive than the discrete points of the category scale. When the VAS method is used patients are asked to indicate on a 100mm long line, marked “least possible pain” on the left-hand side and “worst pain possible” on the right-hand side, how intense the pain is (Collins *et al.* 1997).

3.2. Spondylolisthesis

Spondylolisthesis has been described as the forward translation, or slippage, of the vertebra onto the adjacent caudal, or lower, vertebra. Approximately 4% of the US population has spondylolisthesis by the age of 6 years, increasing by 2% in adults (Uysal *et al*. 2012). It is a common cause of back pain and neurogenic claudication, and 15% of people typically require surgical intervention for treatment (Fay 2012).

Degenerative spondylolisthesis generally occurs when the intervertebral disc or facet joints are degenerated. Sagittal orientation has a role in the forward subluxation of the vertebrae which, according to Berven and Herkowitz (2009), is the reason why degenerative spondylolisthesis commonly occurs at the L4-5 level, coupled with the relative stability of the L5-S1 level and the iliolumbar ligaments.

Spondylolisthesis and the resulting neurogenic claudication are important spinal abnormalities to consider as they are indications for posterior dynamic stabilisation. Neurologic claudication, a main cause of severe leg pain in patients, can be treated using a posterior dynamic stabilisation device that decompresses the intervertebral disc and corrects the slippage of the cephalad vertebra onto the cephalic vertebra. In a study by Li *et al.* (2013) on the clinical outcomes of the Isobar TTL Semi-Rigid Rod System (Scient'x, Bretonneux, France) the authors determined that the Isobar corrected spondylolisthesis in most patients, see Figure 18. They also saw a significant decrease in overall mean VAS for leg pain from 7.9 to 2.5, an indication of the treatment of neurogenic claudication.

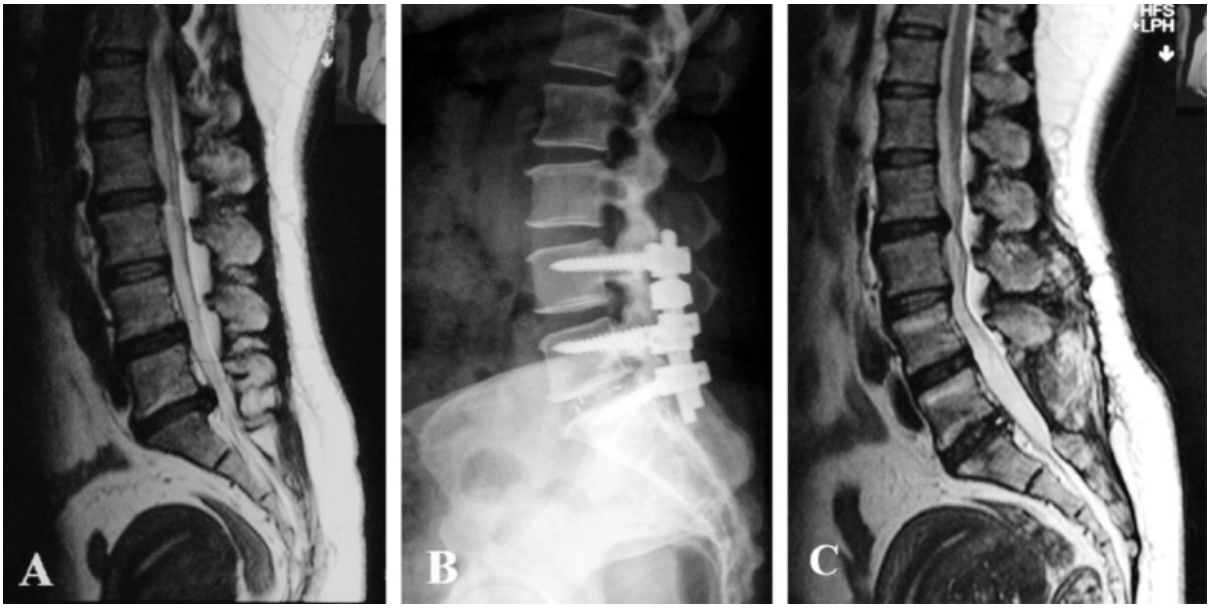

Figure 18: A: Preoperative MRI of a 47-year-old woman with neurogenic claudication, B: Radiograph of instrument level L4-L5 with decompression and the Isobar with adjacent fusion and interbody cage at L5-S1, C: Postoperative MRI showing corrected curvature (Li *et al.* 2013)

Fay *et al* (2013) studied the clinical outcomes of the Dynesys (Zimmer Spine, Minneapolis) for the treatment of spondylolisthesis. They also saw a significant decrease in overall mean VAS for leg pain from 7.4 to 2.5. Pre- and postoperative radiographs of the Dynesys implanted in a 75-year-old man are shown in Figure 19; note how the degree of spondylolisthesis has been decreased.

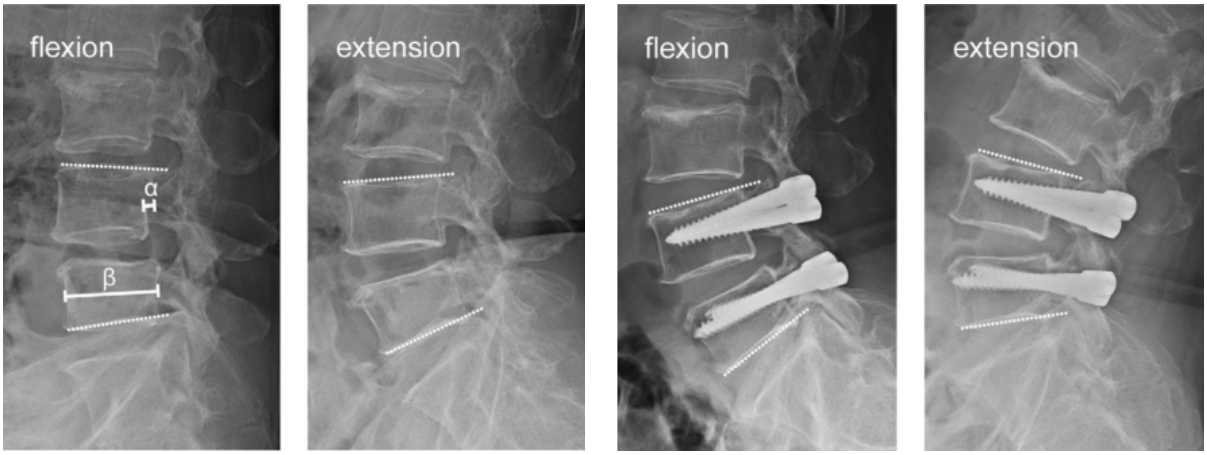

Figure 19: Pre- (A) and postoperative (B) radiographs of the Dynesys implanted showing the decrease in the degree of spondylolisthesis (Fay *et al.* 2013)

3.3. Spinal Stenosis

Lumbar spinal stenosis (LSS) is the compression of the ischaemia of the nerve roots by the osseous, ligamentous or discal structures of the spine (Kobayashi 2006). The spinal cord is compressed through a narrowing of the vertebral canal. Spinal stenosis occurs as a result of degenerative hypertrophic lesions of the facet joints and ligament flavum, or due to intervertebral disc herniation or degeneration (Katz *et al.* 1991).

Patients typically experience leg pain or neurogenic claudication, the latter describing a pain in the buttocks or legs while walking or standing that resolves upon sitting down or a flexion of the spine (Weinstein *et al.* 2008).

Lumbar spinalcanal stenosis (LSCS) is considered one of the most common reasons for spinal intervention (Katz 1995) and is a frequent indication for spinal surgery. The number of people diagnosed with LSCS complaining about lower extremity pain, numbness, and neurological intermittent claudication (NIC) has increased annually (Johnsson 1995).

Diagnosis of lumbar spinal stenosis requires more than imaging techniques; clinicians cannot rely solely on them as computed tomography (CT) and magnetic resonance imaging (MRI)are often unspecific and inconclusive, and generally the symptoms may respond to decompressive surgery (Katz 1991).

3.4. Posterior Element Degeneration

The two posterior facet joints and the intervertebral disc make up the so called 'three-joint complex' and together form a functional spinal unit (FSU). The degeneration of all three joints is significant in spinal degeneration and disease of the intervertebral disc usually precedes facet joint degeneration (An 1999).Facet joints resist extension, axial rotation and shear; excessively high stresses in these movements may cause facet osteoarthritis that may in turn result in spinal stenosis (Wiseman *et al.* 2005).

It is important to understand the mechanism of facet joint degeneration as this condition is generally treated with a facetectomy and discectomy; procedures that inherently destabilise the spine and increase spinal segment motion. This destabilisation is an indication for posterior dynamic stabilisation (Senegas 2002). The Device for Intervertebral Assisted Motion, or DIAM (Medtronic, Memphis, TN), is shown in Figure 20A and is designed to be implanted between the two spinous processes after unilateral partial facetectomy and discectomy in order to decompress the facet joints. In a study by Phillips *et al.* (2006) the authors investigated the biomechanical effect of the DIAM on the lumbar spine, using a cadaveric spinal segment as illustrated in Figure 20B. The study suggests that the DIAM device is effective in restoring normal spinal segmental motion, except in axial rotation. The device decompresses the facet joints, but this decompression, coupled with the device's poor transverse stiffness, meant that the now-distracted facet joints could no longer resist axial rotation correctly.

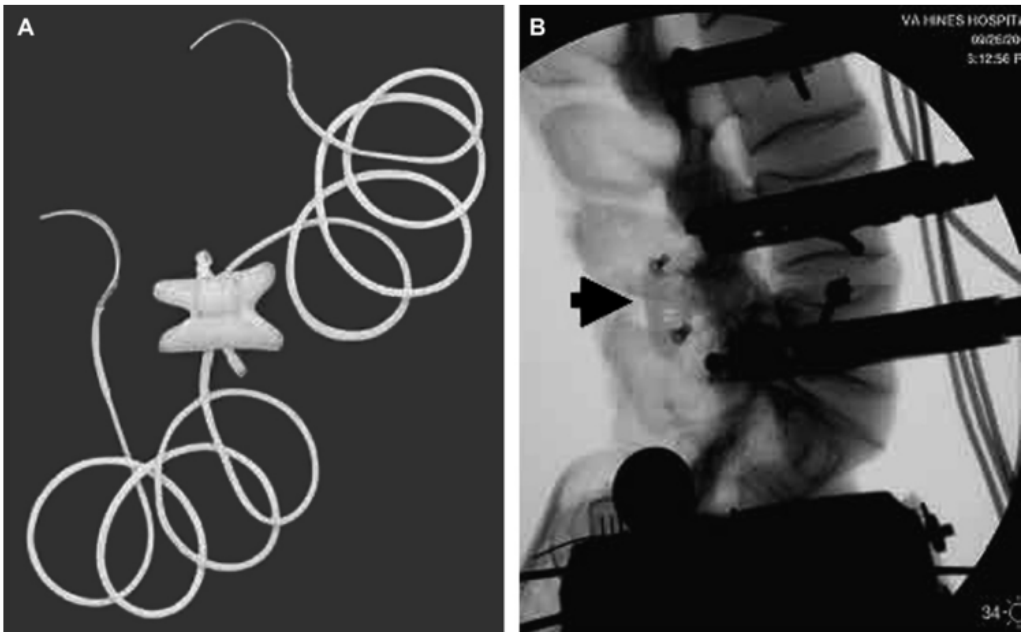

Figure 20: A: The DIAM device, B: The device implanted in a cadaveric spine (Phillips *et al.* 2006)

3.5. Treatment of Lower Back Pain

Chronic lower back pain s caused by instability of the spinal segment, which is secondary to disc degeneration (Lau *et al*. 2007). Lumbar spinal instability is defined as the spinal column losing its ability to maintain its natural pattern of displacement under loading (Haher *et al.* 2001).

The most common treatment methodologies for pain stemming from spinal disorders have evolved into lumbar discectomy and lumbar fusion. Figure 21 illustrates the various treatment options currently available for neck and back pain.

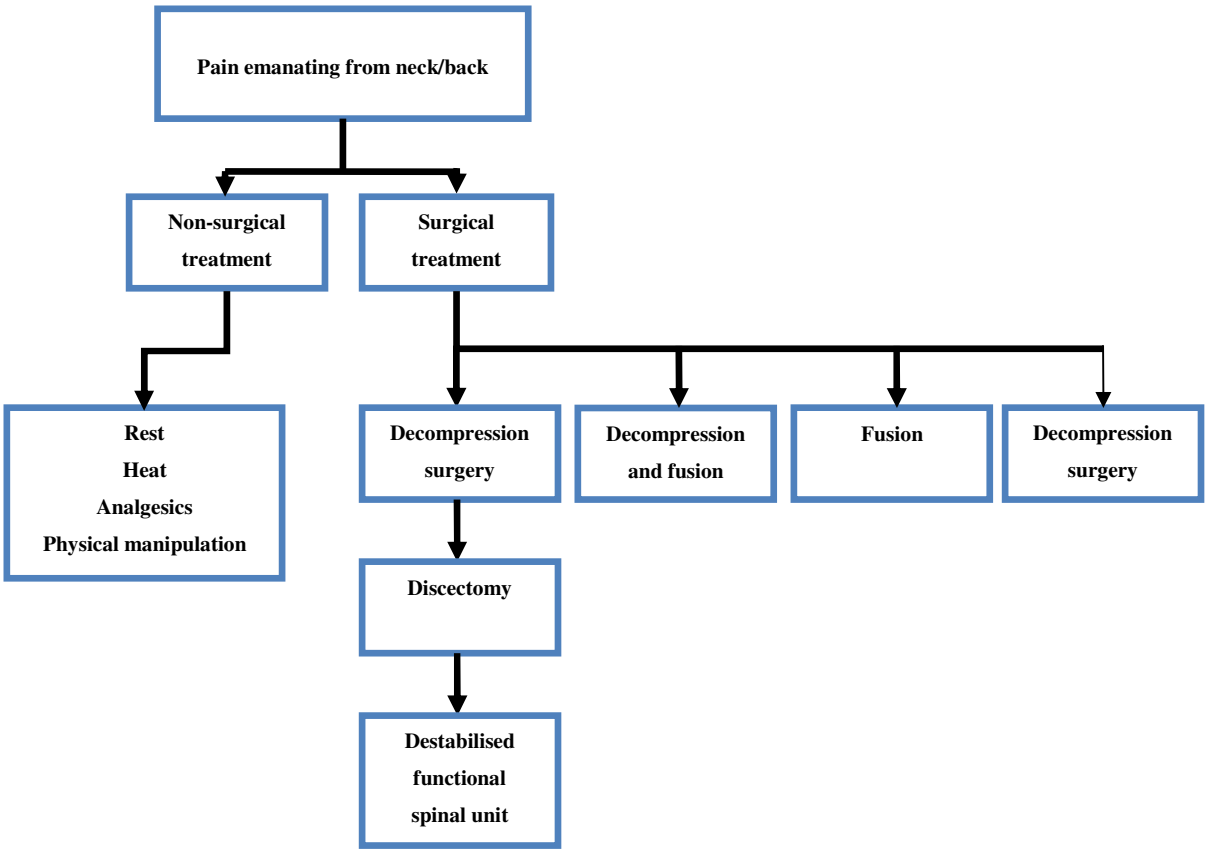

Figure 21: Treatment modalities for neck and back pain

Discectomy is a frequently performed surgical procedure and involves the partial or full removal of the intervertebral disc. The outcomes of a discectomy are measured regardless of the amount of IVD that has been removed. Discectomies also induce segmental instability and result in abnormal pathologic motion, by changing the structure of the disc and hence the load-transferring capabilities, and also increase facet joint loads. Arthroplasty or interbody fusion cages are usually inserted after a discectomy.

According to Lau *et al.* (2007) fusion has been the traditional method for stabilisation of the spinal segment. However, due to the incidence of adjacent segment disease, treatment options have developed into motion preservation devices such as arthroplasty, facet replacement and dynamic stabilisation (Barrey *et al.* 2008).

3.6. Conclusion

Lower back pain may be temporary or chronic; treatment modalities range from physical manipulation to decompression surgery and fusion. Surgery should only be considered as a last resort if responses to non-surgical treatment prove ineffective.

A number of spinal disorders qualify as indications for dynamic stabilisation. Spondylolisthesis is a primary cause of spinal nerve root impingement and neurogenic claudication; causing leg pain. Dynamic stabilisation can correct this condition by correcting the subluxation of the vertebra and restoring the lordotic angle of the functional spinal unit. Spinal stenosis is another abnormality that is indicated for lumbar dynamic stabilisation and can be a result of posterior element degeneration; the compression of the spinal nerves is also corrected through restoring the normal height of the intervertebral disc and unloading the facet joints.

Patient selection is imperative and correct diagnosis of the spinal abnormality should be accurately conducted in order for the possible spinal stabilisation procedure to be successful and effective.

Chapter 4: Dynamic Stabilisation

4.1. Rationale for Dynamic Stabilisation

Dynamic stabilisation devices are designed to unload the degenerated intervertebral disc and facet joints while maintaining physiological spinal motion and reducing associated pain (Chao *et al.* 2011). Cahill *et al.* (2012) suggested that the use of a 'transitional', pedicle-fixated rod eliminates adjacent segment problems in a scoliosis proximal construct when placed on the most proximal end.

Dynamic stabilisation devices are also intended to control the neural posture of the treated segment, control abnormal motion of the degenerated segment and modify the distribution of loads in the intervertebral disc and facet joints (Li *et al.* 2013).

In the study by Park *et al.* (2012), the authors compared the in-vivo kinematics of posterior lumbar fusion, discectomy and dynamic stabilisation with the Dynesys device. In this study it was found that the Dynesys device preserved motion at the segment well. In a separate study on the early clinical outcomes of NFix II dynamic stabilisation device (N Spine, Inc., San Diego, California) the authors found that the device decreased the ODI score of the patient group by an average of 13% and preserved 53% of ROM; a patient group of 40 (15 males, 25 females) was studied.

4.2. Designing for Stability

4.2.1. Dynamic Stabilisation Systems versus Fusion Systems

The main goal of posterior dynamic stabilisation (PDS) systems is to restore the normal motion and kinematics of the spinal segment. These devices have been developed to avoid the familiar disadvantages of traditional fusion systems; fusions eliminate mechanical loads anteriorly from accompanying interbody cages and graft, causing pseudarthrosis and osteoporosis through a phenomenon known as 'stress shielding' (Goel *et al.* 1991).

PDS systems are designed to have a decreased stiffness, theoretically allowing more load transfer through the anterior column and enhancing osteogenesis and interbody fusion according to Wolff's Law (Frost 2003).Any posterior pedicle device results in a load-sharing between itself and the anterior column; a less stiff, dynamic device results in anterior compression and posterior traction while a rigid device results in axial pull-out forces at the ends of the device construct (Templier *et al.*1998), this concept is illustrated in Figure 22.

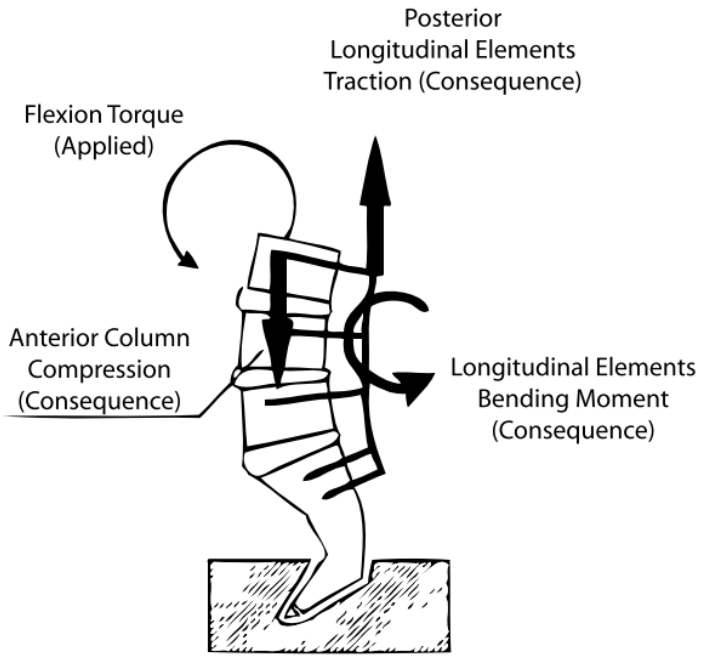

Figure 22: Load-sharing between the device and the anterior column under an applied flexion torque (Templier *et al.* 1998)

4.2.2. Dynamic Stabilisation Stiffness

In order to provide the correct stabilisation of an unhealthy spine, a posterior device must have the correct axial and bending stiffness values to result in the correct ROM during movement.

Schmidt *et al.* (2009) used an extensively validated finite element model (FEM) to predict the stiffness values of a dynamic stabilisation device required in order to stabilise a spinal segment in flexible, semi-flexible and rigid ways. They found that, in order to reduce flexibility of the spinal segment by 30% of that of a healthy spinal segment, the axial and bending stiffness values were relatively low; 45N/mm and 30N/mm respectively. They also recommended choosing appropriate axial and bending stiffness values, for the specific application, from Figure 23 and Figure 24.

In a study performed by Rohlmann *et al.* (2012), an extensively validated FEM was used to simulate 250 variations of a posterior dynamic stabilisation construct in a spine model. The device rod diameter was varied between 6mm and 12mm and the elastic modulus of the rods was varied between 10MPa and 200MPa. The optimised criteria, evaluated through objective functions, included; range of motion, facet joint forces, posterior disc bulges (PDBs) and intradiscal pressures. The authors found that, while taking the PDB into account, 47N/mm was the most ideal axial stiffness. They concluded that, when combining all the criteria with different weighting factors, the most optimised stiffness value was 50N/mm.

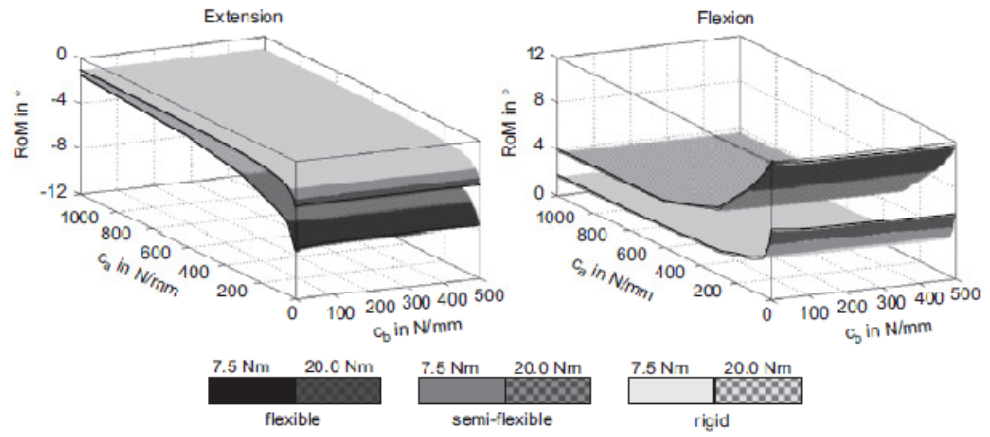

Figure 23: Influence on ROM of axial and bending stiffness values for flexion and extension of the spinal unit (Schmidt *et al.* 2009)

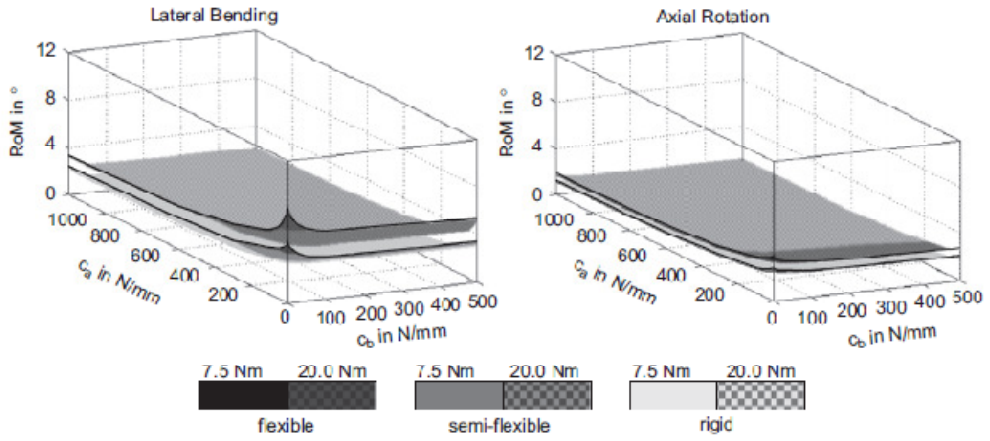

Figure 24: Influence on ROM of axial and bending stiffness values for lateral bending and axial rotation of the spinal unit (Schmidt *et al.* 2009)

In a study by Shilling *et al.* (2011) the authors performed an in-vitro study of the effect on load-bearing and kinematics of the lumbar spinal segment of six different dynamic stabilisation devices. The findings in the study support those of Rohlmann *et al.* (2012) and Schmidt *et al.* (2009) on the effect of the axial and bending stiffness values on ROM in flexion and extension. However, they found that in axial rotation the predominant factors influencing stability, by limiting ROM, may not be limited to axial and bending stiffness values but, in fact, could be more heavily influenced by the shear stiffness values. They pointed out that the Dynesys device, consisting of a cord and a spacer, had the lowest shear stiffness and would have the least stabilising effect transversely as the screw heads would be able to translate easily transversely. The DSS (Paradigm Spine), consisting of a single metal slotted coupler, would have a higher shear stiffness value transversely and would therefore provide more stability in axial rotation.

4.3. Indications and Contraindications for Dynamic Stabilisation

Indications of dynamic stabilisation systems include but are not limited to the following deformities of the lumbar or thoracic spine; degenerative spondylolisthesis with objective evidence of neurologic impairment, kyphosis, and pseudarthrosis (failed previous fusion). According to Stoll *et al.* (2002), indications for posterior dynamic stabilisation devices also include segmental hypermobility, segmental hypomobility and single- or multi-level spinal stenosis.

These devices are also may not be used in the cases of (Paradigm Spine, DSS Instructions for Use):

- Any mental condition
- Any acute, chronic or systemic spinal or localised infections
- Active, metabolic or severe systemic diseases
- Morbid obesity (BMI>40)
- Pregnancy
- Dependency on pharmaceutical drugs
- Severe osteoporosis
- Soft tissue deficit not allowing wound closure
- Pars defect
- Any condition that totally precludes the possibility of fusion
- Inadequate pedicle or vertebral body geometry

4.4. Clinical Results and Device Performance

Li *et al.* (2013) believe that there is a lack of evidence that supports claims that posterior dynamic stabilisation devices avoid adjacent segment disease when compared to classic intervertebral fusion. However, there are clear benefits when using posterior dynamic stabilisation devices, such as range of motion preservation at the treated segment. There are, as expected, complications involved with these devices.

4.4.1. VAS and ODI Scores

In the study performed by Stoll *et al.* (2002) on 83 patients, with various indications and treated with dynamic stabilisation, a significant improvement in ODI scores was observed. In the retrospective study by Li *et al.* (2013) there were significant improvements in VAS and ODI scores in 37 patients treated with the Isobar Semi-rigid Rod (Scient'x, Bretonneux, France). Long-term follow-up VAS

scores changed from 6.3 to 1.1 while back and leg pain VAS scores changed from 7.9 to 1.8. The mean ODI score changed from 46.8% preoperatively to 27.8% postoperatively.

In a study by Canbay et al. (2013) the authors studied the clinical and radiological results of the Cosmic Dynamic Pedicle Screws (Ulrich Medical GmbH). 25 patients, diagnosed with lumbar degenerative disc disease, were included in the study; all patients complained about lower back pain without leg pain. In the 12-month follow-ups of the patients after surgery, 2 patients developed adjacent segment disease (ASD) and after about 2 years both experienced disc hernias at the L5-S1 level, although both patients had Grade 3 degeneration at the L5-S1 level. Table 4 and Table 5 show the VAS and ODI scores, at various stages, of the patients treated with the Cosmic device.

Table 4: VAS scores at various periods of patients treated with the Cosmic device (Canbay *et al.* 2013)

Follow-up point	VAS (out of 10)	
	Median ±SD	Median
Preoperative	7.60 ±1.29	8.00
First year	1.72 ±0.89	2.00
Late period	1.04 ±0.89	1.00

Table 5: ODI scores at various periods of patients treated with the Cosmic device (Canbay *et al.* 2013)

Follow-up point	ODI (percentage out of 50)	
	Median ±SD	Median
Preoperative	57.63 ±16.27	58.00
First year	10.16 ±4.70	8.00
Late period	6.72 ±3.00	6.00

4.4.2. Complications

Due to the non-static nature of dynamic stabilisation devices they are more likely to malfunction in some way when compared with arthrodesis devices, which are static. Mechanical complications and medical complications are discussed separately.

Mechanical Construct Complications

The most extensively studied dynamic stabilisation device in literature is the Dynesys system (Zimmer Spine, Minneapolis, MN). This device, which received FDA clearance in 2004, has had contradictory clinical results, and a number of complications for these types of implants were demonstrated by the Dynesys. The first study involving the Dynesys was performed by Dubois *et al.* (1999).

Mechanical complications of posterior dynamic stabilisation implants may not have a significant influence on clinical outcomes, according to Benezech and Mitulescu (2007), but are important to consider for a device that does not fuse the vertebrae. In their study, they investigated the 45-month

follow-up results of 33 patients treated with the semi-rigid ISOLOCK system. They found 3 cases of screw breakage, 1 of screw cap loosening and 1 of instrument loosening. Stoll *et al.* (2002) also reported that, of the 83 patients treated with the Dynesys system, 10% had screw loosening.

Pedicle screw-based systems generally include a coupler of some sort between the pedicle screws; therefore the screws are effectively constrained in torsion. Because of this, the more clinically relevant failure mode is the pull-out force of the screws (Sanden *et al.* 2001).

Medical Complications

All procedures have associated risks and there are complications that may arise intraoperatively, and general complications include; problems with anaesthesia and allergic reactions among others. Posterior lumbar spinal surgery may cause the following complications intraoperatively (Faraj & Webb 1997, Paradigm Spine DSS Instructions for Use):

- Pedicle fractures
- Cerebrospinal fluid leaks
- Screw misplacement
- Nonunion
- Pain, discomfort
- Degenerative changes
- Metal sensitivity or reactions
- Neurologic injury
- Vertebrae fracture
- Injury to vessels nerves and organs
- Bursitis
- Esophageal perforation
- Hematoma
- Spinal cord impingement
- Paralysis or death

Medical complications that arise due to dynamic stabilisation are common and represent the most important reason for developing these devices.

One of the most common complications of many spinal devices is the occurrence of adjacent segment degeneration (ASD). According to Ghiselli *et al.* (2004) longitudinal studies on lumbar spinal fusions have suggested that the fusion predispose patients to problems on levels adjacent to the fused level including; ASD, increased motion of cephalad adjacent joints and increased adjacent disc compression, both confirmed in cadaveric studies.

In their retrospective study Ghiselli *et al* (2004). determined the rates of ASD, which required either decompression or the insertion of an arthrodesis, to be 16.5% at five years and 36.1% at ten years.

4.5. Conclusion

Posterior dynamic stabilisation devices aim at restoring the normal ROM of the spinal segment. These devices should be designed to have a lower stiffness to allow more load-sharing with the anterior column. This load-sharing should reduce 'stress shielding' and adjacent segment disease.

The ideal axial stiffness values for a posterior dynamic stabilisation device, in flexion and extension, were determined in studies by Schmidt *et al.* (2009), Rohlmann *et al.* (2012) and Schilling *et al.* (2011) to be those below 200N/mm. The authors also concurred that the bending stiffness was negligible when analysing the effect on ROM.

The range of motion at the affected level can be expected to decrease, as the dynamic stabilisation device is intended to limit motion, and this may cause hypermobility at adjacent levels. However, the dynamic stabilisation device is designed to decrease this adjacent hypermobility as far as possible but still relieving the affected level from painful spondylolisthesis and stenosis.

The VAS and ODI scores of the different devices do not vary much; both the Dynesys device and the Cosmic device showed around a 20% decrease in VAS scores in the first year and around a 25% decrease in ODI after the first year postoperatively.

Still more clinical evidence is required to distinguish the benefits of dynamics stabilisation over that of traditional rigid-rid fixation. Dynamic stabilisation devices, with an exception of the Dynesys, are relatively new devices and require more investigation and positive results before they are accepted as the next 'gold standard' in lumbar spinal surgery.

Chapter 5: Biocompatible Materials

5.1. Manufacturing Techniques

Conventional manufacturing techniques, such as computer numerically controlled (CNC) milling, turning and electric-discharge machining (EDM) are currently the preferred methods in manufacturing medical devices. However, other less-conventional techniques are worth considering, as medical device designs can become complex, and could prove to be useful.

5.1.1. Additive Manufacturing

Additive manufacturing, or more commonly referred to as 3D-printing, is a manufacturing process whereby a component is built layer-by-layer by depositing material resin in slices; excess resin is usually cleaned off the part in a chemical bath. 3D-printers use computer-aided design (CAD) software to automatically determine how to construct the desired component (Berman 2012).

Berman also lists advantages to 3D-printing over other manufacturing techniques:

- Cost effective as:
    - There is no scrapping of material
    - Material can be easily recycled for use
    - Manufacturing is automated
    - There is no costly tooling
- Easy to outsource designs
- Easy to modify designs
- Can do a production run of small quantities as though it were for mass production economically

Figure 25: Example of a 3D-printed prototype interspinous process spacer device by Southern Medical

The use of 3D-printing is clearly advantageous in the medical devices industry. Custom implantable devices are easily manufactured specifically for a unique patient to create a perfect-fit device. 3D-printing currently allows the designer to hold a relatively accurate representation of the component that was designed. Figure 25 shows an example of a 3D-printed device, printed from a titanium alloy.

There are, however, concern about the use of 3D-printing currently as the technology is not developed enough to be adopted into everyday manufacturing. There are limitations on what materials can be printed, and materials that are currently printable are very expensive plastics and metals. 3D-printing is also not accurate enough and cannot be considered for components requiring high-precision manufacturing. There are also valid concerns over inter-layer strength, where delamination can occur if a 3D-printed component is load-bearing.

5.1.1. Composite Flow Moulding

Composite flow moulding is a patented process, developed by ETH Zurich, and is commercially applied by Icotec AG in Switzerland. This process is particularly useful when moulding parts made from the continuous, unidirectional carbon fibre-reinforced polymers. These composites are provided in their standard form as pultruded rods. There are three main steps involved in this process, an illustration of which is shown in Figure 26.

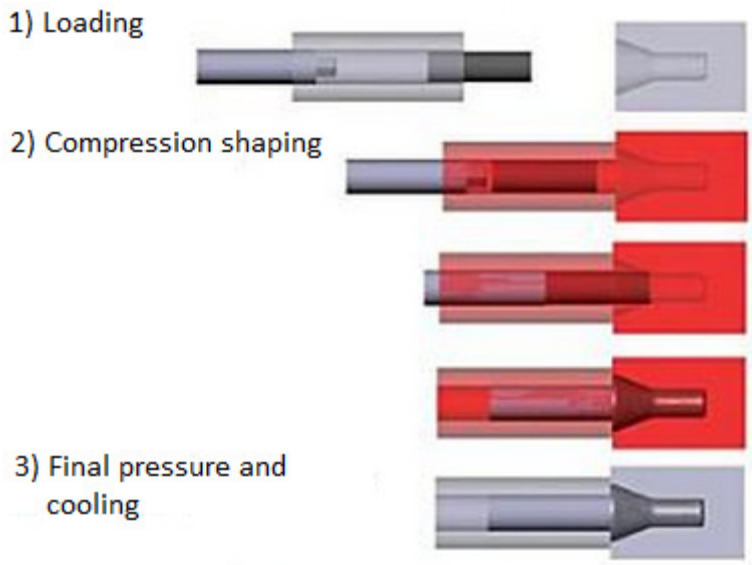

Figure 26: Composite flow moulding process (courtesy of Icotec AG)

In step one the pultruded rods are heated to above the melting point of the polymer matrix inside a heating barrel. This barrel is moved toward a machined steel mould that has a split line that is used to remove the moulded part. Step two involves inserting a plunger, with a significantly high force, into the barrel and forcing the softened rod into the mould cavity. Once the material has taken up the mould cavity the temperature is decreased, in step three, to below that of the glass transition (approximately 143°C) while applying a follow-up pressure.

The advantages of this manufacturing method include the ability of moulding composite polymer parts that contain 60% to 65% volume fraction of continuous carbon fibre. This high volume fraction of carbon fibre results in a material with superb strength and stiffness properties.

Machining these carbon fibre-reinforced polymers can be achieved through relatively conventional methods. The material suppliers recommend diamond-tip tooling in most cases as the material is known to be quite abrasive and may cause significant wear on regular tooling. Machining conditions for normal PEEK and carbon fibre-reinforced (CFR) PEEK, as recommended by suppliers such as Invibio Ltd. (Technology Centre, Hillhouse International, Thornton Cleveleys, Lancashire, UK) are listed in Table 6.

Table 6: Machining conditions for normal PEEK-OPTIMA and carbon fibre-reinforced PEEK-OPTIMA (Invibio Ltd.)

Process	Units	PEEK-OPTIMA	CFR-PEEK-OPTIMA
Sawing			
Clearance angle	°	15-30	15-30
Rake angle	°	0-5	10-15
Cutting speed	m/min	500-800	200-300
Pitch	mm	3-5	3-5
Coolants	Compressed air		
Drilling			
Special instructions	Drill bits experience 'zero velocity' at tip; milling is preferred		
Clearance angle	°	5-10	6
Rake angle	°	10-30	5-10
Cutting speed	m/min	50-200	80-100
Feed rate	mm/rev	0.1-0.3	0.1-0.3
Coolants	Compressed air		
Milling			
Special instructions	Use a five-axis milling machine to achieve a 15° milling angle	Use silicon carbide- or diamond-tipped tooling	Use diamond-tipped tooling
Clearance angle	°	5-15	15-30
Rake angle	°	6-10	6-10
Cutting speed	rpm	<=15000	<=15000
Feed rate	<=0.5mm/tooth		
Coolants	Compressed air		
Turning			
Special instructions	-	Use silicon carbide- or diamond-tipped tooling	Use diamond-tipped tooling
Clearance angle	°	6-8	6-8
Rake angle	°	0-5	2-8
Side angle	°	45-60	45-60
Cutting speed	m/min	250-500	150-200
Feed rate	mm/rev	0.1-0.5	0.1-0.5
Coolants	Compressed air		
Comments	• Tool nose radius >=0.5mm • Internal corners to be filleted with radius >=0.2 • Machine in the direction of carbon fibres for CFR-PEEK		

5.2.Material Selection

In this section various aspects about biomaterials are explored, such as material properties. The selection of material is based on the intended application of the device. The materials should not be considered in isolation; by using different materials together, one may create a hybrid device that combines the advantages of various mechanical and biological properties.

5.2.1. Mechanical Properties

Material properties are important factors that can determine the level of successful integration of an implant. Aseptic loosening of the implant is largely attributed to stress shielding, which is developed due to a large difference in the Modulus of Elasticity between the implant and the surrounding bone tissue (Au *et al.*2007).

Biomaterials are classed into four categories: metals, ceramics, polymers and composites of these. Figure 27compares the Modulus of Elasticity of various biomaterials. Note that PEEK has a Modulus of Elasticity close to that of cortical bone, this means that the amount of stress shielding between the two should be low.

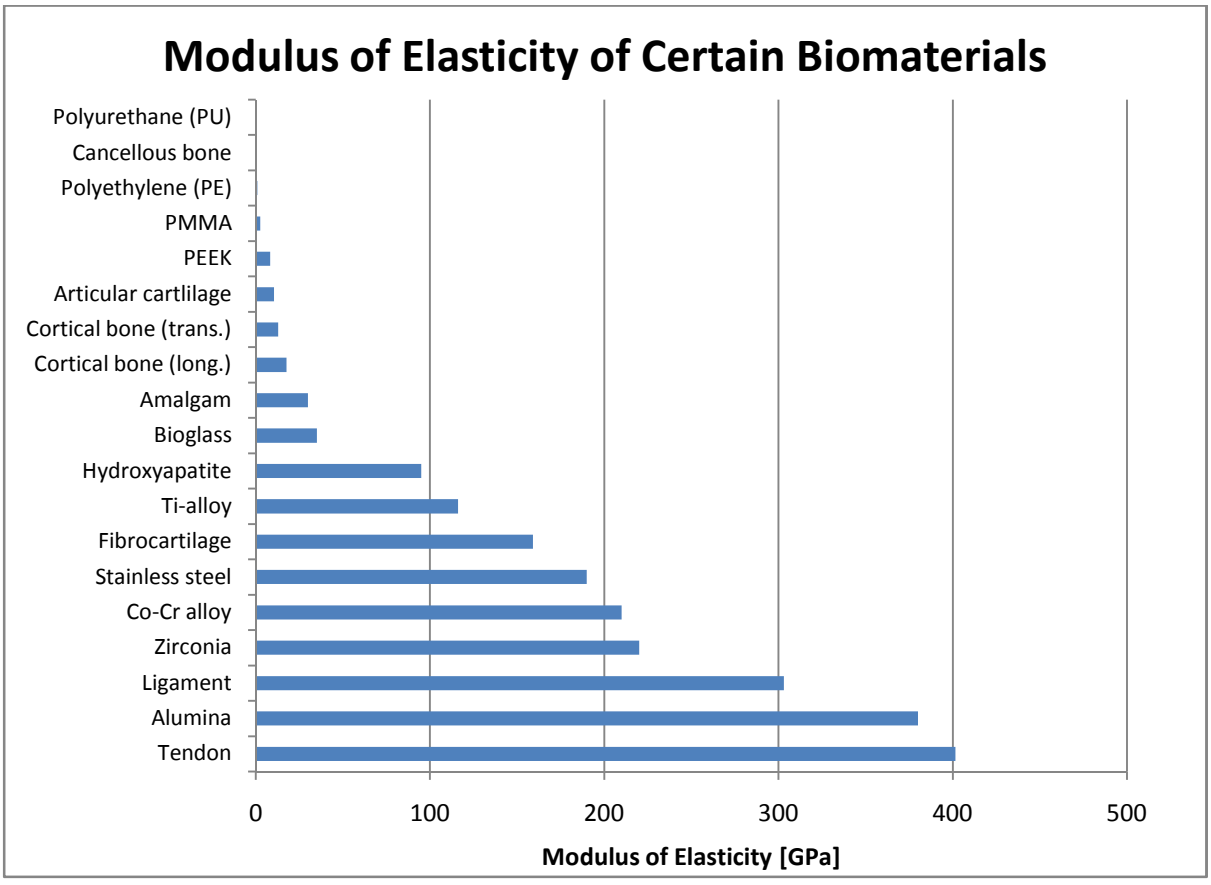

Figure 27: Modulus of Elasticity for a range of biomaterials (Adapted from Ramakrishna *et al.* 2001)

An implant is subjected to mechanical as well as chemical-biological loading components that affect its mechanical properties over time. The implant surface is critically affected by the environmental conditions; such as proteins, which have an impact on the fatigue life of titanium alloy implants (Fleck and Eifler 2010).

5.2.2. Biocompatibility

According to Kiepnafel *et al.* (1999) the extents of the biocompatibility of materials are categorised into the groups bioinert, biointolerant and bioactive. Table 7 lists various biomaterials and their extents of biocompatibility and reactive bone formation, the latter describing the degree to which bone forms adjacent to the implant surface.

Table 7: Metals and polymers and their respective extents of biocompatibility and reactive bone formation

Class	Material	Extend of Biocompatibility	Reactive bone formation	Source
Metals	Co-Cr-based alloys	Bioinert	Contact osteogenesis	Kiepnafel *et al.* 1999
	Stainless steel	Biotolerant	Distance osteogenesis	
	Ti-based alloys	Bioinert	Contact osteogenesis	
Polymers	PMMA	Biotolerant	Distance osteogenesis	
	PEEK	Biotolerant	Intervened osteogenesis	Kurtz and Devine 2007

Metallic biomaterials that are used frequently in orthopaedic implants include alloy of stainless steels, cobalt and titanium. Commercially pure (CP) titanium and Ti6Al4V titanium alloy with extra-low interstitials (ELI) are the two most common and widely used titanium alloys for biomedical applications (Niinomi 2003). The surface properties of titanium alloys, especially CP titanium, are known result in a build-up of a spontaneous, stable and inert oxide layer. The properties that are associated with titanium's biocompatibility are its low electronic conductivity, high corrosion resistance and thermodynamic state at physiological pH levels, among others (Elias *et al.* 2008).

5.2.3. Osseointegration

In order to achieve effective osseointegration, according to Goodman *et al.* (2013), it is critical to develop methods that allow the efficient loading of biomolecules onto the implant surface as well as the controlled the release of these molecules. Kiepnafel *et al.* (1999) describe this primary function as cellular proliferation onto the implant surface.

Screw-loosening is a well-known complication with posteriorly anchored devices, particularly in osteoporotic patients, and is the main cause of the loss of construct stability (Wittenberg *et al*. 1991).

One classical method, in the attempt to increase construct stability, was to inject polymethylmethacrylate (PMMA), more commonly known as bone cement, into the bone before screw insertion. There has, however, been concern about the leakage of cement and subsequent release of monomers into the bloodstream. Another concern expressed over the use of PMMA is the exothermic reaction associated with the polymerisation process of the cement (Feith, 1975).

Presently, the most efficient methods for improving the osseointegrative properties of the implant surface are through surface-modification processes, such as grit-blasting, anodising or applying a porous plasma-coated layer of titanium. Götz *et al.* (2004) have suggested that the laser-texturing of Ti6Al4V, in combination with surface blasting, may be a very 'interesting' technology to consider when specifying an implant surface for the primary function of osseointegration.

The use of hydroxyapatite (HA) coating on an implant surface is another method used when attempting to increase the construct stability. According to Moroni *et al.* (1998), HA coating may improve the bone-metal stability without the disadvantages of PMMA. Studies performed by Sanden *et al.* (2000, 2001) have shown that HA-coated pedicle screws outperform non-coated pedicle screws in terms of bone-metal interface strength.

5.2.4. Wear Resistance

Wear, or fretting, is described by Geringer *et al.* (2006) as a mechanical friction of two surfaces in contact under small displacements in a corrosive environment when moving relative to one another. The degree of wear depends on the amplitude of the displacement and the type of wear mechanism, i.e. stick, partial slip, or full slip.

The environment in which the two surfaces are situated plays a major role in the amount of wear that takes place, the chloride solutions that an implant is exposed to can lead to accelerated wear rates (Duisabeau *et al*. 2004).

5.2.5. Galvanic Properties

Implanting a device that comprises of dissimilar metals, or inappropriately combined metals, can result in galvanic corrosion; understanding the process of galvanic corrosion is critical in selecting combinations of materials that, when implanted, will successfully avoid this problem.

Table 8: Acceptable and unacceptable metal and alloy combinations (Adapted from Shetty 1989)

Dissimilar Metal Combinations	Galvanic
Ti-6Al-4V/Cast Co-Cr-Mo	Acceptable
Wrought Co-Cr-W-Ni/Cast Co-Cr-Mo	Acceptable
Wrought Co-Cr-W-Ni/Forged Co-Cr-Mo	Acceptable
CP Titanium/Forged Co-Cr-Mo	Acceptable
CP Titanium/Cast Co-Cr-Mo	Acceptable
CP Titanium/Ti-6Al-4V	Acceptable
22-13-5 Stainless/316L Stainless	Acceptable
316L Stainless/Cast Co-Cr-Mo	Do Not Use
316L Stainless/ Ti-6Al-4V	Do Not Use
316L Stainless/CP Titanium	Do Not Use
316L Stainless/Forged Co-Cr-Mo	Do Not Use
316 Stainless/Wrought Co-Cr-W-Ni	Do Not Use
22-13-5 Stainless/Cast Co-Cr-Mo	Do Not Use
22-13-5 Stainless/Ti-6Al-4V	Do Not Use
22-13-5 Stainless/CP Titanium	Do Not Use
22-13-5 Stainless/Forged Co-Cr-Mo	Do Not Use
22-13-5 Stainless/Wrought Co-Cr-W-Ni	Do Not Use

Table 8 list combinations of metals and alloys that are acceptable and unacceptable in combination in terms of galvanic reactivity. According to Shetty, galvanic corrosion occurs when two different metals with differing electrochemical characteristics are in contact with one another; an ‘active’ metal in contact with a ‘noble’ metal results in electron transfer from the former to the latter. The ‘active’ metal, losing electrons, oxidises and this is visible as rust and pitting.

Shetty also advises caution, though, as two dissimilar metals that are compatible in terms of galvanic reactivity statically may not be as compatible when there is micromotion between the two. This motion may wear away the protective surface oxide films, changing the corrosion characteristics altogether.

5.2.6. Other Considerations

Radiographic imaging is often used to diagnose the abnormalities of the spine; and the use of carbon fibre-reinforced polymers allows the use of magnetic resonance imaging, X-rays and computed tomography (CT) scans without migrating due to any magnetic-induced torque or force and without creating large imaging artefacts (Scholz *et al.* 2011).

Using non-metallic designs for orthopaedic implants permits the use of magnetic resonance imaging (MRI) without problematic imaging artefacts; stainless steel and aluminium produce large artefacts in radiographic imaging (Ramakrishna *et al.*2001). Titanium creates much smaller artefacts when compared to these metals; and carbon fibre-reinforced polymers created even smaller artefacts under MRI, this is illustrated in Figure 28.

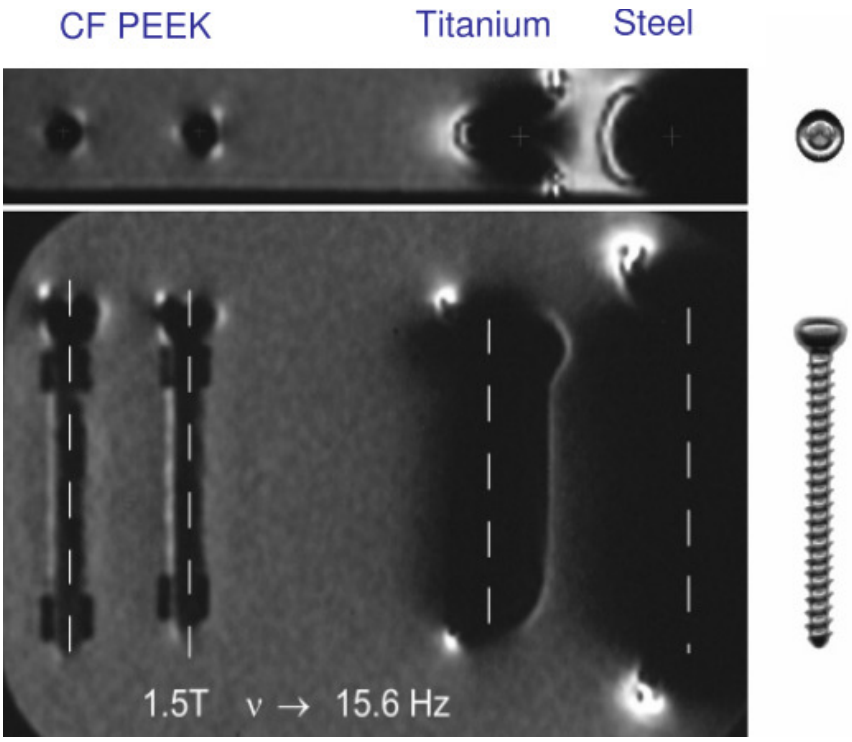

Figure 28: MRI artefacts of screws manufactured from titanium, stainless steel and carbon fibre-reinforced PEEK (Green 2006)

5.3. Conclusion

The selection of material for use in orthopaedic implants must take various factors into account; biocompatibility, mechanical properties, osseointegration and imaging properties. The correct material selection can determine how much load-sharing between the implant and vertebral column takes place.

Titanium is the most widely used implant for osseointegration applications in orthopaedic devices. The use of titanium in primary fixation is popular as it can be used not only as an anchoring screw but it promotes bone growth on its surface. Metals such as cobalt-chrome-molybdenum are also biocompatible.

PEEK is a proven biomaterial and has been extensively used in orthopaedic implants. Composites that use PEEK, such as carbon fibre-reinforced PEEK, have increased stiffness and excellent imaging capabilities; creating small artefacts in MRI images.

Chapter 6: Competitor Products

Motion-preserving devices are categorised into four main types (Serhan *et al*. 2011): total disc replacement (TDR), prosthetic nucleus replacement, posterior dynamic devices, and facet replacement. The latter two are the types of devices relevant to this study as they are usually anchored in the pedicles and are implanted posteriorly.

Table 9 summarises the most popular dynamic stabilisation devices currently being clinically tested. The following design factors are included for comparative purposes; material, fixation method, and type of dynamic coupler.

Table 9: Comparison of competitor products

Manufacturer	Device Name	Regulatory Status	Materials	Fixation Method	Dynamic Coupler	Illustration	Source
Zimmer Spine	Dynesys®	FDA cleared in 2004	Polycarbonate Urethane (PCU), Polyethylene-terephthalate and Titanium	Pedicle screws	Compression of PCU tube	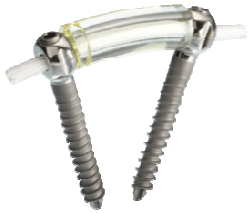	Faye L-Y *et al.* 2012
Graf	Graf ligamentoplasty	Unknown	Titanium, polyester	Pedicle screws	Braided polyester bands	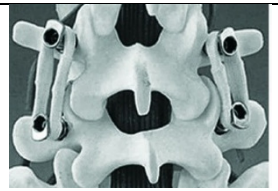	Schroeder *et al.* 2011
N Spine, Inc.	NFix II System	Unknown	PCU and Titanium	Polyaxial pedicle screws	Compression of PCU tubes		Acosta *et al.* 2008
Medtronic	BalanC™	Unknown FDA, CE Marked	PEEK rod, silicone filler	Pedicle screws	PEEK U-shape with silicon filler	 	BalanC™ Surgical Manual
Medtronic	CD HORIZON® PEEK Rod	Unknown FDA, CE Marked	PEEK, titanium markers	Pedicle screws	Flexible polymer	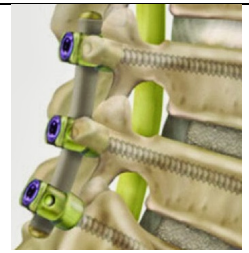	CD HORIZON® Surgical Manual

Manufacturer	Device Name	Regulatory Status	Materials	Fixation Method	Dynamic Coupler	Illustration	Source
Medtronic	CD HORIZON® AGILE™	Unknown - Implant recalled due to failures	Titanium, PCU spacer	Pedicle screws	PCU spacer, central cable	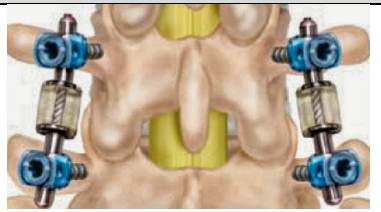	CD HORIZON® AGILE™ Surgical Manual
Medtronic	Device for Intervertebral Assisted Motion (DIAM)	Intend seeking FDA approval	Silicone within polyester jacket	Cables around spinous processes	Silicone "bumper"	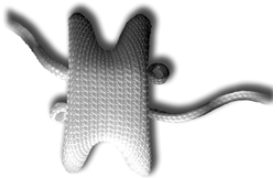	Phillips *et al*. 2006
Medtronic	X-stop®	FDA cleared in 2005	Titanium and PEEK	Side-wings holding spinous process	Spacer		Serhan *et al*. 2011
BioSpine Corp.	BioFlex	Unknown	Nitinol shape memory	Pedicle screws	Coil spring		X. Courville *et al*. 2008

Manufacturer	Device Name	Regulatory Status	Materials	Fixation Method	Dynamic Coupler	Illustration	Source
Applied Spine Technologies Inc.	Stabilimax®	FDA study started 2007 (terminated)	Unknown	Pedicle screws	Dual-spring	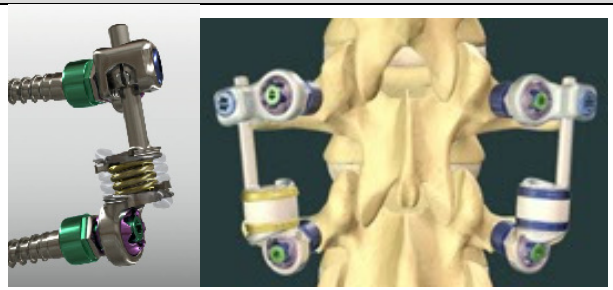	X. Courville *et al*. 2008
Scient'X	IsoBar	FDA cleared (warning letters issued 2010, 2011)	Titanium	Pedicle screws	Flexible rod		Serhan *et al.* 2011
Scient'X	ALADYN[3] Dynamic Plate	Unknown	Titanium	Pedicle screws	Unknown		ALADYN[3] Surgical Manual

Manufacturer	Device Name	Regulatory Status	Materials	Fixation Method	Dynamic Coupler	Illustration	Source
Globus Medical	TRANSITION®	Unknown FDA, CE Marked	Polyurethane, titanium (unknown cord material)	Pedicle screws	Polyurethane bumpers with central cord	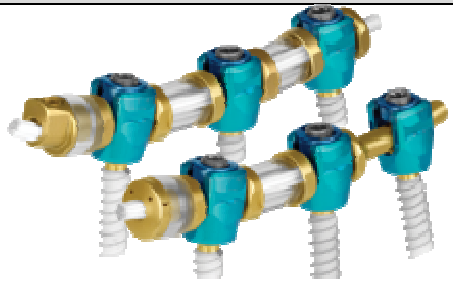	TRANSITION ® Surgical Manual
Globus Medical	AccuFlex	FDA cleared, discontinued	CoCrMo	Pedicle screws	Flexible titanium rod with machined grooves		Serhan *et al.* 2011
Abbott Spine	Wallis System	FDA trials started 2007	PEEK and woven-polymer	Woven-polymer	PEEK interspinous spacer		Serhan *et al.* 2011
Ulrich Medical	Cosmic™	CE Marked	Unknown	Pedicle screws	Hinged pedicle screws for motion	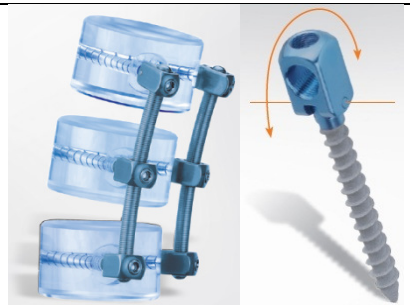	Cosmic Surgical Manual
Paradigm Spine	DSS	Unknown FDA, CE Marked	Titanium	Pedicle screws	Titanium 'spring'	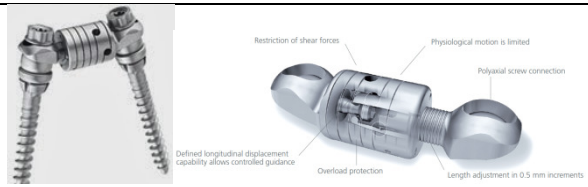	Wilke *et al.* 2009

Manufacturer	Device Name	Regulatory Status	Materials	Fixation Method	Dynamic Coupler	Illustration	Source
Synthes	NFLEX	Unknown FDA, CE Marked	Titanium alloy with polymer 'bumpers'	Pedicle screws	Compression of polymer 'bumpers'	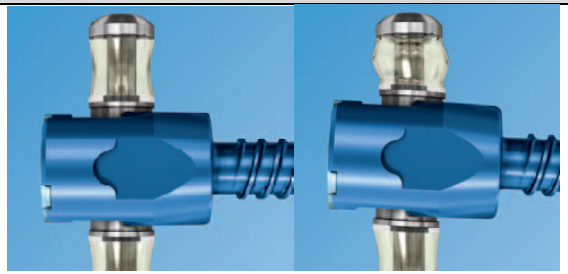	NFLEX Surgical Manual
DePuy	Expedium™ PEEK Rod	Cleared for fusion	PEEK Rod, treated with radiopaque Barium Sulphate ($BaSO_4$) for visualisation. Titanium markers	Pedicle screws	Flexible PEEK rod	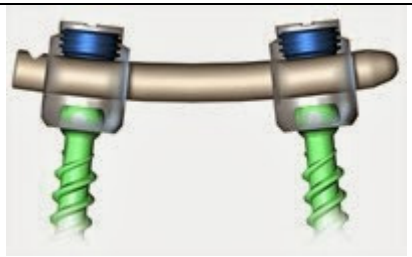	Expedium™ PEEK Rod Surgical Manual
Eden Spine	PERFX-2™	Unknown	Titanium (only known material)	Pedicle screws	Hinged joint, translation and flexion-extension	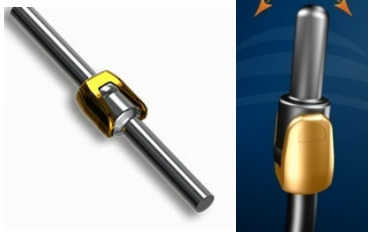	PERFX-2 Surgical Manual
SpineVision	Flex+™	CE Marked	Titanium, polymer sheath, unknown cord material	Pedicle screws	Flexible polymer sheath and tension cord	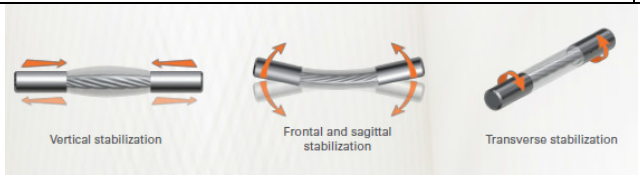	Flex+ Surgical Manual

Manufacturer	Device Name	Regulatory Status	Materials	Fixation Method	Dynamic Coupler	Illustration	Source
Medyssey	WavefleX™	Unknown	Titanium Grade 5	Pedicle screws	Wire-cut wave spring geometry		WavefleX Surgical Manual
Jemo Spine	SPINOFLEX™	CE Marked	Nitinol	Pedicle screws	Pre-formed spring		SPINOFLEX™ Surgical Manual
Jemo Spine	Niti™	CE Marked	Nitinol	Pedicle screws	Flexibility of Nitinol rod		Niti™ Surgical Manual
Jemo Spine	OMEGA™	CE Marked	Nitinol	Pedicle screws	Flexible Nitinol sections	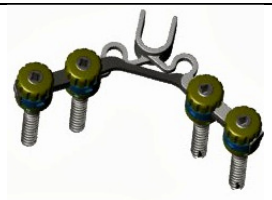	OMEGA™ Surgical Manual

Manufacturer	Device Name	Regulatory Status	Materials	Fixation Method	Dynamic Coupler	Illustration	Source
SpineLab	Elaspine™	Unknown	Polymer	Pedicle screws	Flexible polymer-based rod	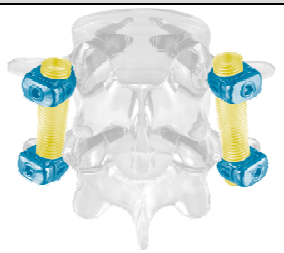	Elaspine™ Surgical Manual

6.1. Material Selection

The material selection for present posterior dynamic stabilisation devices is limited to cobalt-chromium-molybdenum, PEEK, PCU, titanium, nitinol or a flexible proprietary polymer.

Many existing devices have been manufactured from materials that allow a decreased stiffness while also having a good fatigue life.

6.2. Device Constraint

The kinematics of the posterior device should be such that it mimics the natural motion of the joint as closely as possible. In order to do this, the kinematics that should be considered are bending moment and associated displacement, instantaneous centre of rotation (ICR), range of motion (ROM) and degrees of freedom (DOF).

Table 10 lists the considered parameters for flexion/extension and axial rotation of healthy spines, from various sources; the testing method used to determine these parameters is also listed. These parameters are useful in determining loads and displacement inputs for the design of the device.

Table 10: Kinematic parameters of intact, healthy spines from various sources

Kinematic parameter		**Source**									
		Flexion/extension (sagittal plane)								**Axial rotation (transverse plane)**	
		Schmidt *et al.* 2008			Bifulco *et al.* 2012			Xia *et al.* 2010		Cunningham *et al.* 2006	Wachowski *et al.* 2010
Applied bending moment [N·m]		1.5	4.5	7.5	N/A			N/A		N/A	N/A
										N/A	N/A
										N/A	N/A
Mean ICR position [mm]	Level	L4-L5			L2-L3			L2-L3	L3-L4	N/A	L1-L5
	x	≈0	3	9	2.33	9.53	3.61	-19.0	-20.5	N/A	See Figure 29
	z	≈0	-0.5	-1	9.87	9.14	4.81	N/A			
	Relative to	Centre of intervertebral disc			Centre of inferior vertebral body			Anterior edge of superior vertebral body		N/A	
Mean sagittal rotation [degrees]		N/A			7.08	9.95	7.18	N/A		N/A	N/A
Mean sagittal translation [mm]		N/A			3.49	4.16	4.58	-0.3	-0.6	N/A	N/A
Interpedicular displacement [mm]		N/A			N/A			N/A		2.3-2.7	N/A
Healthy spine ROM [degrees]		6 (flexion), 4 (extension), 4.3 (LB), 2.5 (AR)			N/A			N/A		N/A	N/A
Method used		FEM			Fluoroscopic imaging (3 patients)			Model simulation using 3D MRI		In-vitro analysis	3D position-measuring system

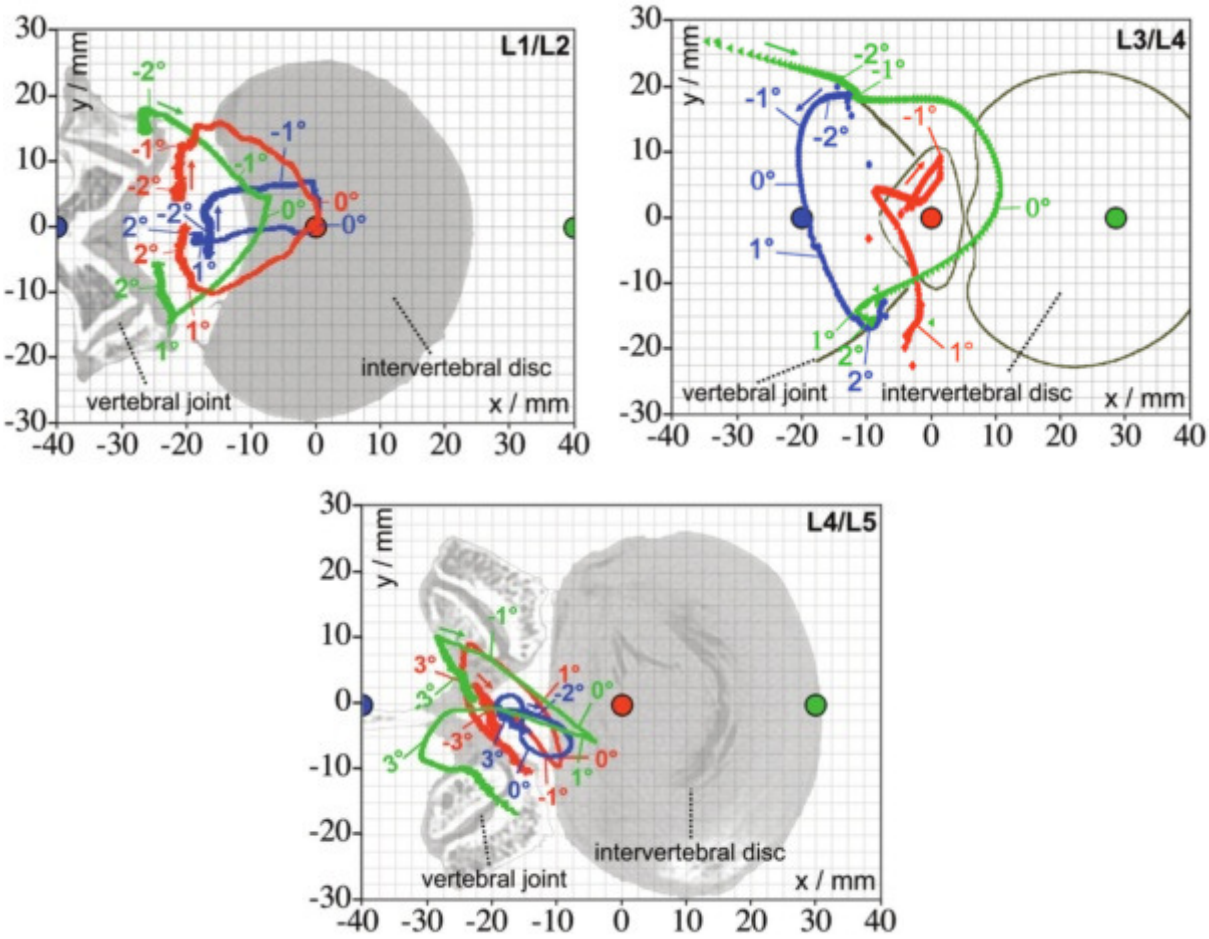

Figure 29: ICR migration during axial rotation for three lumbar segments (Wachowski *et al.* 2010)

Figure 29 illustrates the results of a study by Wachowski *et al.* (2010) in which the authors studied the migration of the ICR for different lumbar segments during motion. Schmidt *et al.* (2009) found that in right lateral bending, the ICR remained close to the sagittal plane under 1.5 Nm, moved 8mm to the right of the sagittal plane under 4.5 Nm and 10mm under7.5 Nm. In axial rotation it was found that the ICR moved toward the compressed facet joint.

6.3. Range of Motion

Table 11 compares the sagittal range of motion (SROM) results after dynamic stabilisation of certain spinal segments. Schulte *et al.* (2008) reported a SROM of 2.0° after Dynesys instrumentation, a 68% reduction from that of the intact spine. Cheng reported a SROM of 1.3° after Dynesys instrumentation, a 75% reduction from that of the intact spinal segments. Meanwhile, Park *et al.* (2012) reported a SROM of 2.1°. The Dynesys system also affects ROMs in the coronal and axial planes. Cheng *et al.* (2007) observed 2.0° of lateral bending and 4.2° of axial rotation which, from the intact spine, is a 61% decrease and a 2.4% increase in lateral bending and axial rotation respectively

after Dynesys instrumentation. Schulte *et al.* (2008) observed 2.2° of lateral bending and 3.3° of axial rotation representing a 70% reduction and a 15% reduction from an intact spine.

Table 11: Comparison of results from various studies of the SROM after dynamic stabilisation

	Motion (SD) [°]			Method of test	Levels measured	Measurement	Loads
	Flexion-extension	Flexion	Extension				
Freudiger *et al.* (1999)	-	4.3 (0.9)	-	In vitro	L3...L5	Magnetic field-based	18.3 Nm
Cheng *et al.*(2007)	1.28 (0.42)	-	-	In vitro	L3-L4	Cameras	6 Nm
Schulte *et al.* (2008)	2.0 (0.8)	1.0 (0.4)	1.0 (0.4)	In vitro	L1...L5	Position sensor	5 Nm
Cakir *et al.*(2009)	4.1 (3.7)	-	-	In vivo	L4-L5	Clinical radiographs	Physiological max.
Kim *et al.*(2011)	3.9 (5.0)	-	-	In vivo	L2...S1	Clinical radiographs	Physiological max.
Park *et al.* (2012)	2.1 (1.3)	1.0 (0.9)	1.5 (1.3)	In vivo	L2...S1	Radiostereometric analysis	Physiological max.

In a study by Jahng *et al.* (2013) the authors a validated FEM model to predict the effect of implanting four different devices; Dynesys, NFlex, PEEK rods and conventional titanium rods in a L4-L5 spinal segment. The results show that the NFlex device showed an ICR closest to that of the intact spine and also showed the largest ROM in comparison with the other devices; 42% in flexion and 56% in extension of that of the intact spine.

The PEEK rod in the study by Jahng *et al.* (2013) demonstrated a ROM in all movements similar to that of the rigid titanium rod system, except in axial rotation where the PEEK rods demonstrated the largest ROM of all the constructs. PEEK rods have recently started being investigated as posterior semi-rigid fixation devices. According to Yoshihara (2013) PEEK rods have advantages over conventional titanium rods. PEEK has a lower elastic modulus, close to that of cortical bone, and would still offer a rigid fusion while transferring more load anteriorly by bending. PEEK would also offer better imaging as it is radiolucent. However, more clinical studies on the use of PEEK rods for spinal fusion are required in order to justify the benefits (Chang *et al.* 2013).

6.4. Methods of Fixation

Primary fixation should be achieved by means of anchoring the implant to the vertebrae. Primary fixation is very common among posterior dynamic stabilisation devices as the pedicle offers the perfect position for placing a screw.

Pedicle screws do have a high incidence in breakage, loosening and bending (Okuyama *et al.* 2001). These incidences have decreased, though, due to the screw shaft diameters increasing, and by tapering the shank of the screw (Ashman *et al.* 1989, Okuyama *et al.* 1983).

Pedicle screws are not suitable for osteoporotic patients as the lack of BMD of the vertebrae results in a higher incidence of screw pull-out or loosening (Hu 1997). In the study performed by Hasegawa *et al.* (2005) the authors concluded that it may be advantageous to coat the pedicle screws with hydroxyapatite (HA) for use in osteoporotic bone. This type of coating may help in stability and bonding between the screw and bone in the early postoperative stage.

Primary fixation should also keep the implant anchored until secondary fixation, or osseointegration, can take place.

6.5. Conclusion

As Table 9 illustrates, there is a wide variety of dynamic stabilisation products in the market already. This makes it difficult to design a unique device. A number of these devices are already FDA-approved, if only as fusion devices, and other devices may be acquiring approval in the next few years.

More recently it has become popular to provide PEEK rods, with claimed advantages being (Ponnappan *et al.* 2009):

- That PEEK would provide a less stiff construct than a conventional titanium alloy rod
- The construct results in reduced stresses at the bone-screw interface
- Improved imaging, reduced scattering and artefacts, due to the radiolucent PEEK

However, clinical results are rare and comprehensive-enough studies are yet to be conducted on the use of these rods (Schroeder *et al.* 2011).

Material selection is currently limited to titanium alloys, PEEK, polyurethane, nitinol and CCM. Enhancements to screw osseointegration surfaces include using PMMA and HA.

The objective of these devices is a common design parameter; reducing the ROM by about 70% by designing the device to have a specific axial stiffness.

Chapter 7: Product Development Process

This research does not cover all the necessary requirements for a medical device to be approved by ISO 13485 standards. Therefore, not all the user requirements for such approval are covered in the scope of this dissertation.

7.1. Design Control

The design control process of a medical device ensures that the end product of the design process is a device that performs satisfactorily when compared to the user requirements. In order to produce such a device verification of the design and validation of the initial device are required. The typical design control process is illustrated in Figure 30.

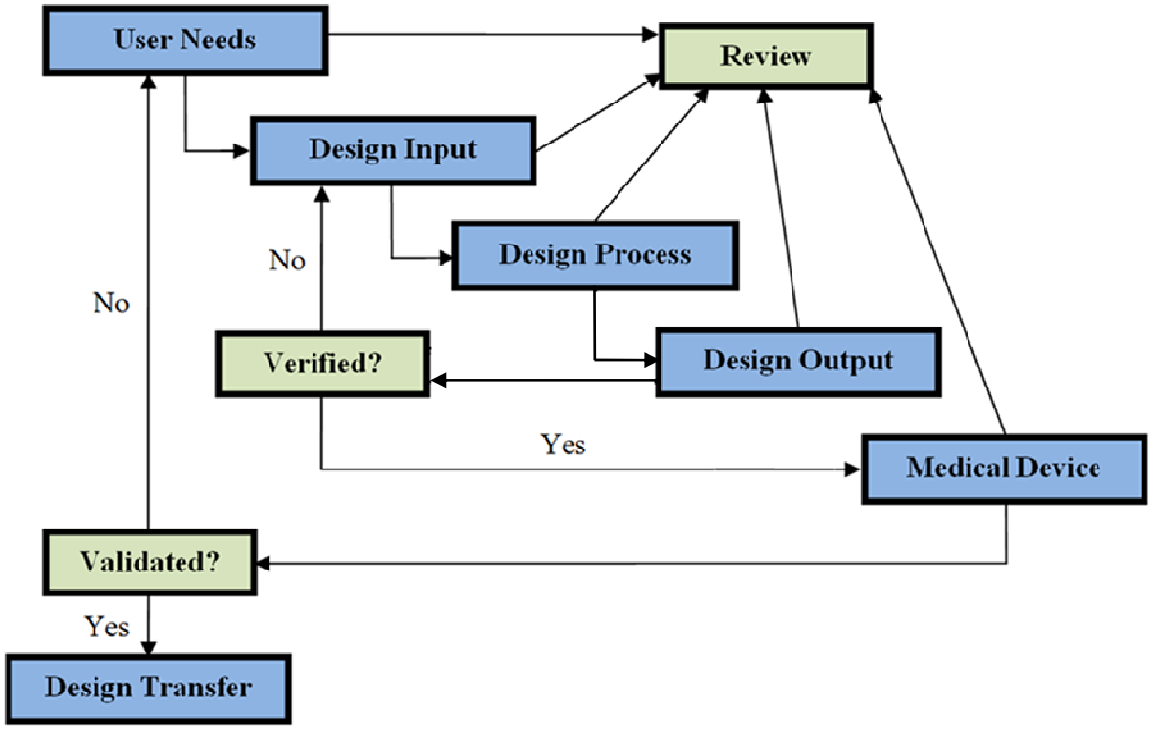

Figure 30: Design control process (adapted from the FDA Design Control Guidance 1997)

From this flowchart the following process is derived and will be followed during the design stage:

1. User needs and intended uses serve as the design initiation
2. User needs are translated into design inputs
3. Design inputs are processed and translated into design outputs

4. Verification of the design outputs ensure that they satisfy the design inputs; by means of a literature review and/or design review
5. If the design outputs are not verified, new design outputs must be generated in the design process
6. Validation of the designed medical device, performed experimentally, ensures that the design satisfies user needs

7.2. User Needs and Design Initiation

The design process begins with a design initiation; this may be in the form of a design request from the user or, in the case of a manufacturer sales team, a formal request for investigation into a certain device design from the sales representatives. In this way the user requirements are communicated and the design inputs are determined for each requirement by the engineering team.

7.3. Design Input

The design inputs for the device are listed in Table 12.

Table 12: Design inputs, outputs, verifications and validations

User Requirements	Design Input	Design Verification/Validation	
User Need/Intended Use	**Design Requirement**	**Verification**	**Validation**
Safety Requirements			
1. Device is biocompatible	a. Device conforms to biocompatibility standards for a permanent spinal implant	Chapter 5.2., Chapter 7.4.2.	2-year clinical follow-up
2. Postoperative imaging is safe	b. Device is safe under MR imaging: heating, force, torque	Chapter 5.2., Chapter 7.4.2.	Clinical experience data
	c. Implant is visible under X-Ray and CT	Chapter 5.2., Chapter 7.4.2.	Clinical experience data
Functional Requirements			
3. Device fits L1-L5 disc spaces between pedicles	d. Provide multiple device lengths	Chapter 7.4.4.	Clinical experience data
4. Device has a satisfactory usable life	e. Device conforms to standards regarding fatigue life	Chapter 7.5.	Clinical experience data and future fatigue tests
5. Device provides a satisfactory amount of spinal segment support	f. Device reproduces the correct stiffness level required for spinal stability	Chapter 7.5.	Clinical experience data
Marketing Requirements			
6. Device is easy to use	g. Use existing posterior fixation instrumentation as far as possible	Surgical procedure comparison with competitor products	Device is compatible with existing instrumentation
7. Postoperative imaging	h. Surrounding anatomy, i.e. adjacent intervertebral discs and spinal cord, to be clearly visible under post-operative imaging	Chapter 5.2., Chapter 7.4.2.	-
Manufacturability Requirements			
8. Device is designed for manufacturability	i. Dimensions and tolerances assessed for ease of manufacturing and cost saving	Chapter 5.1.	Consistent quality throughout each batch of devices manufactured

7.4. Design Output

The start to this design was the stiffness required for a posterior lumbar pedicle-screw-based device to provide sufficient spinal segment support. The design of the device was divided into the following sections:

- Device stiffness
- Material selection
- Primary fixation
- Dynamic coupler
- Connection between primary fixation and coupler

7.4.1. Device Stiffness

The basis of the conceptual design is determining the ideal stiffness of the device. In order to decrease the spinal segment ROM by approximately 40% in flexion and extension, the device must have a certain axial stiffness. As was found in literature (see 4.2. Designing for Stability) the axial stiffness values that affected ROM most significantly were those below 200N/mm, while the effect of the device's bending stiffness was not as significant. A simple calculation is performed in order to obtain an estimated device axial stiffness value.

Using Figure 31 and Figure 23 the following can be determined, assuming a destabilisation of 40% of a healthy spine ROM:

$\beta = 0.6(4°) \approx 2.4°$

And; $\delta = 0.045(\tan 2.4°) = 1.89mm$

$M = F \cdot d$

$\therefore F = {}^{7.5}/_{45 \times 10^{-3}} \approx 166.67N$

$k_{tot} = {}^{F}/_{\delta} = {}^{166.67}/_{1.89} \approx 88.19\ N/mm$

For two springs in parallel: $k_1 = k_2 = {}^{75.76}/_{2} \approx 44\ N/mm$

This axial stiffness result is in agreement with the axial stiffness values determined by Wilke *et al.* in 2009 (50N/mm) and also by Schmidt *et al.* in 2009 (45N/mm) required for a dynamic stabilisation device.

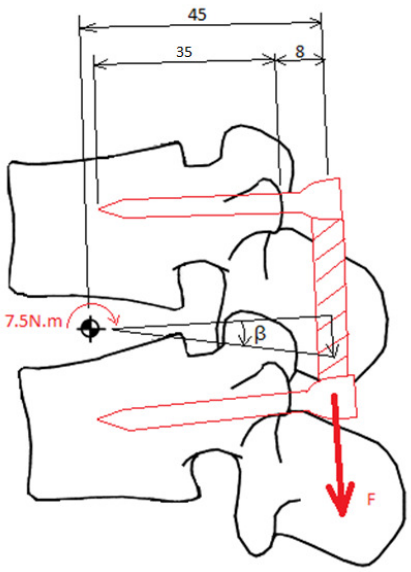

Figure 31: Free body diagram (FBD) to determine device axial stiffness

In a study performed by Cunningham *et al.* (2006) it was found, radiographically, that the average total lumbar spine pedicle displacement was between 2.3mm and 2.7mm. Because the aim of this dynamic stabilisation device is to limit the ROM of the pre-op spinal segment by at least 60%, the range of maximum axial displacement values will be limited to between 1.38mm and 1.89mm, or 1mm to 2mm for flexion. In extension, the compression of the device will be limited to 1mm.

7.4.2. Material Selection

The material of the device is an important factor in obtaining the correct stiffness of the construct. The user requirements of the device; biocompatibility, imaging safety, fatigue properties and stiffness, galvanic properties and manufacturability must all be considered when selecting the material.

The material selection between components that may move relative to one another or are in contact with one another is important. The dynamic coupler may be made from various metallic biomaterials such as cobalt-chrome-molybdenum (CCM) based alloys or the commonly used titanium alloys based on Ti6Al4V with extra-low interstitials (ELI). These two materials, however, should not be used in combination if they components they are manufactured from will be moving against one another as titanium or CCM wear debris, as fine particles, may cause cell damage (Evans 1994). Therefore, in the dynamic coupler, the materials used will either be the one or the other. The connection between the coupler and the primary fixation may, however, include both materials as they were found to be similar in terms of galvanic properties and would not cause galvanic corrosion. Considering performances under fatigue, the dynamic coupler will not include the titanium alloy (Ti6Al4V ELI) as

it is notch-sensitive under cyclic loading; it will, however, be used in the pedicle screws due to its osseointegration properties.

7.4.3. Primary Fixation

The method of primary fixation is achieved by using a constraining mechanism, such as a pedicle screw, to allow for cellular proliferation and osseointegration.

7.4.4. Dynamic Coupler

The dynamic coupler should be designed such that it provides the correct stabilisation for the spinal segment. In order to achieve this stabilisation the device needs to, according to the user requirements; fit in the anatomical space between pedicles, have the correct axial stiffness and allowable displacement to limit spinal segment range of motion.

Table 13 summarises the criteria, as determined in literature and competitor product reviews.

Table 13: Criteria for the dynamic stabilisation coupler

Criterion	Requirement
Coupler length	• <24mm (see Table 12) • Multiple lengths
Coupler stiffness	50N/mm axial (see 7.4.1. Device Stiffness)
Coupler displacement (see 7.4.1. Device Stiffness)	Compression: 0mm-1mm
	Distraction: 1mm-2mm

7.4.5. Connection between Primary Fixation and Coupler

The type of connection between the screw and the dynamic coupler is important as it may determine the level of success of the device. If the connection is not strong enough the cyclic loads experience by the system may lead to loosening of the connection which is a serious failure mode.

There were two types of connections explored; one connection used a top-loading cylindrical clamping method where the dynamic coupler had ends in the form of cylindrical rods that were seated in a U-shaped polyaxial screw head. The cylindrical clamp concept is illustrated in Figure 32; this concept allowed for more misalignment as the polyaxial head could tilt around a ball-joint screw head on the inside just below the U-shape seating. The other connection used a spherical clamp; in this

concept the objective was to ‘wedge’ the components together using spherically-shaped components. This design allows the load to be transferred directly against the screw shank instead of using the cylindrical friction clamp in concept 1. This spherical clamp concept is illustrated in Figure 33.

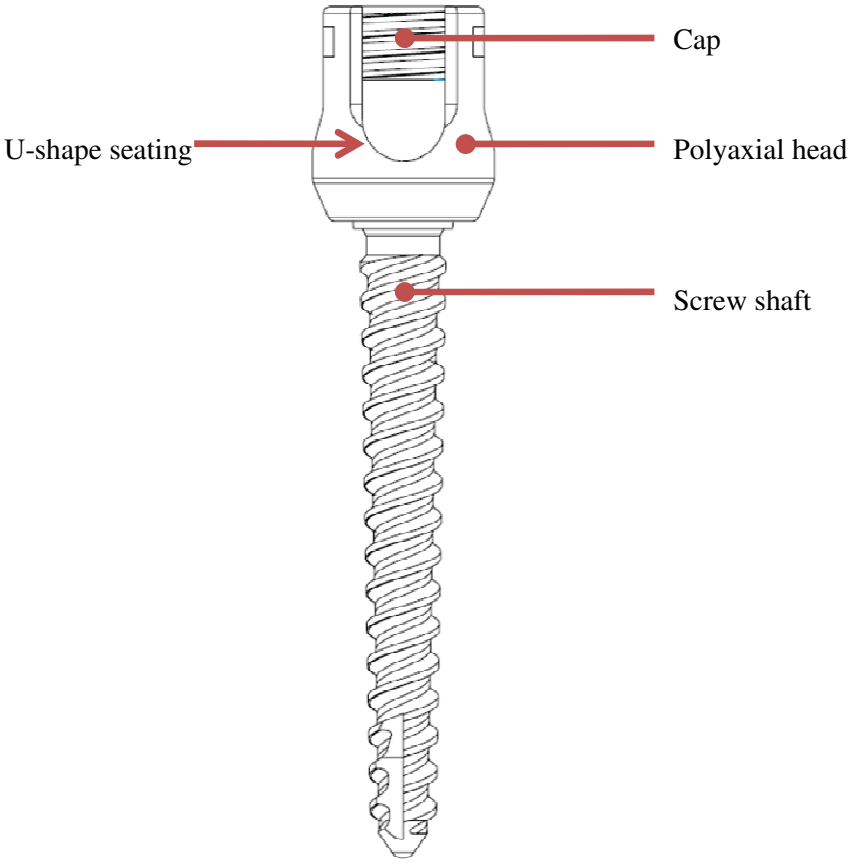

Figure 32: Concept 1; cylindrical clamp connection

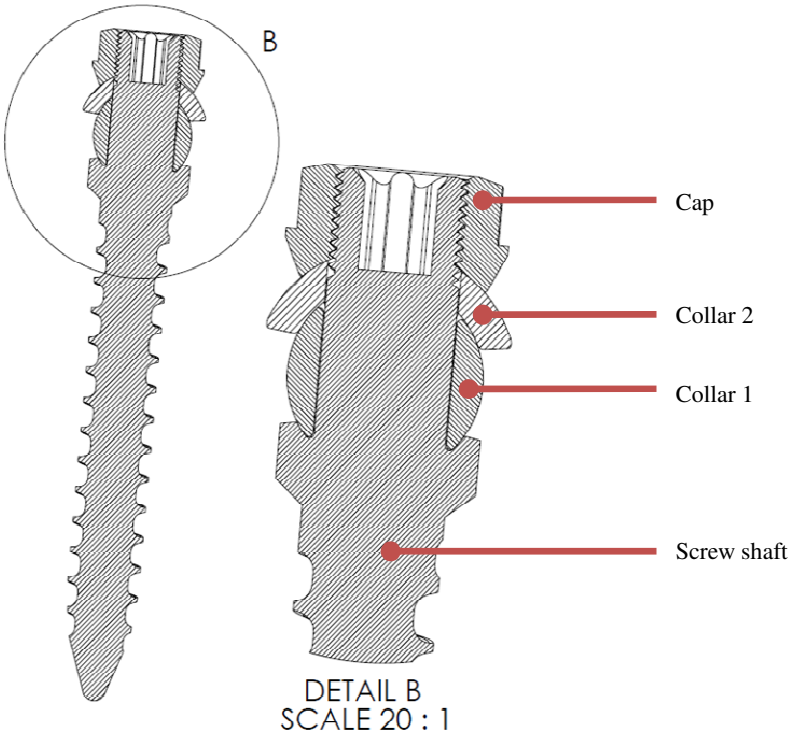

Figure 33: Concept 2; spherical clamp connection

7.4.6. Concept Generation

Concept generation is a creative process whereby a number of ideas are generated and evaluated against a scoring matrix. The design inputs are addressed as far as possible with the design outputs in order to meet user requirements.

The concepts were evaluated using the following criteria, with corresponding weighting; manufacturing complexity (3), surgical technique complexity (3), relative motion of surfaces in contact (10), coupler-screw connection (10), smoothness of motion (10), and fatigue life (10).

The four concepts that were generated between 2012.11 and 2013.08 were considered. The concept from 2013.08 scored the highest out of the considered concepts, however due to financial constraints the concept was not feasible to rapid prototype.

7.4.7. Concept Selection

Concept 2012.11 was selected as it used a dynamic coupler that had both a compression and tension stop to prevent excessive travel. This coupler incorporated a simple helical spring and was also easily customised during the design phase to obtain the required stiffness.

The concept selected is illustrated in Figure 34. The figure shows the detail of the coupler mechanism and associated component materials; a combination of an outer sleeve, an inner sleeve (both of which are to be manufactured from CCM) and the coiled spring. The inner sleeve has a tapered, slotted end with a fine-pitched inner thread and a rim to provide a distraction stop; the slots allow the tapered end to flex inward upon assembly. The inner thread, once it has the male threaded shaft inserted, keeps the rim open and inside the outer sleeve undercut as it is also tapped into the slotted section.

The inner threaded shaft can be turned further in or out depending on the inter-screw length required for the specific patient. The spherical-clamp collars on either end allow for a friction clamp to keep the angle between the dynamic coupler and the screws fixed.

The helical spring component is to be designed such that the number of active coils allows for enough coils to anchor the ends of the spring sufficiently, while saving as much space as possible to fit within the 25mm length limit as specified in the user requirements.

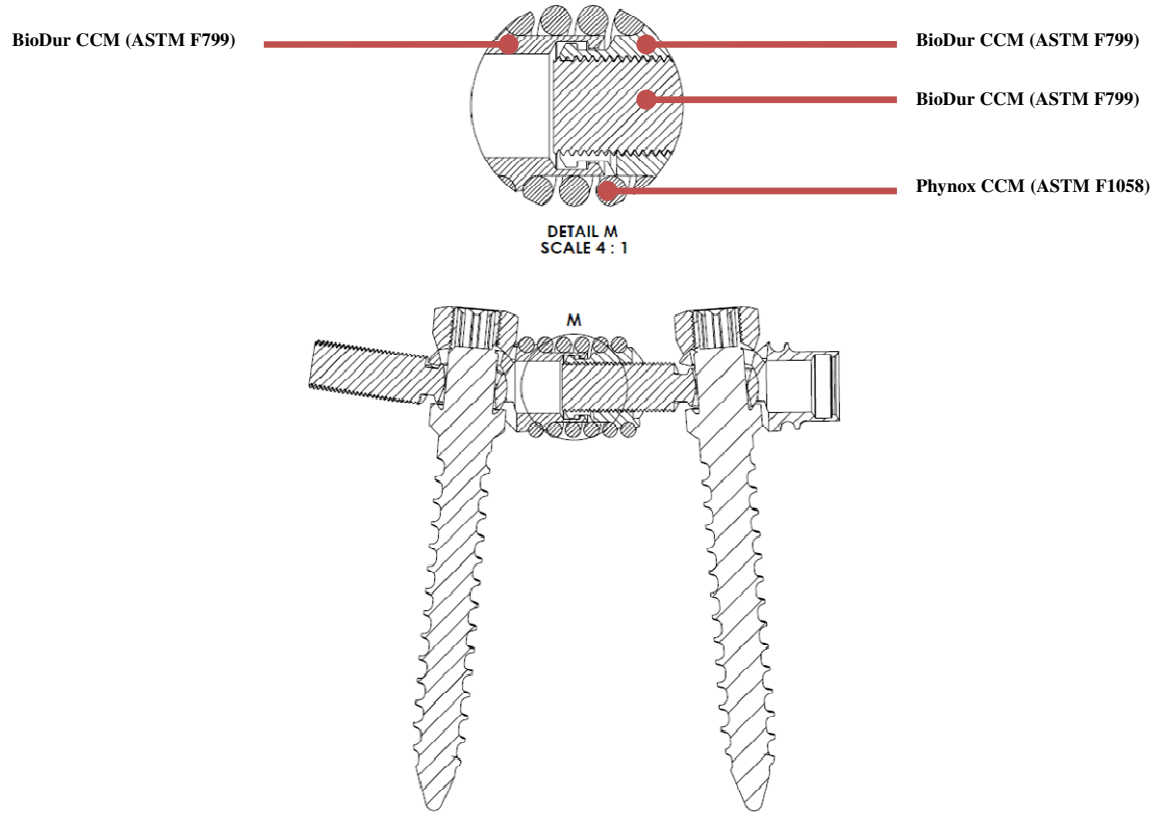

Figure 34: Dynamic coupler detail, prototype revision A-001 (Concept 2012.11)

7.5. Design Verification

Design verification is the process of using reviewed literature, physical testing or calculations to show that the output satisfies the design inputs.

7.5.1. Spring Optimisation

The following optimisation process was followed in determining the ideal spring to design (see Table 13):

1. For a range of outer coupler diameters, explore a range of wire diameters
2. For each wire diameter find the number of coils that satisfy the requirements of 50N/mm spring stiffness (see the spring calculations in Appendix B: Spring Optimisation)
3. Filter the resulting springs with a total free length of less than 24mm
4. Filter the top 30 springs and sort according to shear stress and total spring length
5. Filter the results by removing springs with a relatively high shear stress and length and a least number of active coils
6. Make a final decision on which spring to use from the remaining list

Please see Appendix B: Spring Optimisation for the raw data for this process.

7.5.2. Spring Calculations

The results of the spring calculations are included in Appendix C: Spring Calculator. The resulting spring stiffness values obtained for compression and extension were49N/mm and 25N/mm respectively. The shear stress value calculated, a maximum of 269MPa, is far below the fatigue limit of the material; the fatigue curve for this material is provided in Figure 35.

Using the properties of the material (stainless steel spring wire EN 10270) anticipated for the rapid prototype device the stiffness value calculated for the spring is 25.19N/mm in compression.

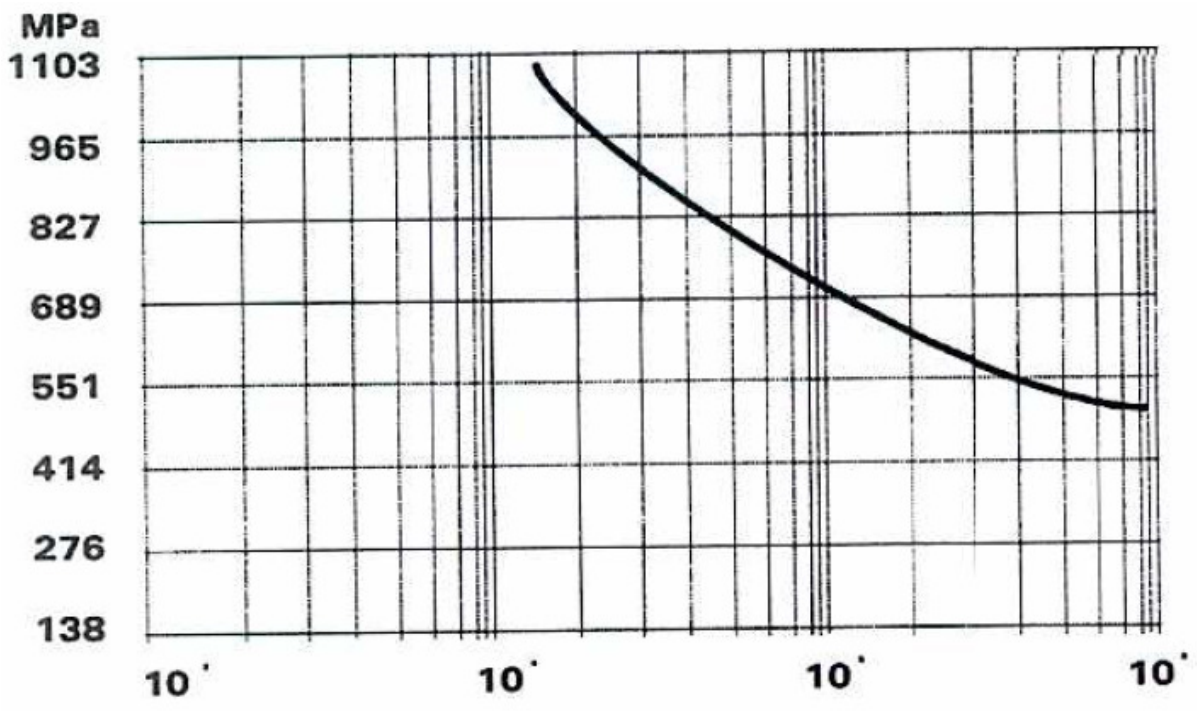

Figure 35: Fatigue curve for Phynox (CCM-based) in the form of a spring, wire diameter 1.5mm (Ugitech: www.ugitech.com)

7.5.3. Finite Element Analyses

In order to verify that the device meets the design inputs it was necessary to simulate the design under typical loading conditions using finite element modelling (FEM). The finite element analyses (FEA) were performed using the SimXpert Student Edition 2012 (MSC Software).

A rendering of the dynamic coupler to be simulated is shown in Figure 36; the coupler is a four-piece device with two collars for pedicle screw anchorage, an inner sleeve that has the axial displacement stops and the actual coiled spring mounted on the one collar and on the inner sleeve. Each of these four components are analysed separately to verify the strength calculations done on them. The components are separately simulated as the Student Edition of SimXpert only allows a limited number of geometry curves, elements and, therefore, nodes allowed for an analysis.

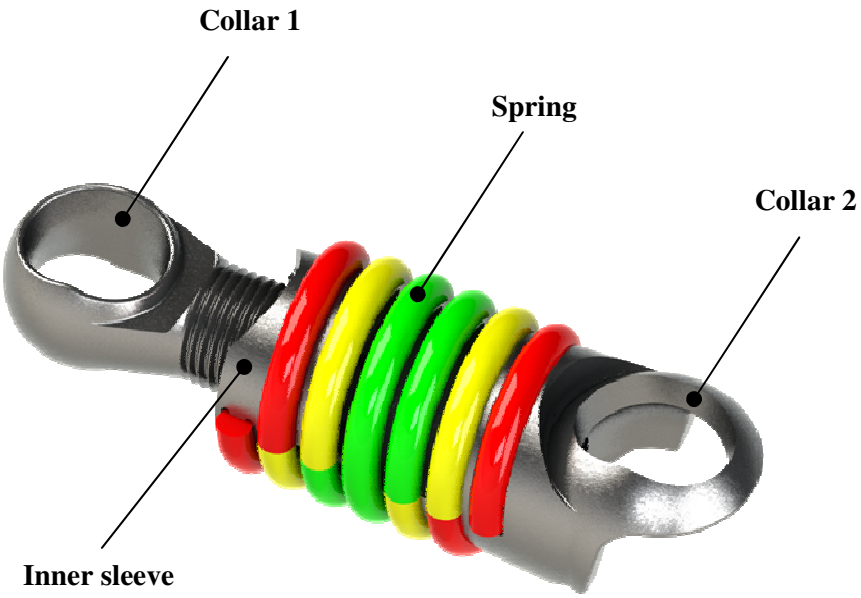

Figure 36: Dynamic coupler

Spring

To verify the spring stiffness a simple model of the spring was analysed. The model incorporated the two active coils as designed for. The spring is to be made from Phynox; as described before this is a CCM-based alloy with excellent fatigue properties.

Simplifying Model

In order to simplify the load case for the spring, a simplifying model was created that simulated the active coils, represented by the green coils in Figure 36. The model was simplified by ignoring the coils that played no part in the determining the stiffness of the assembly; these inactive coils were replaced by solid cylinders so that only the active coils' contributions to stiffness was analysed.

Boundary Conditions

The boundary conditions for this simplified spring model included fixing the circular surface on one end of the spring in all directions, and applying the total load on the other circular surface; these conditions are also illustrated in Figure 37. In the simplified model, 1231 solid quadratic elements were used with the average element size of 6.86mm.

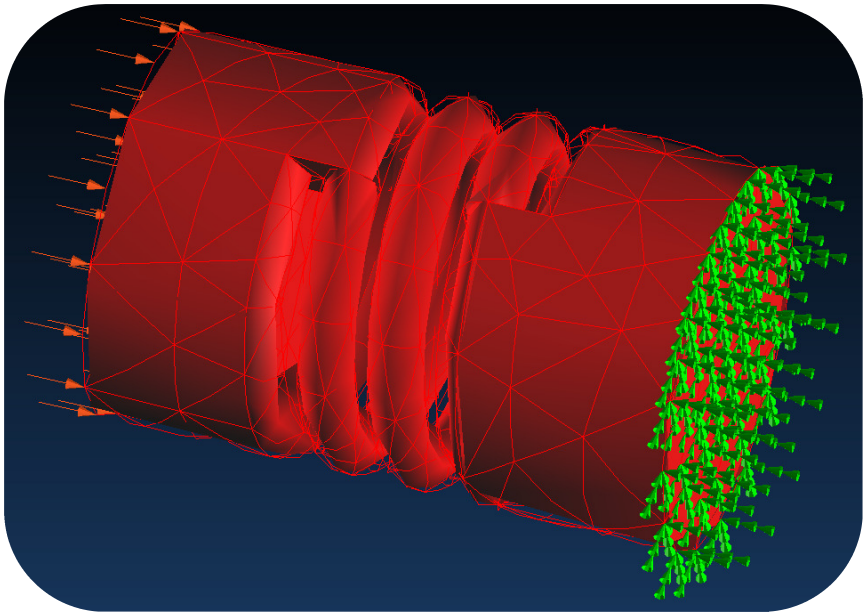

Figure 37: Boundary conditions applied to the model

Simulation Parameters

To simulate the compression of the spring model that incorporated two active coils, the parameters listed in Table 14 were used.

Table 14: Parameters used for the spring FEA

Parameter	Value
Element type	Solid quadratic
No. of elements	1231
Average element size	6.86mm
Young's Modulus	208GPa
Poisson's Ratio	0.3
Shear Modulus	$G = {[0.5(208 \times 10^9)]}/{(1 + 0.3)} = 80GPa$

Results and Discussion

Under the 50N compressive load that was applied to the model the FEA predicted an axial displacement of 1.05mm; this is illustrated in Figure 38. This correlates well with the calculated value of 1mm displacement under a 50N compression load.

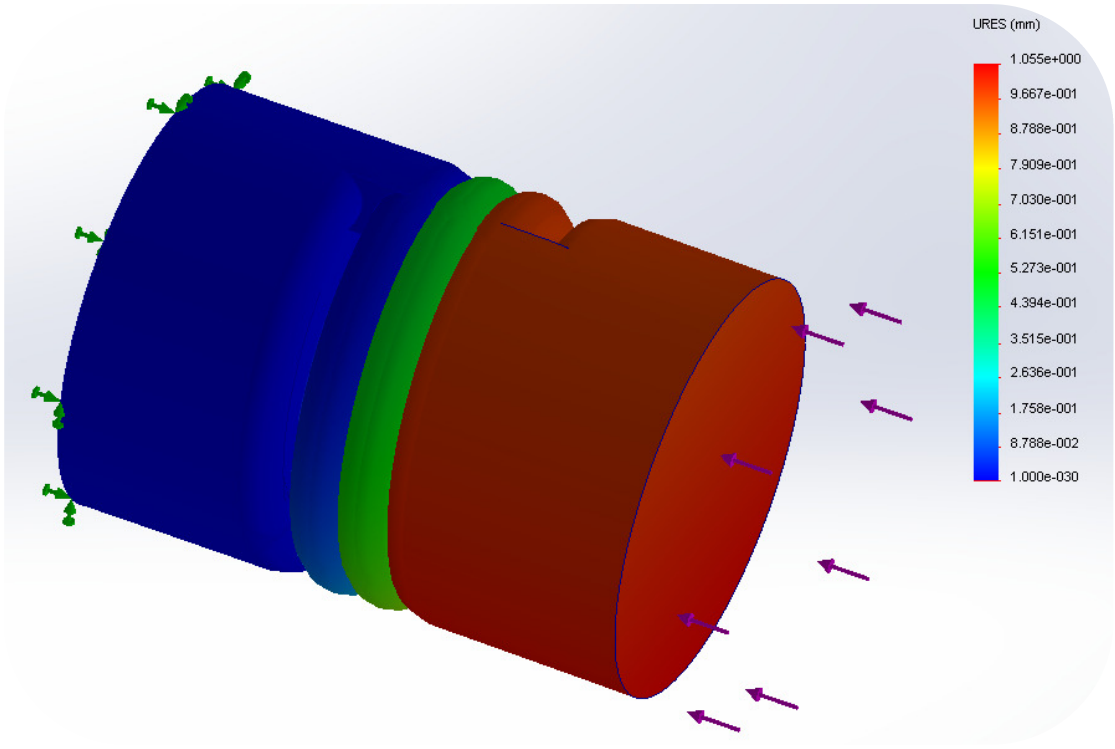

Figure 38: Resultant displacement under a 50N load

Comparison with Other Devices

When comparing the axial stiffness value with that of similar devices, the device is most similar to the DSS™ (Paradigm Spine); 49N/mm was obtained in the calculations, which is almost exactly that achieved by the DSS (50N/mm). In an in-vitro study by Schilling *et al.* (2011) the authors determined the effects of design parameters, or stiffness values, on the kinematics and load-bearing of spinal segments with four different dynamic stabilisation devices and one fusion device. The stiffness values of the devices were measured by the authors and are listed in Table 15.

Table 15: Summary of design parameters, including setup images, of the devices (adapted from Schilling *et al.* 2011)

Description	Image	Axial stiffness [N/mm]	Bending stiffness [N/mm]
Spring tube concept (STC)	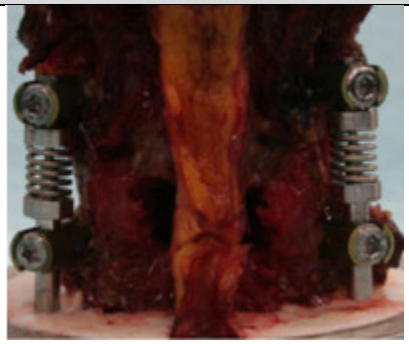	10	15

Leaf spring concept (LFC) or WavefleX™	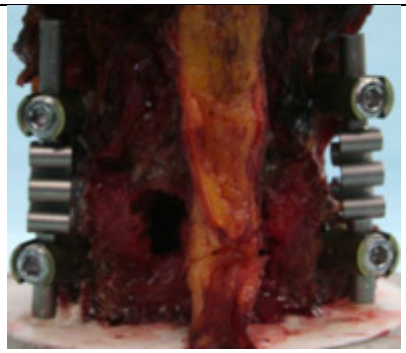	70	3
DSS™	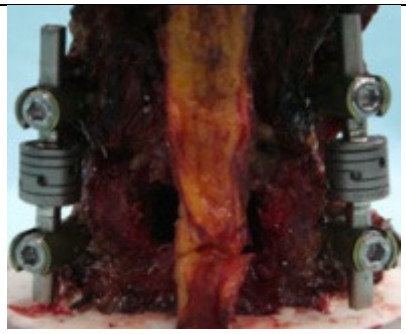	50	5
Dynesys	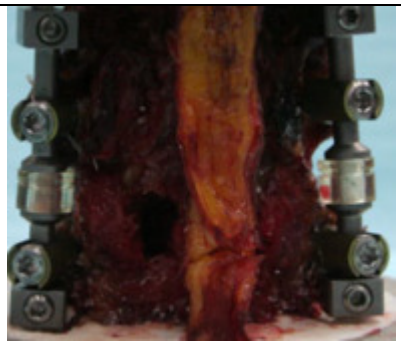	230	6

The authors determined the bending stiffness values using a very simple method; using a sample size of five, the authors clamped the one end of the device and applied a load, 30mm from the clamped end, until the deflection was 1.5mm. To determine the current device's bending stiffness in a similar manner it was only simulated using a finite element analysis (FEA) to get a general idea of the stiffness transversely. The result of this simple simulation is illustrated in Figure 39; note that the load that caused the deflection of the end where it was applied was 7.65N. This resulted in a bending stiffness of 5.1N/mm, very similar to the result of the DSS (5N/mm) in the study by Schilling *et al.* (2011). It is noted that it is challenging to assess the bending stiffness of a dynamic stabilisation device as it may depend on several factors of the design.

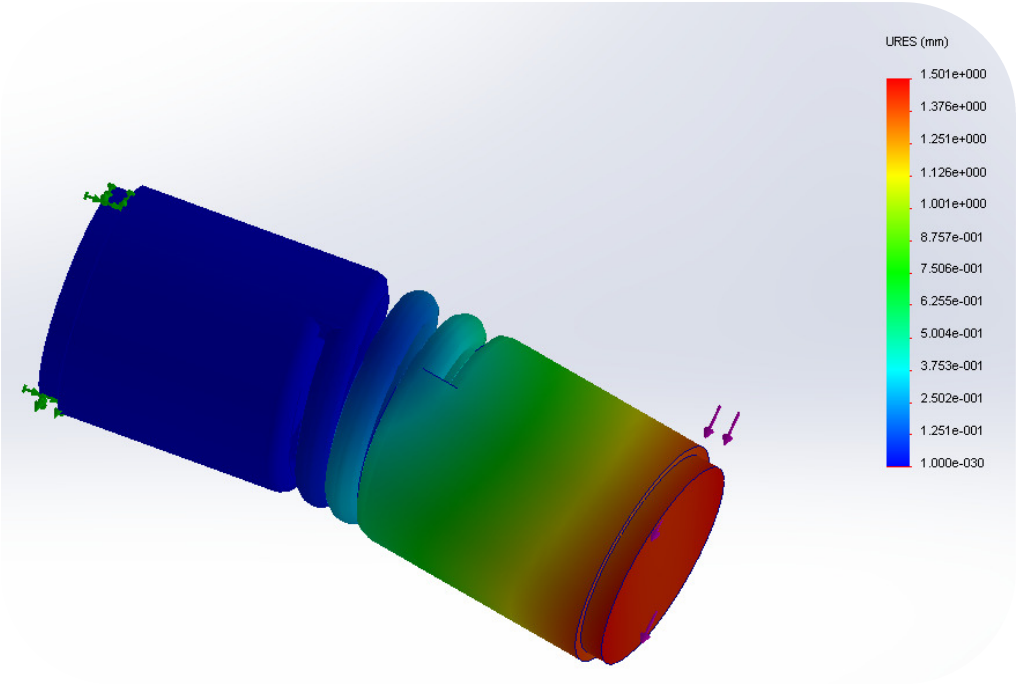

Figure 39: FEA result of a simple bending stiffness of the simplified spring model (using a cantilever length of 30mm)

Spinal Stabilisation and Effect on Kinematics

To estimate what effect the dynamic stabilisation device would have on a spinal segment in terms of kinematics, its comparison with similar devices is used. At this stage of the design process it must be noted that the current design is similar to that of the DSS; showing similar performance in terms of stiffness as discussed before.

In an FEA study by Galbusera *et al.* (2011) the authors used a finite element model of the L2-L5 lumbar spinal segment, by inserting models of pedicle screws and fusion devices as well as dynamic stabilisation devices; the FlexPlus and DSS; at the L4-L5 level to determine the effect of these devices on spinal biomechanics.

The results showed that the two 'dynamic' devices being inserted resulted in a reduction in range of motion of the segments while, compared to the rigid devices, preserved some mobility. The range of motion reductions resulting from each device for flexion and extension are presented in Figure 40 and Figure 41 respectively.

The current device, as it is similar to the DSS, would have a similar effect on the ROM and spinal mobility of that of the DSS. The result of the DSS caused a ROM reduction of about 35% in flexion and 40% in extension. These values are similar to the values initially calculated for the current device; a reduction in ROM of 40% was designed for, see Section 7.4.1. Device Stiffness. It is therefore assumed, because of the similarity between the properties of the current design and those of the DSS

that the current design will meet the user requirements of stabilisation of the spinal segment by the correct amount. It is also noted that in the study by Galbusera *et al.* (2011) that the DSS device also had a comparatively lower increase of adjacent segmental motion, and hence hypermobility, which would lower the likelihood of developing adjacent segment disease.

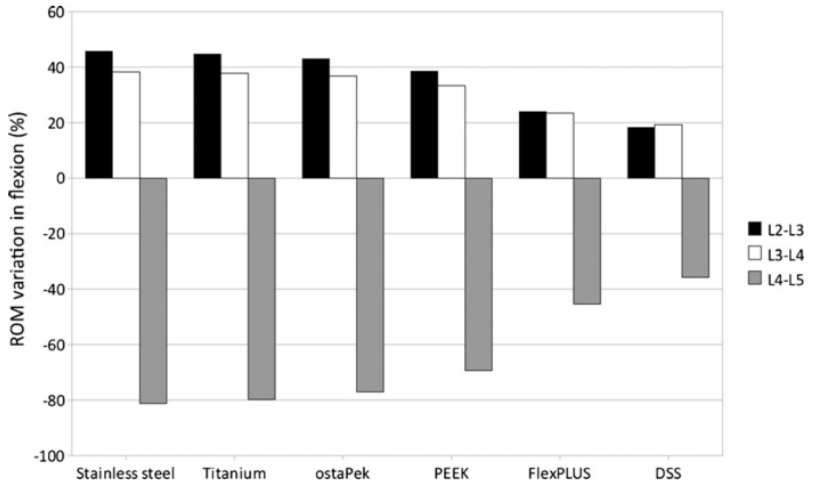

Figure 40: ROM variation for flexion due to the instrumentation at the various spinal segments (Galbusera *et al.* 2011)

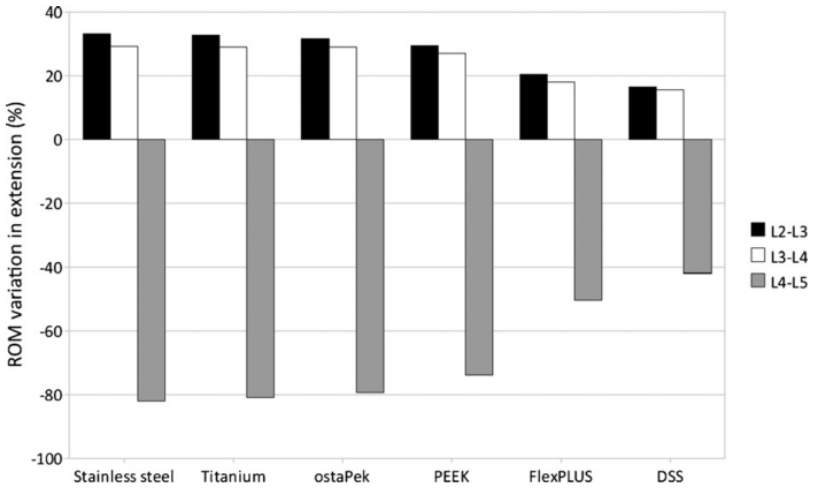

Figure 41: ROM variation for extension due to the instrumentation at the various spinal segments (Galbusera *et al* 2011)

The resultant anterior column loading of the device would also be similar to that of the DSS device. Figure 42 shows the von Mises stress distributions in the intervertebral discs (IVDs) of the models of; the intact spinal segment, the spinal segment instrumented with conventional titanium rods and the spinal segment instrumented with the DSS. Note how the stress in the IVD is higher in the titanium rod as the rods are stiffer. The DSS, a significantly less stiff device, causes a lower stress during flexion when the anterior edge of the IVD is compressed.

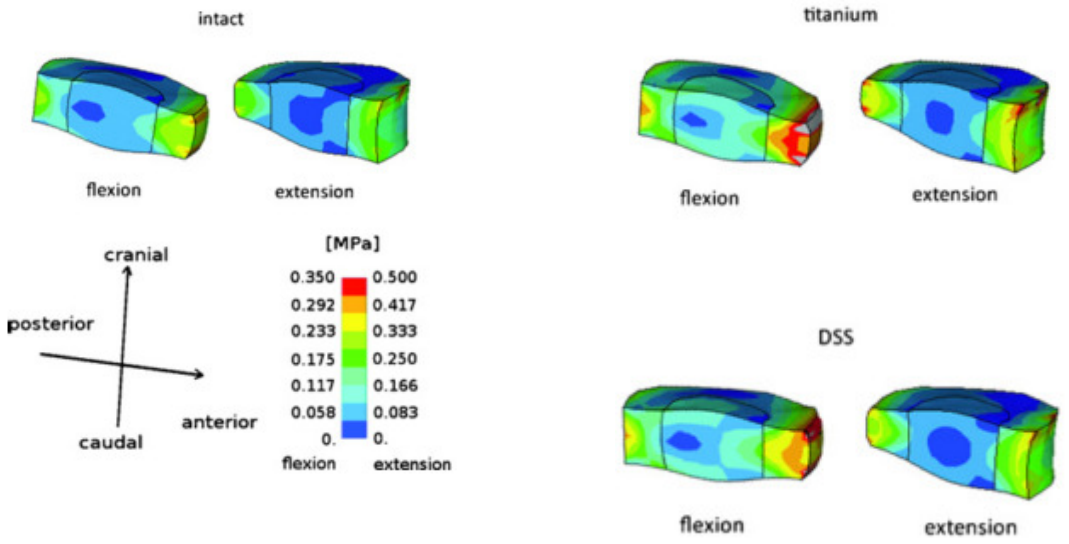

Figure 42: Comparison of von Mises stress in the intervertebral disc of the intact spinal segment, conventional titanium rods and the DSS device (adapted from Galbusera *et al.* 2011)

A device that is too stiff could cause anterior disc bulges and could increase the chances of disc herniations. In a study by Heuer *et al.* (2012) the authors investigate the intervertebral disc loading during all spinal segment motions of an intact spine, as well as with rigid fusion rods and dynamic stabilisation device. The results for flexion from this study are illustrated in Figure 43. Note how the DSS device causes less disc bulging than the rigid fixation rods.

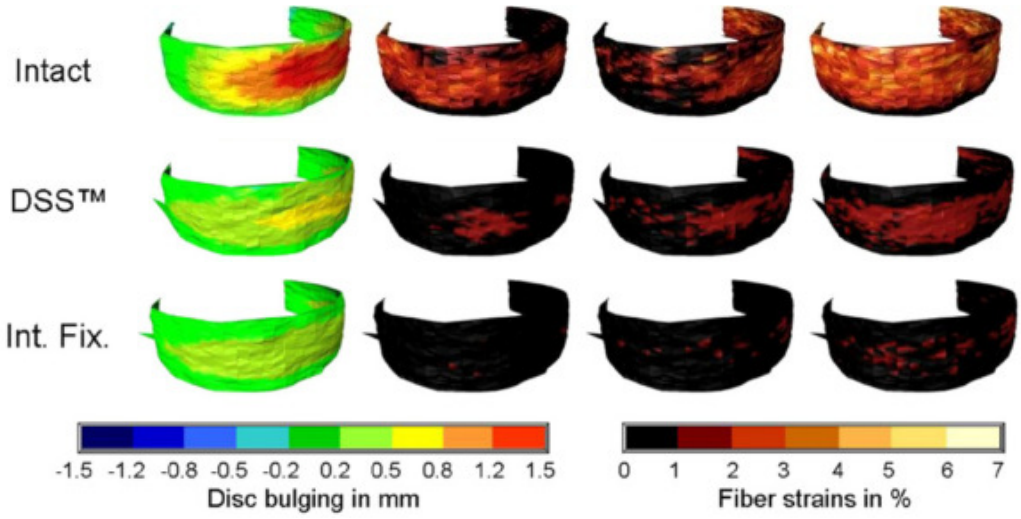

Figure 43: Disc bulging and fibre strain during flexion under 7.5 Nm for an intact spinal segment, DDS-instrumented and fused with rigid rods (Heuer et al. 2012)

Pedicle Screw

The pedicle screw is an important part of the dynamic stabilisation device and can determine whether or not the device fails. The stress under the dynamic loading was determined using a FEA and this result was then verified using fundamental calculations. The parameters used in the FEA of the screw are listed in Table 16.

Parameters and Boundary Conditions

The parameters used for the FEA of the pedicle screw are listed in Table 16. The boundary conditions included fixing the screw thread in all directions and applying a total load of 100N to the screw shank where it is anticipated the load would be transferred to through the collar of the device; collar 1 in Figure 36.

Table 16: Parameters used for the screw FEA

Parameter	Value
Element type	Solid quadratic
Young's Modulus	104GPa
Poisson Ratio	0.34
Shear Modulus	$G = {[0.5(104 \times 10^9)]}/{(1 + 0.34)} = 38.8GPa$

Results and Discussion

The results predicted by the FEA show that the maximum von Mises stress in the screw is about 38.66MPa and occurs on the root diameter at the top of the screw thread; shown in Figure 44. The resultant displacement where the load is applied is about 1.7×10^{-3}mm; shown in Figure 45.

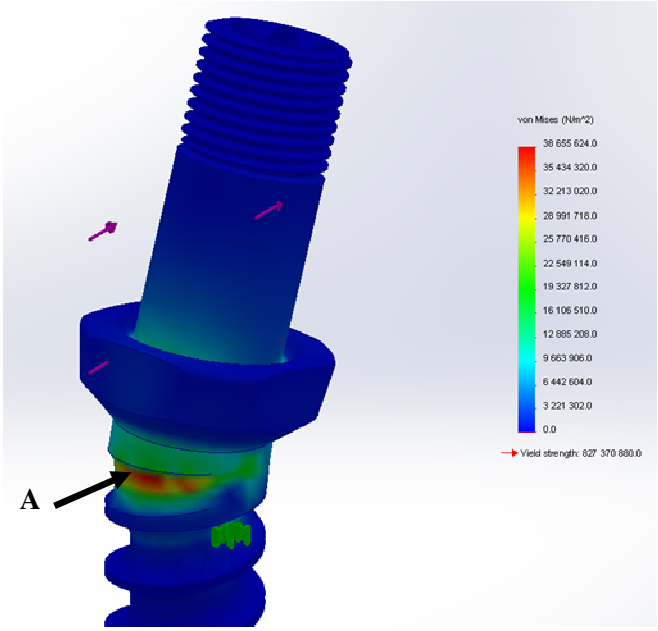

Figure 44: Von Mises stress of the pedicle screw

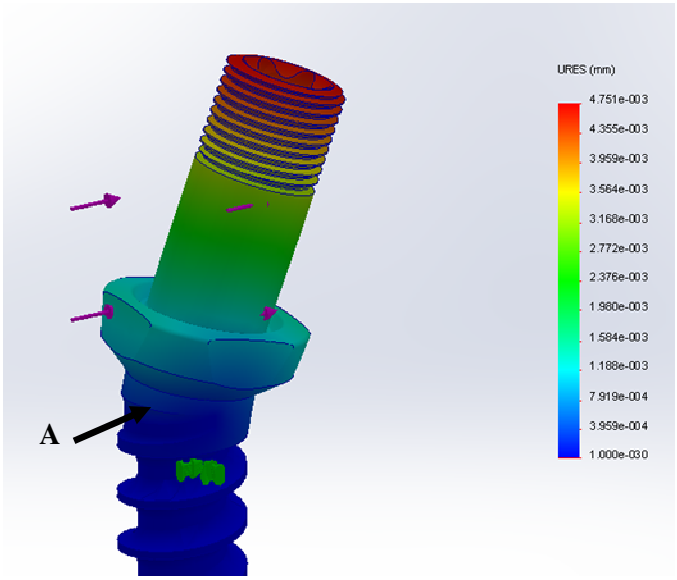

Figure 45: Resultant displacement of the screw shank

An illustration of where the load, representing the load that the collar exerts on the screw shank, during loading is shown in Figure 46; note the point A where the expected bending is expected once the screw is anchored in the bone.

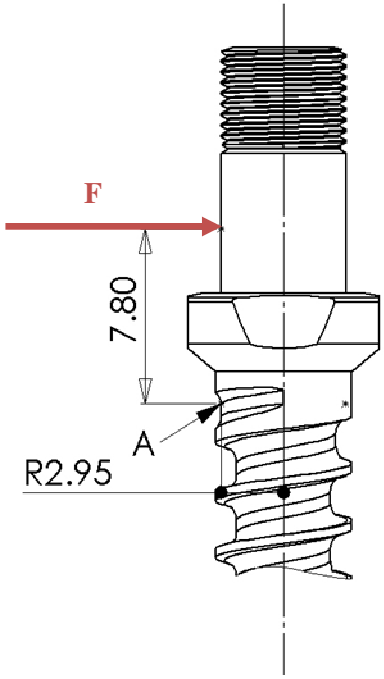

Figure 46: Illustration of the point of application of the load

$$I = \frac{1}{4}\pi\left(2.95 \times 10^{-3}\right) = 5.95 \times 10^{-11} m^4$$ **Equation 1: Moment of inertia**

$$\delta = \frac{PL^3}{3EI} = \frac{100(0.0078)^3}{3(104\times10^9)(9.52\times10^{-11})} = 1.6 \times 10^{-3} mm$$ **Equation 2: Deflection**

$$\sigma_{max} = \frac{Mc}{I} = \frac{(100)(0.0078)(2.95\times10^{-3})}{5.95\times10^{-11}} = 38.67 MPa$$ **Equation 3: Maximum stress**

These results correlate well with the FEA results, thus acting as verification. The maximum stress occurs on the minor diameter of the screw thread just above where the screw would be anchored in the bone.

The maximum von Mises stress is around 39MPa; this is far below the fatigue life of Ti6Al4V ELI titanium alloy, indicating that this cyclic loading will not cause failure of the screw before $1x10^7$ cycles.

7.5.4. Verification Conclusion

The required axial stiffness value for a posterior dynamic stabilisation device to limit spinal segmental motion by the amount found in literature, as well as the stiffness suggested by various authors, is around 50N/mm in compression.

The value of 50N/mm in compression was obtained after initial calculations using a spring optimisation process and final spring calculations. The finite element analyses carried out on the simplified spring model predicted an axial deflection result similar to that of the calculated value

under a 50N load; this verified the device design input by showing that the present design would limit the range of motion of the affected spinal segment by the correct amount and stabilise the segment while lowering the chance of adjacent segment disease. The present design was also compared to that of the DSS system (Paradigm Spine), determined in vitro and theoretically by Schilling *et al.* (2011) and Galbusera *et al.* (2011), and it was found that the present design would, to a certain extent, produce similar results in ROM reduction and spinal stabilisation.

There are inherent limitations to the verifications performed; finite element analyses are only estimations. One may be able to create a model that is as close as possible to the actual device but the simulation is still only an estimation of the real setup.

7.7. Design Validation

Design validation is the process of testing a low-volume production run of the device, or a first-off prototype; as was the case in this project. The verifying calculations warranted the advance in the procedure to perform validation on the first rapid prototype device.

The selected concept conceived during the design process was implemented in the form of a prototype that could be physically tested to validate the device stiffness.

7.7.1. Testing Protocol

Aim: The stabilisation capabilities of the representative prototype device are unknown; the aim of this validation is therefore to:

- Determine the stiffness of the representative prototype device
- Measure the principal dimensions of the device
- Assess the bending capabilities of the device and determine where there may be issues regarding wear

Materials and Methods:

The validation tests were performed on the rapid prototype device using a simple test setup. A progressive compression test and a progressive tensile test were performed. Figure 47 shows the test setup. The prototype device was clamped on either end; one in the vice connected to the linear actuator, and the other end in a clamp connected to the force gauge. The load was increased steadily and measured at random intervals to obtain load-versus-displacement values to determine the axial stiffness of the device. The axial displacement was measure using a digital calliper.

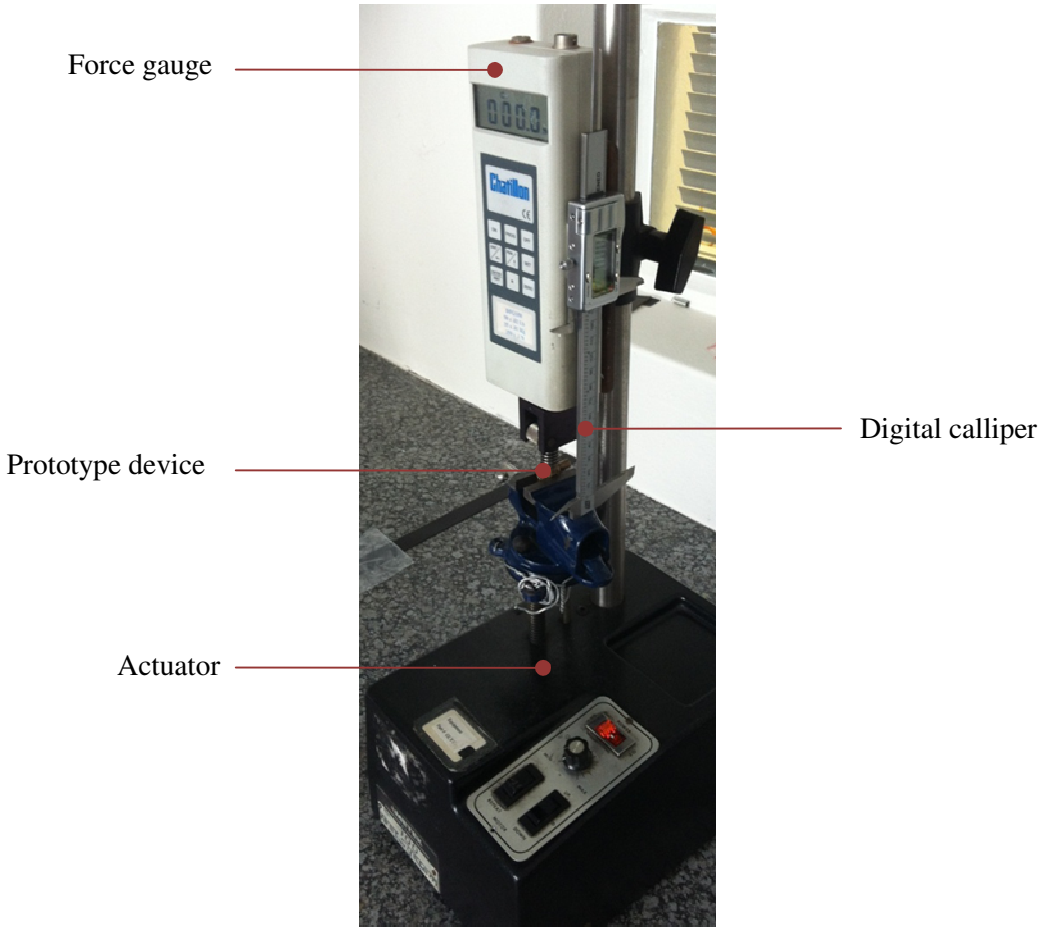

Figure 47: Validation test setup

Test Equipment

The test equipment used in this validation included a calibrated force gauge to measure the exerted load on the device, a calibrated digital calliper to measure the axial displacement and a linear actuator to exert the load; see Figure 47 for the test setup. The actuator was easily controlled using a fine potentiometer.

Device Description

The investigated device is presented in Figure 48. The use of conventional manufacturing methods, requiring custom-made tooling, proved to be unfeasible for first-off prototypes. In order to produce this first-off device, a rapid prototyping technique was used. 3D-printing was the rapid prototyping method chosen for this device as it included some complex geometry that would take time and expensive tooling to manufacture using conventional methods.

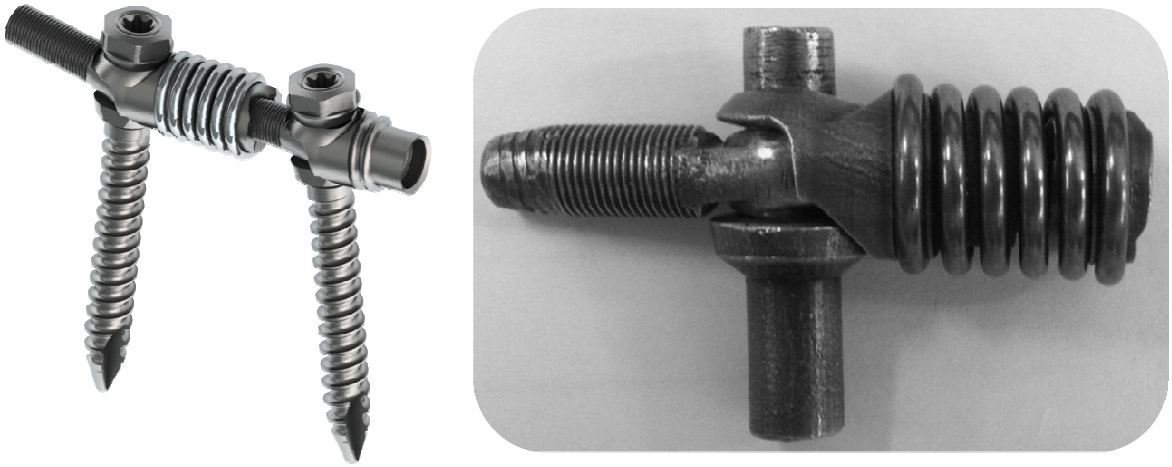

(A) **(B)**

Figure 48: The rapid prototype device (revision A-001); Rendering (A), 3D-printed device (B)

Descriptions and specifications of the tested prototype device are listed in Table 17.

Table 17: Description of validation test components

Validation test component description	
Device revision	A-001
Components	Helical spring
	Collar mount
	Threaded mount
	Threaded rod collar
	Screw shaft representation
Materials	Helical spring: S.S. spring wire (EN 10270-1 drawn)
	Other components: Bronze
Manufacture method	Rapid prototype (3D-printing)
Test date	2013.10.20

The rapid prototype device is produced differently to that of the anticipated production-ready device; these differences are listed in Table 18.

Table 18: Differences in manufacture method and materials between the prototype and anticipated production device

	Rapid prototype	**Production-ready**
Processes	3D-printed, drawn wire	Turning, milling, EDM, drawn wire
Helical Spring	S.S. spring wire (EN 10270)	Phynox: CCM-based alloy (ASTM F1058)
Collars	Bronze	BioDurCCM alloy (ASTM F799)

7.7.2. Results and Discussion

The results of the force-displacement test are provided in Figure 49. A linear-fit line was inserted to determine the approximate gradient, and hence device axial stiffness, of the curve.

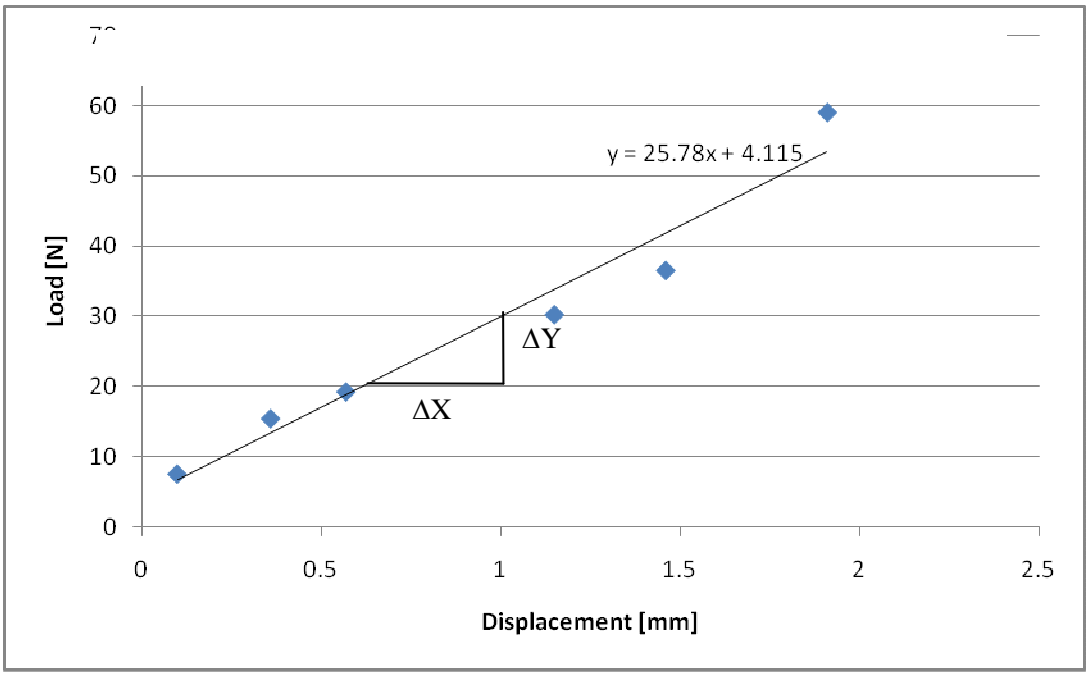

Figure 49: Load-displacement curve for prototype A-001

The resultant gradient of the linear-fit line, and stiffness of the device, is as follows:

$$k = {\Delta Y}/{\Delta X} = {(30 - 20)N}/{(1 - 0.625)mm} = 26.67N/m$$

This stiffness value correlates well with the calculated value of 25.19N/mm in compression. This test, although very limited, validates the stiffness of the rapid prototype device. This implies that the concept would have the anticipated stiffness once it is in production-ready phase as the only change would be that of the material to obtain the required stiffness of 50N/mm.

7.7.3. Validation Conclusion

The validation of the rapid prototype device was conducted to validate the design; the verification calculations warranted this validation to test whether or not the medical device prototype meets the user needs.

The testing included performing a load-displacement test on a single prototype device to determine its axial stiffness. The result obtained was about 26.67N/mm and was determined by calculating the

gradient of the linear-fit line of the data. This result correlated well with the stiffness value calculated during the verification phase; an axial stiffness of 25.19N/mm in compression.

There are limitations to the validation test that should be pointed out. These limitations affect the results of the tests and included:

- An inaccurate representation of the method anchoring either end of the dynamic coupler
- Not all the 3D-printed components could be assembled due to the inaccuracy of the manufacturing process, therefore simulating a full assembly was not possible
- As only one device was tested the results were not significant statistically

Addressing these limitations would certainly have improved the accuracy of the test result. Also, a larger sample size is required for these tests; although this was not feasible.

The rapid prototype device, using stainless steel spring wire (EN 10270) as the spring material, was validated according to the user requirements of having the correct stiffness; a change in material, or using Phynox, would result in the stiffness required for the production-ready specification of 50N/mm.

Chapter 8: Conclusion

This chapter concludes the research on the development of a posterior dynamic stabilisation implant indicated for thoraco-lumbar disc degeneration. Perspective is provided of the relevance of the research, the salient findings are consolidated, and aspects meriting further investigation are discussed.

8.1. Perspective of the Work

The functional spinal unit of the lumbar spine is placed under loading that can cause wear of the three-complex joint of each level. This wear can lead to spinal disorders that significantly affect the range of motion of each spinal segment and can lead to lower back pain that affects the patient and the economy as a whole.

Degenerative Disc Disease

Degenerative disc disease increases the rate of disc degeneration, which is a natural process, and causes a misalignment of the spine. This misalignment may result in impingement of spinal nerves leading to pain. Disc degeneration is thought to be caused by various factors such as; mechanical loading, genetic predisposition and nutritional effects.

Currently the most effective solution to alleviation from pain resulting from spinal stenosis due to disc degeneration is to intervene with a mechanical device that redistributes the load transferred through the spinal segment and preserves some motion. This intervention should be achieved using solid engineering principles in designing a device that has the correct stiffness properties to provide spinal segment stabilisation.

Posterior Element Degeneration

Posterior element degeneration, or degeneration of the facet joints, is often a result of intervertebral disc degeneration. When these facet joints degenerate the one surgical intervention technique is to perform a facetectomy; this removal of parts of the joint results in their inability to resist loading transversely, or in axial rotation. This scenario requires a posterior dynamic stabilisation device to stabilise the spine in the transverse plain.

Posterior Dynamic Stabilisation Development

The *gold standard* treatment for lumbar spinal disorders is currently to fuse the vertebrae at the affected level. This fusion certainly relieves pain for the patient but inherently causes complications such as adjacent segment disease. This adjacent segment disease is a result of the level, adjacent to the

fusion, becoming hypermobile and the intervertebral disc wearing at a faster rate. The fusion, created using rigid rods between pedicle screws, changes the normal load distribution between the posterior elements and the anterior vertebral column by carrying the entire load. This change results in an unloading of the intervertebral disc and results in 'stress shielding' that can cause osteoporosis when these fusion rods are used with an intervertebral fusion cage, which is often the case.

The next logical step in the advancement of posterior lumbar devices is to develop a device that limits the range of motion of the lumbar spinal segment, relieving pain, but that still allows some motion so as to prevent adjacent hypermobility and degeneration. There is not enough clinical evidence, as of yet, that supports the theory that dynamic stabilisation devices prevent this complication. However, theoretically it is clear that these devices are advantageous over conventional fusion techniques; they have been shown to preserve some of the range of motion of the spinal segment and they can be easily designed to achieve the correct amount of stabilisation.

8.2. Consolidation of the Work Done

The aim of this work was to develop a posterior dynamic stabilisation device that is indicated for intervertebral lumbar disc degeneration and posterior element, or facet, degeneration. To achieve this it was necessary to design a device that provided the correct stabilisation of the spinal segment.

Through reviewing relevant, and contemporary where possible, literature the following procedure was followed:

- Anatomy and functional spinal unit kinematics were explored
- Loading of the lumbar spine was researched
- The origins of lower back pain were identified
- Summaries and comparisons were made between competitor products
- Clinical results of other devices were investigated
- Biomaterials that could potentially be used were reviewed
- A design process was followed in order to develop, design, verify and validate a prototype device

From the research done in the above process it was found that, to adequately stabilise the spine, the device should:

- Have biomaterials that are compatible with one another
- Provide an axial stiffness that adequately limits the spinal segment range of motion
- Have certain dimensions to ensure it fits most inter-segmental anatomies

To ensure that the materials were compatible, they were chosen such that there would be no galvanic dissimilarities. The spring material was chosen to be a specialist cobalt-chrome-molybdenum alloy that has excellent fatigue properties. The other components were designed to be manufactured from another CCM-based alloy and not Ti6Al4V (Titanium Grade 5 ELI) as it was found to be notch-sensitive under cyclic loading.

Design Verification and Validation

Concepts for the posterior lumbar dynamic stabilisation device were evaluated according to specific criteria in order to select the best one. Due to financial constraints the most feasible device to rapid prototype was selected. It incorporated a helical compression spring mounted on two collar ends that allowed axial translation and were easily assembled. The collars would be mounted onto pedicle screws using spherical friction clamps.

The rapid prototype device was manufactured to estimate the effect it would have as a stabilisation device. The prototype was not manufactured from materials anticipated for a production-ready device; instead materials that could be used to 3D-print the device were used. The design was verified according to the design inputs through calculations and finite element analyses (FEAs). The axial stiffness obtained was 49N/mm in compression and around 25.19N/mm in distraction. These values were successfully correlated with the FEAs.

The resulting design of the device, during verification, was also compared to similar devices. One such device, the DSS (Paradigm Spine) was found to be very similar in stiffness properties and geometry; this comparison was used to evaluate and estimate how well the current design would be able to stabilise a spinal segment. Verifications of the FEAs that predicted stresses in the components were also performed; all components, under the specified cyclic loading, had significantly high factors of safety (FOS) and all FEA results were correlated well with applicable hand calculations.

The design was validated according to the user requirement of providing the correct spinal stabilisation. This was accomplished by performing a load-displacement test on the rapid prototype device. The stiffness of the prototype device was validated; the test result was an axial stiffness of 26.67N/mm which correlated well with the calculated value of 25.19N/mm.

8.3. Conclusion

It is apparent that work initiated during this project should not be concluded at present; it provides a framework for further, more detailed work. This study performed the design process up until the first rapid prototype device. This makes it a limited study and future work is therefore required to fully develop such a device.

Production-ready Device

In order to develop a device that accurately satisfies the user requirements, the device that is developed and tested must represent the final production-ready device as far as reasonably possible; this was not possible in this study due to financial constraints.

The production-ready device may even be manufactured entirely differently and from different materials; such as those used in the other concepts that were generated. The use of a carbon fibre-reinforced poly-ether-ether-ketone (CFR-PEEK) would be advantageous as it would provide superior imaging capabilities, smoother translation, a simpler single-piece design and superb fatigue properties. This type of device would also be compatible with existing pedicle screws and instrumentation that are developed by Southern Medical (Pty) Ltd. and would therefore result in significant cost savings and operation time savings.

Biomechanical Testing and Clinical Studies

The production-ready device would have to be validated using biomechanical tests to evaluate the effect it has on spinal segment range of motion. This type of test incorporates implanting the device in cadaveric spines and assessing the motion of the segments.

Clinical studies would also need to be performed on the production-ready device to assess: ease of surgical operation, operating time, hospital stay length and VAS and ODI scores at patient follow-up periods.

8.4. Recommendations

Long-term clinical data that illustrate how advantageous posterior dynamic stabilisation devices are is severely lacking. This type of data is required to assess how effective the devices are in the long-term and to determine possible associated complications that were not foreseen or identified during short-term follow-up studies. In order to gather this type of information it is recommended that clinical trials, the results of which are added to a local register, are performed and strictly followed-up by practitioners and manufacturers in order to further develop the medical devices.

Chapter 9: References

Acosta, F. L., et al. (2008). Early Clinical & Radiographic Results of NFix II Posterior Dynamic Stabilization System. SAS Journal, 2(2), 69–75. doi:10.1016/S1935-9810(08)70021-5

Adams, M.A., Freeman, B.J.C., Morrison, H.P., Nelson, I.W., Dolan, P. (2000) Mechanical initiation of intervertebral disc degeneration. Spine 2000; 25(13):2625–36.

Adogwa, O., et al. (2011). Long-term outcomes of revision fusion for lumbar pseudarthrosis: clinical article. Journal of neurosurgery. Spine, 15(4), 393–8. doi:10.3171/2011.4.SPINE10822

An, H. S. (1999). The relationship between facet joint osteoarthritis and disc degeneration of the lumbar spine : an MRI study, 396–401.

Ashman R.B., Galpin RD, Corin J.D., Johnston C.E. II. (1989) Biomechanical analysis of pedicle screw instrumentation systems in a corpectomy model. Spine 1989;14:1398–405.

Austin, H., (2008). Wear of PEEK All-Polymer Articulations for Cervical Spinal Disc Arthroplasty. Masters Dissertation, University of Waterloo

Bao, Q., McCullen, M., et al. (1996). Review The artificial disc: theory, design and materials. Biomaterials. Vol. 17, pp 1157-1167. Retrieved from Elsevier 07/01/2010.

Barrey, C. Y., Ponnappan, R. K., Song, J., Vaccaro, A. R. (2008). Biomechanical Evaluation of Pedicle Screw-Based Dynamic Stabilization Devices for the Lumbar Spine: A Systematic Review. SAS Journal, 2(4), 159–170. doi:10.1016/S1935-9810(08)70035-5

Berman, B. (2012). 3-D printing: The new industrial revolution. Business Horizons, 55(2), 155–162. doi:10.1016/j.bushor.2011.11.003

Benezech J., Mitulescu A. (2007) Retrospective patient outcome evaluation after semi-rigid stabilization without fusion for degenerative lumbar instability. Eur J OrthopSurgTraum. 2007;17:227-234.

Berven, S. H., Herkowitz, H. N. (2009). Evidence-Based Medicine for the Spine: Degenerative Spondylolisthesis. Seminars in Spine Surgery, 21(4), 238–245. doi:10.1053/j.semss.2009.08.007

Bifulco, P., Cesarelli, M., Cerciello, T., Romano, M. (2012).A continuous description of intervertebral motion by means of spline interpolation of kinematic data extracted by videofluoroscopy. Journal of Biomechanics, 45(4), 634–41. doi:10.1016/j.jbiomech.2011.12.022

Bogduk, N. And Twomey, L.T. (1987, 1991). Clinical Anatomy of the Lumbar Spine, 1st and 2nd editions, Churchill Livingston, Edinburgh.

Boos N, Webb JK. (1997). Pedicle screw fixation in spinal disorders: a European view. Eur. Spine J. 1997;6(1):2-18.

Canbay et al. (2013). Posterior dynamic stabilization for the treatment of patients with lumbar degenerative disc disease: long-term clinical and radiological results. Turkish Neurosurgery, 23(2), 188–97. doi:10.5137/1019-5149.JTN.6459-12.0

Cahill P.J., Wang W., Asghar J., et al. (2012). The use of a transition rod may prevent proximal junctional kyphosis in the thoracic spine following scoliosis surgery: a finite element analysis. Spine 2012;37:E687–95.

Cakir B., Carazzo C., Schmidt R., Mattes T., Reichel H., Käfer W. (2009). Adjacent segment mobility after rigid and semirigid instrumentation of the lumbar spine. Spine (Phila Pa 1976) 2009;34:1287–91.

Chao, S., Malloy, J.P., Bono, C.M. (2011).Complications Specific to Motion-Sparing Devices in the Lumbar Spine. Seminars in Spine Surgery, 23(2), 123–134. doi:10.1053/j.semss.2010.12.015.

Cheng B.C., Gordon J., Cheng J., Welch W.C. (2007). Immediate biomechanical effects of lumbar posterior dynamic stabilization above a circumferential fusion. Spine (Phila Pa 1976) 2007; 32: 2551–7.

Collins, S.L., Moore, R.A., McQuay, H.J. (1997) The visual analogue pain intensity scale: what is moderate pain in millimetres?, Pain, Volume 72, Issues 1–2, August 1997, Pages 95-97, ISSN 0304-3959, 10.1016/S0304-3959(97)00005-5.

Courville, X., Torretti, J., Sengupta, D. K. (2008). Dynamic Stabilization: Principles and Current Clinical Practice. Seminars in Spine Surgery, 20(2), 146–153. doi:10.1053/j.semss.2008.02.009

Crisco, J.J., Panjabi, M.M., Yamamoto, I., Oxland, T.R. (1992). Euler stability of the human ligamentous lumbar spine. Part II: Experiment, Clinical Biomechanics, Volume 7, Issue 1, February 1992, Pages 27-32, ISSN 0268-0033, http://0-dx.doi.org.innopac.up.ac.za/10.1016/0268-0033 (92)90004-N.

Cunningham B., Colleran D., Holsapple G., et al. (2006). Lumbar Spine Kinematics: a Radiographic assessment of the Change in Interpedicular Distance throughout the Range of Motion. In: SAS Proceedings - Symposia Handouts, Abstracts of Podium Presentations and Poster Presentations. Montreal, Quebec, Canada; May 9–13, 2006:58.

Drake, R.L., Vogl, A.W., Mitchell, A.W. (2010). Gray's Anatomy for Students. Second Edition. 2010. ISBN: 978-0-443-06952-9.

Dubois G., de Germay B., Schaerer N.S., et al: (1999). Dynamic neutralization: a new concept for restabilization of the spine, in Szalski, M., Gunzburg, R., Pope, M.H. (ed). Lumbar Segmental Instability. Philadelphia, Lippincott Williams & Wilkins, 1999, 233 - 240

Ebraheim, N. a., Hassan, A., Lee, M., Xu, R. (2004).Functional anatomy of the lumbar spine. Seminars in Pain Medicine, 2(3), 131–137. doi:10.1016/j.spmd.2004.08.004

Eijkelkamp, M.F., Groningen, U. of. (2002). On the development of an artificial intervertebral disc. Retrieved from http://www.narcis.nl/publication/RecordID/oai%3Aub.rug.nl%3Adbi%2F43565cc917913

Elias, C.N., Lima, J.H.C., Valiev, R., Meyers, M.A. (2008). Biomedical Applications of Titanium and its Alloys, (March), 1–4.

Errico, T.J., (2004). Why a mechanical disc? The Spine Journal. 151S-157S. Retrieved 07/01/2010 from Science Direct.

Evans, E.J. (1994). Cell damage in vitro following direct contact with fine particles of titanium, titanium alloy and cobalt-chrome-molybdenum alloy. Biomaterials, 15(9), 713–7. Retrieved from http://www.ncbi.nlm.nih.gov/pubmed/7948594

Faraj, A.A. Webb, J. K. (1997). Early complications of spinal pedicle screw. European spine journal : official publication of the European Spine Society, the European Spinal Deformity Society, and the European Section of the Cervical Spine Research Society, 6(5), 324–6. Retrieved from http://www.pubmedcentral.nih.gov/articlerender.fcgi?artid=3454598&tool=pmcentrez&rendertype=abstract

Fay, L.-Y., Wu, J.-C., Tsai, T.-Y., Wu, C.-L., Huang, W.-C., Cheng, H. (2012). Dynamic stabilization for degenerative spondylolisthesis: Evaluation of radiographic and clinical outcomes. Clinical neurology and neurosurgery. doi:10.1016/j.clineuro.2012.05.036

Feith, R. (1975). Side effects of acrylic cement, implanted to bone. ActaOrthopScand 1975; (Suppl.): 161.

Fleck, C., Eifler, D. (2010). Corrosion, fatigue and corrosion fatigue behaviour of metal implant materials, especially titanium alloys. International Journal of Fatigue, 32(6), 929–935. doi:10.1016/j.ijfatigue.2009.09.009

Freudiger, S., Dubois, G., Lorrain, M. (1999). Dynamic neutralisation of the lumbar spine confirmed on a new lumbar spine simulator in vitro. Arch Orthop Trauma Surg. 1999;119:127–32.

Frost, H.M. A. (2003). Update of bone physiology and Wolff's Law for clinicians. Angle Orthodontist.2004, 74:3-15.

Fujiwara, A., Tamai, K., An, H.S., et al. (2000). The relationship between disc de- generation, facet joint osteoarthritis, and stability of the degenerative lumbar spine. J Spin Dis. 2000;13:444–50.

Galbusera, F., Bellini, C. M., Anasetti, F., Ciavarro, C., Lovi, A., Brayda-Bruno, M. (2011). Rigid and flexible spinal stabilization devices: a biomechanical comparison. Medical Engineering &Physics, 33(4), 490–6. doi:10.1016/j.medengphy.2010.11.018

Gédet, P., Haschtmann, D., Thistlethwaite, P. a, Ferguson, S. J. (2009).Comparative biomechanical investigation of a modular dynamic lumbar stabilization system and the Dynesys system. European spine journal : official publication of the European Spine Society, the European Spinal Deformity Society, and the European Section of the Cervical Spine Research Society, 18(10), 1504–11. doi:10.1007/s00586-009-1077-7

Ghiselli, G., Wang, J. C., Bhatia, N. N., Hsu, W. K., Dawson, E. G. (2004). Adjacent segment degeneration in the lumbar spine. The Journal of bone and joint surgery. American volume, 86-A(7), 1497–503. Retrieved from http://www.pubmedcentral.nih.gov/articlerender.fcgi?artid=2796347&tool=pmcentrez&rendertype=abstract

Goel, V.K., Lim, T.H., Gwon, J. et al. (1991). Effects of rigidity of an internal fixation device. A comprehensive biomechanical investigation. Spine. 1991; 16:S155-161.

Goodman, S. B., Yao, Z., Keeney, M., Yang, F. (2013).The future of biologic coatings for orthopaedic implants. Biomaterials, 34(13), 3174–83. doi:10.1016/j.biomaterials.2013.01.074

Götz, H.E., et al. (2003). Effect of surface finish on the osseointegration of laser-treated titanium alloy implants, Biomaterials, Volume 25, Issue 18, August 2004, Pages 4057-4064, ISSN 0142-9612, http://dx.doi.org/10.1016/j.biomaterials.2003.11.002.

Green, S. (2006) Carbon Fibre-reinforced PEEK-OPTIMA® Composite Materials for use in Surgical Implant Applications. April 2006. Presentation.

Gulbrandsen, P., Madsen, H. B., Benth, J. S., Laerum, E. (2010). Health care providers communicate less well with patients with chronic low back pain--a study of encounters at a back pain clinic in Denmark. Pain, 150(3), 458–61. doi:10.1016/j.pain.2010.05.024

Haher, T.R., Yeung, A.W., Ottaviano, D.M., Merola, A.A., Caruso, S.A. (2001). The inverse effects of load transfer and load sharing on axial compressive stiffness. The spine journal : official journal of the North American Spine Society, 1(5), 324–9; discussion 330. Retrieved from http://www.ncbi.nlm.nih.gov/pubmed/14588309

Hart, B.L., Deyo, R.A., Cherkin, D.C. (1995) Physician office visits for low back pain. Spine 1995; 20: 11-19.

Hasegawa, T., Inufusa, A., Imai, Y., Mikawa, Y., Lim, T.-H., An, H. S. (2005). Hydroxyapatite-coating of pedicle screws improves resistance against pull-out force in the osteoporotic canine lumbar spine model: a pilot study. The spine journal : official journal of the North American Spine Society, 5(3), 239–43. doi:10.1016/j.spinee.2004.11.010

Heuer, F., Schmidt, H., Käfer, W., Graf, N., Wilke, H.-J. (2012). Posterior motion preserving implants evaluated by means of intervertebral disc bulging and annular fibre strains. Clinical Biomechanics (Bristol, Avon), 27(3), 218–25. doi:10.1016/j.clinbiomech.2011.09.004

Holm, S., Maroudas, A., Urban, J.P.,Selstam, G., Nachemson, A. (1981). Nutrition of the intervertebral disc: solute transport and metabolism. Connect Tissue Res 1981, 8:101-119.

Horner, H.A., Urban, J.P: (2001) Volvo Award Winner in Basic Science Studies: effect of nutrient supply on the viability of cells from the nucleus pulposus of the intervertebral disc. Spine 2001, 26:2543-2549.

Hu, S.S. (1997). Internal fixation in the osteoporotic spine. Spine 1997; 22:S43–8.

Okuyama, K., Abe, E., Suzuki, T., Tamura, Y., Chiba, M., Sato, K. (2001). Influence of bone mineral density on pedicle screw fixation: a study of pedicle screw fixation augmenting posterior lumbar interbody fusion in elderly patients. The spine journal : official journal of the North American Spine Society, 1(6), 402–7. Retrieved from http://www.ncbi.nlm.nih.gov/pubmed/14588296

Jahng, T.-A., Kim, Y. E., Moon, K. Y. (2013). Comparison of the biomechanical effect of pedicle-based dynamic stabilization: a study using finite element analysis. The Spine journal : official journal of the North American Spine Society, 13(1), 85–94. doi:10.1016/j.spinee.2012.11.014

Jansen, N. (2010). Development of a low imaging signature cervical spine disc arthroplasty.Diss. 2010.

Johnsson, K.E. (1995). Lumbar canal stenosis: a retrospective study of 163 cases in southern Sweden. ActaOrthopScand1995; 66:403–405 (1995)

Kaner, T., Sasani, M., Oktenoglu, T., Aydin, A. L., Ozer, A. F. (2010). Minimum two-year follow-up of cases with recurrent disc herniation treated with microdiscectomy and posterior dynamic transpedicular stabilisation. The open orthopaedics journal, 4(90), 120–5.doi:10.2174/1874325001004010120

Katz, J.N., Lipson, S.J., Larson, M.G., McInnes, J.M., Fossel, A.H., Liang, M.H: (1991). The outcome of decompressive laminectomy for degenerative lumbar spinal stenosis. J Bone Joint Surg [Am] 73:809-816, 1991

Katz, J.N. (1995) Lumbar spinal fusion. Surgical rates, costs, and complications. Spine 20(24 Suppl):78S–83S

Kayalioglu, G. (2009). Chapter 4 - The Spinal Nerves, In The Spinal Cord, edited by Charles Watson, George Paxinos and Gulgun Kayalioglu, Academic Press, San Diego, 2009, Pages 37-56, ISBN 9780123742476, http://dx.doi.org/10.1016/B978-0-12-374247-6.50008-0.

Khoueir, P., Kim, K.A., Wang, M.Y. (2007). Classification of posterior dynamic stabilization devices. Neurosurg Focus 2007; 22:E3.

Kienapfel, H. et al., (1999). Implant fixation by bone ingrowth. The Journal of Arthroplasty, 14(3), 355 - 368.

Kim, D.H., Cammisa, F.P., Fessler, R.G. (2006) Dynamic Reconstruction of the Spine.

Kim, C.H., Chung, C.K., Jahng, T.A. (2011). Comparisons of outcomes after single or multilevel dynamic stabilization: effects on adjacent segment. J Spinal Disord Tech 2011; 24:60–7.

Kirkaldy-Willis, W.H., Farfan, H.F. (1982). Instability of the lumbar spine. ClinOrthop. 1982; 165:110–23.

Kobayashi, S., et al. (2006). Imaging of caudaequinaedema in lumbar canal stenosis by using gadolinium-enhanced MR imaging: experimental constriction injury. AJNR. American Journal of Neuroradiology, 27(2), 346–53. Retrieved from http://www.ncbi.nlm.nih.gov/pubmed/16484408

Krag, M.H., Seroussi, R.E., Wilder, D.G., Pope, M.H. (1987). Internal displacement distribution from in vitro loading of human thoracic and lumbar spinal motion segments: experimental results and theoretical predictions. Spine 1987; 12:1001-7.

Kulkarni, A. G., Diwan, A. D. (2005). Prosthetic lumbar disc replacement for degenerative disc disease. Neurology India, 53(4), 499–505. Retrieved from http://www.ncbi.nlm.nih.gov/pubmed/16565543

Lau, S. and Lam, K.S. (2007).Lumbar stabilization techniques. Current Orthopaedics, Volume 21, 25 - 39.

Li, Z., Li, F., Yu, S., Ma, H., Chen, Z., Zhang, H., Fu, Q. (2013). Two-year follow-up results of the Isobar TTL Semi-Rigid Rod System for the treatment of lumbar degenerative disease. Journal of clinical neuroscience : official journal of the Neurosurgical Society of Australasia, 20(3), 394–9. doi:10.1016/j.jocn.2012.02.043

Markolf, K.L., Morris, J.M. (1974). The structural components of the intervertebral disc. J Bone Joint Surg 1974;56-A(4):675687

McAfee, P.C. (1999). Interbody fusion cages in reconstructive operations on the spine. J Bone Joint Surg Am 1999;81:859-80.

McNally, D.S., Shackleford, I.M., Goodship, A.E., Mulholland, R.C. (1996). In vivo stress measurement can predict pain on discography. Spine 1996;21:2580-7.

Moroni, A., Toksvig-Larsen, S., Maltarello, M.C., et al. (1998). Comparison of hydroxyapatite-coated, titanium-coated, and uncoated tapered external-fixation pins. J Bone Joint Surg. 1998;80A:547–54.

Nachemson, A. (1965). The load on lumbar disks in different position of the body. Clinical Orthopaedics Vol. 45, 1965, 107 - 122.

Nachemson, A., Lewin, T., Maroudas, A., Freeman, M.A.F. (1970). In vitro diffusion of dye through the end plates and annulus fibrosis of human lumbar intervertebral discs. Acta Orthop Scand 1970, 41:589-607.

Nachemson, A. L. (1981). Disc pressure measurements. Spine, Vol. 6, No. 1, 1981, 93 - 97.

Niinomi, M. (2003).Recent research and development in titanium alloys for biomedical applications and healthcare goods. Science and Technology of Advanced Materials, 4(5), 445–454. doi:10.1016/j.stam.2003.09.002

Okuyama, K., Abe, E., Sato, K., Kamata, S., Nagata, A., Miyano, T. (1993) Bending strength and pull-out force of pedicle screws (in Japanese with English abstract). Orthop Surg Traumatol 1993;36:1357–63.

Okuyama, et al. (2001). Influence of bone mineral density on pedicle screw fixation: a study of pedicle screw fixation augmenting posterior lumbar interbody fusion in elderly patients. The spine journal : official journal of the North American Spine Society, 1(6), 402–7. Retrieved from http://www.ncbi.nlm.nih.gov/pubmed/14588296.

Olmarker, K. (1990). Thesis, Gothenburg

Ouellet, J. A., Arlet, V. (2004).Surgical anatomy of the pelvis, sacrum, and lumbar spine relevant to spinal surgery. Seminars in Spine Surgery, 16(2), 91–100. doi:10.1053/j.semss.2004.07.008

Panjabi, M.M., Krag, M.H., White, A.A. 3rd, Southwick, W.O. (1977) Effects of preload on load displacement curves of the lumbar spine. The Orthopedic Clinics of North America 1977, 8(1):181-192]

Park, S.-A., Fayyazi, A. H., Yonemura, K. S., Fredrickson, B. E., Ordway, N. R. (2012). An in vivo kinematic comparison of dynamic lumbar stabilization to lumbar discectomy and posterior lumbar fusion using radiostereometric analysis. The International Journal of Spine Surgery, 6(1), 87–92. doi:10.1016/j.ijsp.2012.02.003

Pearcy, M., Portek, I., Shepherd, J. (1984). Three-dimensional x-ray analysis of normal movement in the lumbar spine. Spine 1984; 9 (3): 294-7.

Pearcy, M.J., Tibrewal, S.B. (1984). Axial rotation and lateral bending in the normal lumbar spine measured by three-dimensional radiography. Spine 1984; 9 (6): 582-7.

Phillips, F. M., et al. (2006).Biomechanics of posterior dynamic stabilizing device (DIAM) after facetectomy and discectomy. The spine journal : official journal of the North American Spine Society, 6(6), 714–22. doi:10.1016/j.spinee.2006.02.003

Polikeit, A., Nolte, L.P., Ferguson, S.J. (2003). The effect of cement augmentation on the load transfer in an osteoporotic functional spinal unit: finite-element analysis. Spine 28, 991–996.

Ponnappan, R. K., Serhan, H., Zarda, B., Patel, R., Albert, T., Vaccaro, A. R. (2009).Biomechanical evaluation and comparison of polyetheretherketone rod system to traditional titanium rod fixation. The spine journal : official journal of the North American Spine Society, 9(3), 263–7. doi:10.1016/j.spinee.2008.08.002

Ramakrishna, S., Mayer, J., Wintermantel, E. (2001). Biomedical applications of polymer-composite materials: a review. Compos Sci.Technol. 2001; 61(9):1189–224.

Rohlmann, A., Zander, T., Bergmann, G., Boustani, H. N. (2012).Optimal stiffness of a pedicle-screw-based motion preservation implant for the lumbar spine. European spine journal : official publication of the European Spine Society, the European Spinal Deformity Society, and the European Section of the Cervical Spine Research Society, 21(4), 666–73. doi:10.1007/s00586-011-2047-4

Rousseau, M. A., Bradford, D. S., Hadi, T. M., Pedersen, K. L., Lotz, J. C. (2006). The instant axis of rotation influences facet forces at L5/S1 during flexion/extension and lateral bending. European spine journal : official publication of the European Spine Society, the European Spinal Deformity Society, and the European Section of the Cervical Spine Research Society, 15(3), 299–307. doi:10.1007/s00586-005-0935-1

Sanden, B., Olerud, C., Johansson, C., et al. (2000). Improved extraction torque of hydroxyapatite-coated pedicle screws. Eur. Spine J 2000;9:534–7.

Sanden, B., Olerud, C., Larsson, S. (2001). Hydroxyapatite coating enhances fixation of loaded pedicle screws: a mechanical in vivo study in sheep. Eur. Spine J 2001;10:334–9.

Schulte, T.L., Hurschler, C., Haversath, M., et al. (2008). The effect of dynamic, semi-rigid implants on the range of motion of lumbar motion segments after decompression. Eur. Spine J 2008; 17:1057–65.

Schroeder, G. D., Murray, M. R., Hsu, W. K. (2011).A Review of Dynamic Stabilization in the Lumbar Spine. Operative Techniques in Orthopaedics, 21(3), 235–239. doi:10.1053/j.oto.2011.06.006

Senegas, J. (2002). Mechanical supplementation by non-rigid fixation in de- generative intervertebral segments: the Wallis system. Eur. Spine J 2002; 11:S164–9.

Sengupta, D.K., Mulholland, R.C. (2005). Fulcrum assisted soft stabilization sys- tem: a new concept in the surgical treatment of degenerative low back pain. Spine 30(9):1019-1029; discussion 1030, 2005

Serhan, H., Mhatre, D., Defossez, H., Bono, C.M. (2011). Motion-preserving technologies for degenerative lumbar spine: The past, present, and future horizons. SAS Journal 5 (2011) 75–89.

Shetty, R. (2011). Use of Dissimilar Metals in Orthopaedic Implants. Investigation performed at the Research Laboratories of Zimmer Inc., Warsaw, Indiana.

Schilling, et al. (2011). The effect of design parameters of dynamic pedicle screw systems on kinematics and load bearing: an in vitro study. European spine journal : official publication of the European Spine Society, the European Spinal Deformity Society, and the European Section of the Cervical Spine Research Society, 20(2), 297–307. doi:10.1007/s00586-010-1620-6

Shirazi-Adl, A. and Drouin, G. (1987). Load-bearing role of facets in a lumbar segment under sagittal plane loadings. J.Biomech. 1987. 20(6), 601-613.

Spenciner, D., Greene, D., Paiva, J., Palumbo, M., Crisco, J. (2006).The multidirectional bending properties of the human lumbar intervertebral disc. The spine journal : official journal of the North American Spine Society, 6(3), 248–57. doi:10.1016/j.spinee.2005.08.020

Stoll T.M., Dubois G., Schwarzenbach O. (2002). The dynamic neutralization system for the spine: a multi-centre study of a novel non-fusion system. Eur. Spine J 11:S170-S178, 2002.

Tanaka, N., An, H. S., Lim, T. H., Fujiwara, A, Jeon, C. H., Haughton, V. M. (2001). The relationship between disc degeneration and flexibility of the lumbar spine. The spine journal : official journal of the North American Spine Society, 1(1), 47–56. Retrieved from http://www.ncbi.nlm.nih.gov/pubmed/20352410

Templier, A., et al. (1998). Orthopaedic Surgery & Comparison between two different concepts of lumbar posterior osteosynthesis implants A finite-element analysis, 27–36.

Urban, J. P. G., Roberts, S. (2003). Degeneration of the intervertebral disc, 5(3).doi:10.1186/ar629

Uysal, M., Circi, E., Ozalay, M., Derincek, A., Cinar, M. (2012). The surgical treatment for a rare case of double-level isthmic spondylolisthesis in L4 and L5 lumbar spine: decompression, reduction and fusion. European Journal of Orthopaedic Surgery & Traumatology, (78).doi:10.1007/s00590-012-0993-0

Weinstein, J. N., Rydevik, B. L., Rauschning, W. (1992). Anatomic and technical considerations of pedicle screw fixation. Clinical orthopaedics and related research, (284), 34–46. Retrieved from http://www.ncbi.nlm.nih.gov/pubmed/1395312

Weinstein, J. N., et al. (2008). Surgical versus nonsurgical therapy for lumbar spinal stenosis. The New England journal of medicine, 358(8), 794–810.doi:10.1056/NEJMoa0707136

White, A.A., Panjabi, M.M. (1990). Clinical biomechanics of the spine. Philadelphia: Lippincott.

Wilke, H., Heuer, F., Schmidt, H. (2009). Prospective Design Delineation and Subsequent In Vitro Evaluation of a New Posterior Dynamic Stabilization System, 34(3), 255–261.

Wiseman, C. M., Lindsey, D. P., Fredrick, A. D., and Yerby, S. A. (2005). The effect of an interspinous process implant on facet loading during extension. Spine (Phila Pa 1976.) 4-15-2005. 30(8), 903-907.

Wittenberg, R.H., Shea ,M., Swartz, D.E., et al. (1991). Importance of bone mineral density in instrumented spine fusions. Spine 1991;16:647–52.

Xia, Q., Wang, S., Kozanek, M., Passias, P., Wood, K., Li, G. (2010). In-vivo motion characteristics of lumbar vertebrae in sagittal and transverse planes. Journal of biomechanics, 43(10), 1905–9. doi:10.1016/j.jbiomech.2010.03.023

Yoganandan, N., et al. (2006). Trabecular bone density of male human cervical and lumbar vertebrae. Bone, 39(2), 336–44. doi:10.1016/j.bone.2006.01.160

Zhao, C.-Q., Wang, L.-M., Jiang, L.-S., Dai, L.-Y. (2007). The cell biology of intervertebral disc aging and degeneration. Ageing research reviews, 6(3), 247–61. doi:10.1016/j.arr.2007.08.001

Appendix A: Concept Selection Matrix

Table 19: Concept selection matrix

			Concepts			
					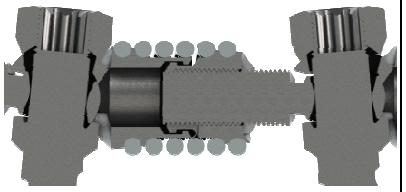	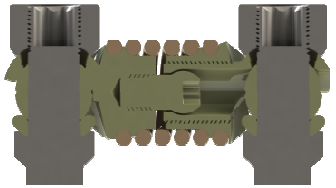
		Date	2013.06	2013.04	2012.11	2013.01
		Description	Coiled spring (CF-PEEK)	U-spring (CF-PEEK)	Adjustable sleeve coupler with coiled spring	Adjustable sleeve coupler with coiled spring and 'ball joint'
		Manufacturing Processes	Injection moulding	Injection moulding	Milling sleeves, turning screws and sleeves, EDM wire-cutting, drawing wire	Milling sleeves, turning screws and sleeves, EDM wire-cutting, drawing wire
		Design Features	Coiled spring, CF-PEEK is radiolucent, very strong and has good fatigue life. Simple one-piece design.	U-spring, CF-PEEK is radiolucent, very strong and has good fatigue life. Simple one-piece design.	Easily adjustable length, strong clamp connection between coupler and screw heads, has displacement stops in both directions.	Easily adjustable length, strong clamp connection between coupler and screw heads, has displacement stops in both directions, has a 'ball joint' central hinge.
Weighting	3	Manufacturing complexity	1	1	5	4
	3	Surgical techn. complexity	7	7	3	3
	10	Relative motion of surf.	2	2	8	8
	10	Coupler-screw conn.	8	8	2	2
	10	Smoothness of motion	7	7	7	7
	10	Fatigue life	8	7	5	5
	46	**Total**	**274**	**264**	**244**	**241**

Appendix B: Spring Optimisation

Step 1

Key	
XX	**Full FOS**
XX	**Compression FOS not met**
XX	**Distraction FOS not met**
XX	***No FOS met***
XX	**Fatigue limit exceeded**

Note: FOS = Factor of Safety

Outside diameter	Wire diameter	Minimum number of active coils	Minimum pitch	Total free length	Active spring length
13	**2.2**	**6**	**2.4**	**24**	14.4
	2.1	**5**	**2.4**	**21.6**	12
	2	**4.4**	**2.3**	**19.3**	10.1
	1.9	**3.9**	**2.3**	**18.17**	8.97
	1.8	***3.6***	***2.3***	***17.5***	8.3
	1.7	***3.3***	***2.3***	***16.8***	7.6
	1.6	***3***	***2.3***	***16.1***	6.9
	1.6	**2.9**	**2.4**	**16.5**	6.9
12	**2.2**	**7**	**2.4**	**26**	16.4
	2.1	**6**	**2.3**	**23**	13.8
	2	**5.5**	**2.2**	**20.9**	12.1
	1.9	**4.7**	**2.2**	**19.1**	10.3
	1.8	***4***	***2.2***	***17.6***	8.8
	1.7	***3.5***	***2.2***	***16.5***	7.7
	1.6	***3.2***	***2.2***	***15.8***	7
	1.5	**2.9**	**2.3**	**15.9**	6.7
11	**2.2**	**9**	**2.3**	**29.9**	20.7
	2.1	**7**	**2.3**	**25.3**	16.1
	2	**6.5**	**2.2**	**23.1**	14.3
	1.9	**5.5**	**2.1**	**19.95**	11.55
	1.8	**4.8**	**2.1**	**18.48**	10.08
	1.7	***4.2***	***2.1***	***17.2***	8.8
	1.6	***3.6***	***2.1***	***16***	7.6
	1.5	**3.3**	**2.1**	**15.3**	6.9

10	**2.1**	**10**	**2.2**	**30.8**	22
	2	**8.5**	**2.2**	**27.5**	18.7
	1.9	**7**	**2.1**	**23.1**	14.7
	1.8	**6**	**2**	**20**	12
	1.7	***5***	***2***	***18***	10
	1.6	***4.3***	***1.9***	***15.77***	8.17
	1.5	***3.8***	***1.9***	***14.8***	7.2
9	**2**	**12**	**2.1**	**33.6**	25.2
	1.9	**9**	**2**	**26**	18
	1.8	**7.5**	**2**	**23**	15
	1.7	**6.5**	**1.9**	**19.95**	12.35
	1.6	***5.5***	***1.8***	***17.1***	9.9
	1.5	***4.6***	***1.8***	***15.5***	8.3
	1.4	**4**	**1.8**	**14.4**	7.2
8	**1.9**	**14**	**2**	**39**	31
	1.8	**11**	**1.9**	**28.5**	20.9
	1.7	**9**	**1.8**	**23.4**	16.2
	1.6	**7.5**	**1.8**	**20.7**	13.5
	1.6	***7***	***1.8***	***19.8***	12.6
	1.5	**6.1**	**1.7**	**17.17**	10.37
7	**1.8**	**19**	**1.9**	**43.7**	36.1
	1.7	**13**	**1.8**	**30.6**	23.4
	1.6	**11**	**1.7**	**25.3**	18.5
	1.5	**9**	**1.6**	**20.8**	14.4
	1.4	**7**	**1.6**	**17.6**	11.2
6	**1.7**	**20**	**1.8**	**43.2**	36
	1.6	**17**	**1.7**	**35.7**	28.9
	1.5	**14.3**	**1.6**	**29.3**	22.9
	1.4	**10.5**	**1.5**	**21.75**	15.75

Step 2

Outside diameter	Wire diameter	Minimum number of active coils	Minimum pitch	Total free length	Active spring length
13	**2.1**	**5**	**2.4**	**21.6**	12
	2	**4.4**	**2.3**	**19.3**	10.1
	1.9	**3.9**	**2.3**	**18.17**	8.97
	1.8	***3.6***	***2.3***	***17.5***	***8.3***
	1.7	***3.3***	***2.3***	***16.8***	***7.6***
	1.6	***3***	***2.3***	***16.1***	***6.9***
12	**2.1**	**6**	**2.3**	**23**	13.8
	2	**5.5**	**2.2**	**20.9**	12.1
	1.9	**4.7**	**2.2**	**19.1**	10.3
	1.8	***4***	***2.2***	***17.6***	***8.8***
	1.7	***3.5***	***2.2***	***16.5***	***7.7***
	1.6	***3.2***	***2.2***	***15.8***	***7***
11	**2**	**6.5**	**2.2**	**23.1**	14.3
	1.9	**5.5**	**2.1**	**19.95**	**11.55**
	1.8	**4.8**	**2.1**	**18.48**	**10.08**
	1.7	***4.2***	***2.1***	***17.2***	***8.8***
	1.6	***3.6***	***2.1***	***16***	***7.6***
10	**1.9**	**7**	**2.1**	**23.1**	**14.7**
	1.8	**6**	**2**	**20**	**12**
	1.7	***5***	***2***	***18***	***10***
	1.6	***4.3***	***1.9***	***15.77***	***8.17***
	1.5	***3.8***	***1.9***	***14.8***	***7.2***
9	**1.8**	**7.5**	**2**	**23**	**15**
	1.7	**6.5**	**1.9**	**19.95**	**12.35**
	1.6	***5.5***	***1.8***	***17.1***	***9.9***
	1.5	***4.6***	***1.8***	***15.5***	***8.3***
8	**1.7**	**9**	**1.8**	**23.4**	**16.2**
	1.6	**7.5**	**1.8**	**20.7**	**13.5**
	1.6	***7***	***1.8***	***19.8***	***12.6***
7	**1.5**	**9**	**1.6**	**20.8**	**14.4**

Step 3

						Compression			Distraction		
Outside diameter	Wire diameter	Minimum number of active coils	Minimum pitch	Total free length	Active spring length	Spring index	T0.66mm (MPa)	T1mm (MPa)	Spring index	T1.33mm (MPa)	T2mm (MPa)
Full FOS											
13	**1.9**	**3.9**	**2.3**	**18.17**	8.97	**50**	**166**	**252**	**24**	**163**	**245**
13	**2**	**4.4**	**2.3**	**19.3**	10.1	**50**	**142**	**215**	**27**	**156**	**236**
12	**1.9**	**4.7**	**2.2**	**19.1**	10.3	**47**	**143**	**217**	**27**	**166**	**249.96**
12	**2**	**5.5**	**2.2**	**20.9**	12.1	**46**	**120**	**182**	**29**	**154**	**231**
13	**2.1**	**5**	**2.4**	**21.6**	12	**50**	**123**	**186**	**30**	**148**	**223**
12	**2.1**	**6**	**2.3**	**23**	13.8	**50.11**	**114**	**172**	**33.4**	**153**	**230**
11	**2**	**6.5**	**2.2**	**23.1**	14.3	**49**	**117**	**178**	**33.8**	**164**	**247**
Partial FOS											
13	1.6	3	2.3	16.1	6.9	44.2	244	370	15	164	246
13	***1.7***	***3.3***	***2.3***	***16.8***	***7.6***	**45**	**205**	311	**18**	**163**	**245**
13	***1.8***	***3.6***	***2.3***	***17.5***	***8.3***	**47**	**181**	**275**	**21**	**163**	**244**
11	**1.8**	**4.8**	**2.1**	**18.48**	**10.08**	**48**	**156**	**241**	**28**	**187**	281
11	**1.9**	**5.5**	**2.1**	**19.95**	**11.55**	**49**	**139**	**210**	**31**	**178**	**268**
9	**1.7**	**6.5**	**1.9**	**19.95**	**12.35**	**48**	**154**	**233**	**33**	**215**	323
10	**1.8**	**6**	**2**	**20**	**12**	**48**	**143**	**217**	**32**	**193**	290
8	**1.6**	**7.5**	**1.8**	**20.7**	**13.5**	**45**	**156**	**237**	**33**	**231**	348
7	1.5	9	1.6	20.8	14.4	43	159	241	34	249	374
9	**1.8**	**7.5**	**2**	**23**	**15**	**51**	**139**	**210**	**38**	**205**	309
10	**1.9**	**7**	**2.1**	**23.1**	**14.7**	**49**	**125**	**191**	**35**	**181**	**272**

8	1.7	9	1.8	23.4	16.2	48	137	207	37	214	323

No FOS											
10	1.5	3.8	1.9	14.8	7.2	46	237	359	22	227	341
9	1.5	4.6	1.8	15.5	8.3	46	215	327	26	245	370
10	1.6	4.3	1.9	15.77	8.17	48	205	312	26	222	333
12	1.6	3.2	2.2	15.8	7	49	248	375	18	187	281
11	1.6	3.6	2.1	16	7.6	49	231	350	22	207	311
12	1.7	3.5	2.2	16.5	7.7	51	217	330	22	187	282
9	1.6	5.5	1.8	17.1	9.9	46	178	270	29	228	344
11	1.7	4.2	2.1	17.2	8.8	47	185	280	25	195	293
12	1.8	4	2.2	17.6	8.8	49	178	269	25	179	269
10	1.7	5	2	18	10	49	173	264	29	210	316
8	1.6	7	1.8	19.8	12.6	50	172	260	36	248	372

Step 4

						Compression			Distraction		
Outside diameter	Wire diameter	Minimum number of active coils	Minimum pitch	Total free length	Active spring length	Spring index	T0.66mm (MPa)	T1mm (MPa)	Spring index	T1.33mm (MPa)	T2mm (MPa)
13	***1.8***	***3.6***	***2.3***	***17.5***	***8.3***	**47**	**181**	275	**21**	**163**	**244**
12	1.8	4	2.2	17.6	8.8	49	178	269	25	179	269
13	***1.9***	***3.9***	***2.3***	***18.17***	***8.97***	**50**	**166**	252	**24**	**163**	**245**
13	**2**	**4.4**	**2.3**	**19.3**	10.1	**50**	**142**	**215**	**27**	**156**	**236**
12	**1.9**	**4.7**	**2.2**	**19.1**	10.3	**47**	**143**	**217**	**27**	**166**	249.96
11	**1.9**	**5.5**	**2.1**	**19.95**	**11.55**	**49**	**139**	**210**	**31**	**178**	268
12	**2**	**5.5**	**2.2**	**20.9**	12.1	**46**	**120**	**182**	**29**	**154**	231
13	**2.1**	**5**	**2.4**	**21.6**	12	**50**	**123**	**186**	**30**	**148**	223
12	**2.1**	**6**	**2.3**	**23**	13.8	**50.11**	**114**	**172**	**33.4**	**153**	230
11	**2**	**6.5**	**2.2**	**23.1**	14.3	**49**	**117**	**178**	**33.8**	**164**	247
10	**1.9**	**7**	**2.1**	**23.1**	**14.7**	**49**	**125**	**191**	**35**	**181**	272

Step 5

						Compression			Distraction		
Outside diameter	Wire diameter	Minimum number of active distraction coils	Minimum pitch	Total free length	Active spring length	Spring index	T0.66mm (MPa)	T1mm (MPa)	Spring index	T1.33mm (MPa)	T2mm (MPa)
12	1.8	4	2.2	17.6	8.8	49	178	269	25	179	269

Appendix C: Spring Calculator

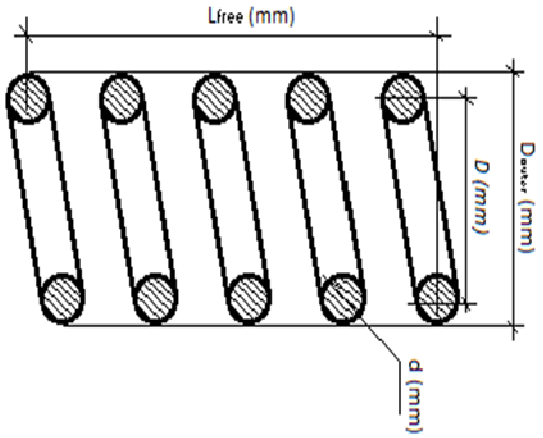

$$\tau_{max} = \frac{8WD}{\pi d^3} F_{max} \qquad G = \frac{E}{2(1+\nu)}$$

$$F_{max} = k\left(L_{free} - L_{solid}\right) \qquad k = \frac{Gd^4}{8D^3 n_a}$$

$$W = \frac{4C-1}{4C-4} + \frac{0.615}{C} \qquad C = \frac{D}{d}$$

Requirements:		
	Displacement (mm)	K value (N/mm)
Compression:	0.66	50.00
Distraction:	1.33	>20

Variables		
Outside diameter	D_{outer} (mm)	12.00
Wire diameter	d (mm)	1.80
Number of active distraction coils	n_{adist}	4.00
Pitch	P (mm)	2.20
Total Number of dead mounting coils	n_{dead}	2.00

Material Properties for Phynox (Cobalt-Chromium-Nickel Alloy)		
Young's Modulus	E (GPa)	208.00
Poisson's Ratio	-	0.30
Fatigue strength	MPa	500.00
Yield	MPa	NA
Shear strength	MPa	NA
Ultimate tensile strength	MPa	>900
Shear fatigue limit	MPa	280.00 (Approx.)

Outputs

Spring index	c	6.67	(Between 4 and 12)	Good	
Shear modulus	*G (N/mm^2)*	*80000.00*			
Wahl correction factor		*1.22*			
Mean diameter	*D (mm)*	*10.20*			

Compression

Number of active compression coils	$n_{a\ comp}$	2.00			
Maximum compression	(mm)	0.80		Good	
Compression spring stiffness	k (N/mm)	49.46	Approx. 50	≈49	N/mm
Force @ 0.66mm compression	*N*	32.64			
Shear stress @ 0.66mm compression	T0.66mm (MPa)	178.04		Good	
Force @ 1mm compression	*N*	49.46			
Shear stress @ 1mm compression	T1mm (MPa)	269.76		Good	

Distraction

Distraction spring stiffness	k (N/mm)	24.73		≈25	N/mm
Force @ 1.33mm distraction	N	32.89			
Shear stress at 1.33mm distraction	T1.33mm (MPa)	179.39		Good	
force @ 2mm distraction		49.46			
Shear stress at 2mm distraction	T2mm (MPa)	269.76		Good	

Complete spring

Total number of coils	n_{total}	6.00	
Total free length	mm	15.00	
Spring constant	N/mm	16.49	
Designed total compression force	N	32.64	
Designed total distraction force	N	32.89	
Maximum design compression	mm	1.98	
Maximum design distraction	mm	1.995	
Shear stress @ 2mm displacement	MPa	179.84	
Fully Compressed spring length	mm	10.80	